POTENTIAL PLATINUM DNA-METALLOINTERCALATORS:

SYNTHESIS, CHARACTERISATION AND ^{1}H NMR STUDIES ON [Pt(diimine)(*N*,*N*-di(*n*-butyl)-*N'*-acylthioureato)]$^+PF_6^-$ COMPLEXES IN SOLUTION

A dissertation submitted to the
UNIVERSITY OF CAPE TOWN

in fulfilment of the requirements for the degree of
MASTER OF SCIENCE

By

CLAIRE JOANNA LAWRENCE
B.Sc.(Hons.) (University of Cape Town)

Department of Chemistry
University of Cape Town
Rondebosch
7700
South Africa

May 1997

ACKNOWLEDGEMENTS

I would sincerely like to thank:

- My supervisor, Assoc. Prof. Klaus R. Koch, for his motivation, enthusiasm and guidance throughout my studies.

- Dr Cheryl Sacht, for her valuable comments and assistance.

- My parents, for always being there for me. Your interest and encouragement throughout my university career has been immeasurable.

- Mrs Elizabeth Wilson, for her continual interest.

- Dr Krassie Dimitrova and Ms Margie Nair for their assistance with the NMR experiments.

- Mr William Hendriks for his friendly assistance in the laboratory.

- To all the staff and students of the Chemistry Department, especially those on the third floor, Mr Francois Wevers, Mr Darren Handforth and Ms Yali Wang. A special thankyou goes to Mr Jörn Miller for proof-reading my thesis. Thank you all for your endless help and encouragement.

- The University of Cape Town and The Foundation for Research and Development for financial assistance.

ABSTRACT

A series of mixed-ligand [Pt(diimine)(*N,N*-di(*n*-butyl)-*N'*-acylthioureato)]$^+PF_6^-$ complexes has been synthesised and fully characterised (where diimine is: 1,10 phenanthroline; 4,7-diphenyl-1,10-phenanthroline; 2,2'-bipyridyl; 4,4'-dimethyl-2,2'-bipyridyl and 4,4'-di-*tert*-butyl-2,2'-bipyridyl and acyl is: benzoyl or naphthoyl).

A study of the ^1H NMR resonance spectra of these complexes in acetonitrile-d_3 revealed a pronounced concentration effect, which indicates that self-association is occurring in solution. Temperature dependence studies were also undertaken. For each complex, dimerisation constants (K^D) were calculated from significant chemical shift changes as a function of concentration. It has been postulated that the mode of association is regioselective since large upfield shifts are observed for the diimine protons. This can be attributed to the anisotropic effect of the ring current from one diimine member of the aggregate upon its neighbour. The effect of solvent on the self-association of these complexes was also investigated.

Experimental results were analysed using a computer program, which allowed for the best estimation of the association constant (K^D), as well as the chemical shift values at infinite dilution (δ_o-monomer) and high concentration (δ_∞-dimer). These values were optimised simultaneously using a linear regression of the chemical shift *vs.* concentration data. The thermodynamic parameters (ΔG, ΔH and ΔS) for the dimerisation of these complexes in acetonitrile-d_3 solution, were estimated from van't Hoff plots.

The nature of the diimine ligands as well as the acylthiourea moieties has been found to have a significant effect on the extent of dimerisation in solution. By systematically varying the diimine moiety of the complexes, the role of ligand geometry on the self-association interaction was investigated. Self-association constants in the range of 1.72 $dm^3\ mol^{-1}$ for [Pt(4,4'-ditbutbipy)-DiBuNTu]$^+PF_6^-$ to 114.1 $dm^3\ mol^{-1}$ for [Pt(4,7-diphenylphen)DiBuBTu]$^+PF_6^-$ have been measured in acetonitrile-d_3 at 25 °C.

ABBREVIATIONS

DiBuBTu	*N,N*-di(*n*-butyl)-*N'*-benzoylthiourea
DiBuNTu	*N,N*-di(*n*-butyl)-*N'*-naphthoylthiourea
bipy	2,2'-bipyridyl
4,4'-ditbutbipy	4,4'-di-*tert*-butyl-2,2'-bipyridyl
4,4'-dimethylbipy	4,4'-dimethyl-2,2'-bipyridyl
phen	1,10-phenanthroline
4,7-diphenylphen	4,7-diphenyl-1,10-phenanthroline
$Pt(bipy)Cl_2$	2,2'-bipyridyldichloroplatinum(II)
$Pt(4,4'\text{-ditbutbipy})Cl_2$	4,4'-di-*tert*-butyl-2,2'-bipyridyldichloroplatinum(II)
$Pt(4,4'\text{-dimethylbipy})Cl_2$	4,4'-dimethyl-2,2'-bipyridyldichloroplatinum(II)
$Pt(phen)Cl_2$	1,10-phenanthrolinedichloroplatinum(II)
$Pt(4,7\text{-diphenylphen})Cl_2$	4,7-diphenyl-1,10-phenanthrolinedichloroplatinum(II)
$[Pt(phen)DiBuBTu]^+PF_6^-$	1,10-phenanthroline-*N,N*-di(*n*-butyl)-*N'*-benzoylthioureato(*S,O*)platinum(II) hexafluorophosphate
$[Pt(phen)DiBuNTu]^+PF_6^-$	1,10-phenanthroline-*N,N*-di(*n*-butyl)-*N'*-naphthoylthioureato(*S,O*)platinum(II) hexafluorophosphate
$[Pt(4,7\text{-diphenylphen})DiBuBTu]^+PF_6^-$	4,7-diphenyl-1,10-phenanthroline-*N,N*-di(*n*-butyl)-*N'*-benzoylthioureato(*S,O*)platinum(II) hexafluorophosphate
$[Pt(4,7\text{-diphenylphen})DiBuNTu]^+PF_6^-$	4,7-diphenyl-1,10-phenanthroline-*N,N*-di(*n*-butyl)-*N'*-naphthoylthioureato(*S,O*)platinum(II) hexafluorophosphate
$[Pt(bipy)DiBuBTu]^+PF_6^-$	2,2'-bipyridyl-*N,N*-di(*n*-butyl)-*N'*-benzoylthioureato(*S,O*)-platinum(II) hexafluorophosphate

[Pt(bipy)DiBuNTu]$^{+}PF_6^{-}$	2,2'-bipyridyl-*N,N*-di(*n*-butyl)-*N'*-naphthoylthioureato(*S,O*)-platinum(II) hexafluorophosphate
[Pt(4,4'-dimethylbipy)DiBuBTu]$^{+}PF_6^{-}$	4,4'-dimethyl-2,2'-bipyridyl-*N,N*-di(*n*-butyl)-*N'*-benzoylthioureato(*S,O*)platinum(II) hexafluorophosphate
[Pt(4,4'-dimethylbipy)DiBuNTu]$^{+}PF_6^{-}$	4,4'-dimethyl-2,2'-bipyridyl-*N,N*-di(*n*-butyl)-*N'*-naphthoylthioureato(*S,O*)platinum(II) hexafluorophosphate
[Pt(4,4'-ditbutbipy)DiBuBTu]$^{+}PF_6^{-}$	4,4'-di-*tert*-butyl-2,2'-bipyridyl-*N,N*-di(*n*-butyl)-*N'*-benzoylthioureato(*S,O*)platinum(II) hexafluorophosphate
[Pt(4,4'-ditbutbipy)DiBuNTu]$^{+}PF_6^{-}$	4,4'-di-*tert*-butyl-2,2'-bipyridyl-*N,N*-di(*n*-butyl)-*N'*-naphthoylthioureato(*S,O*)platinum(II) hexafluorophosphate
DNA	deoxyribonucleic acid
RNA	ribonucleic acid
Å	angstrom unit, 10^{-10} m
ppm	parts per million (NMR)
Hz	hertz, s^{-1}
ΔG	Gibbs free energy change
ΔH	enthalpy change
ΔS	entropy change
K^D	association or dimerisation constant
R	Universal gas constant
T	Temperature (in Kelvin)
δ	chemical shift (NMR)
δ_o	chemical shift of monomer (NMR)
δ_∞	chemical shift of dimer (NMR)

ln	natural logarithm
lit.	literature
m.p.	melting point
Bu	butyl
Me	methyl
tert	tertiary
THF	tetrahydrofuran
KSCN	potassium thiocyanate
CH_3CN	acetonitrile
CD_3CN	deuterated acetonitrile
$CDCl_3$	deuterated chloroform
D_2O	deuterium oxide
+FAB	positive fast atom bombardment
COSY	H-H correlated spectroscopy
PAD	pre acquisition delay

TABLE OF CONTENTS

CHAPTER 1

INTRODUCTION

1 INTRODUCTION

1.1 PLATINUM COMPLEXES AS ANTICANCER DRUGS

Metal ions play an essential role in numerous biological processes[1,2]. They are required in virtually all processes involving nucleic acid biochemistry; and the study of the structure and function of biological macromolecules can be elucidated by their attachment[3,4]. The interaction of transition metal ions with nucleic acids or their constituent bases has been used to investigate[5]:

- the role of metals in nucleic acid metabolism
- selective heavy-metal labelling (for example lanthanide cations)[6] to aid in structure determination and in the sequencing of nucleic acids by electron microscopy
- the development of antitumour agents, notably platinum(II) based complexes, and their mechanism of interaction with nucleic acids

For these reasons, there is continuing interest in metal complexes that interact with deoxy-ribonucleic acid (DNA) molecules in solution. The group of interactions between metal ions and DNA can be classified into four categories as follows[1]:

- those that involve covalent inner-sphere binding of the metal to nucleic acids
- those that involve non-covalent outersphere binding

Aqua-ions of various transition metals bind to DNA mostly through phosphate moieties. Their destabilising or stabilising effect depends on the metal type and relative quantity. Stabilisation of double-stranded DNA, may occur when metal cations act to neutralise the phosphate negative charges. In contrast, interactions of transition metals with the DNA bases leads to destabilisation of the nucleic acid helical structure. For example lead(II) and copper(II) ions bind to phosphate groups at very low metal concentrations. However,

higher concentrations of these metals result in interactions with DNA bases which promote transitions of the DNA helix to the random coil state[7].

- strand breakage

Metal ions can promote the cleavage of nucleic acids. Copper(I) phenanthroline complexes have been found to cleave DNA in an oxygen dependent reaction[8]. Metalloporphyrins intercalate into G-C regions in double-stranded DNA and then after activation, cleave the nucleic acid strands[9]. Generally, in enzymatic systems metal ions activate the phosphate ester bond for hydrolysis (electrophilically by direct co-ordination or by delivery of co-ordinated nucleophiles).

- intercalation

The classical intercalation model involves the insertion of planar molecules between neighbouring base pairs. Intercalators may have neutral or cationic, non-planar substituents protruding into one of the DNA grooves. Typical examples are the phenanthridinium intercalators (ethidium and propidium) and the anthracycline intercalators (daunomycin and adriamycin)[10].

As early as 1931[11] the use of metal complexes of Cu, Cr, Mn, Fe, Pb, Co, Ni, Ru, Rh and Os as antitumour agents were studied. Later, this range was expanded to include complexes of Mg, Zn, Hg, Pd and Ir. The results of these extensive investigations, however, served mainly to illustrate that platinum complexes still appeared to exhibit the greatest antitumour activity at the lowest metal concentration. Platinum complexes are also particularly suited as biological probe reagents. A considerable number of complexes (predominantly with a halide or nitrogen donor ligand[12]) are slightly water soluble which is a prerequisite for a biological probe reagent. With few exceptions, platinum complexes exhibit a square planar or octahedral geometry, in +2 and +4 oxidation states respectively. More importantly, the chemistry of platinum is well known, thus facilitating the design of complexes with desired properties. Furthermore, the co-ordination chemistry of platinum(II) is characterised by kinetic inertness.

In 1964, Rosenberg *et al* discovered the antitumour properties of *cis*-diamminedichloro-platinum(II), '*Cisplatin*', and it is now one of the most commonly used drugs[13] in the treatment of certain types of cancer. This complex was first synthesised and characterised by Peyrone in 1844, (Peyrone's chloride)[14], and it is considered to be the parent compound of a unique group of inorganic co-ordination complexes used as anticancer drugs[15]. In these complexes platinum is essential for the anticancer activity.

Cisplatin is used commercially to treat numerous cancers such as testicular, ovarian, head and neck cancers. However, it is plagued by serious side effects such as nephrotoxicity, myelosuppresion, nausea and vomiting, and has been found to have little effect on breast and colorectal tumours[16]. For these reasons, analogues which do not develop cross-resistance with *Cisplatin*, which are active over a larger range of tumours, and most importantly, which induce fewer side effects, need to be developed[16]. This has stimulated much research on the synthesis and design of new complexes, as well as the mechanism of DNA-platinum complex interactions[17]. Developments in design have centred on the use of functionalised amines and/or mixed amines to selectively influence the potency, solubility and toxicity characteristics of the platinum complexes. In general, studies on the interaction mechanism have revealed that the platinum(II) complexes interact with DNA via two modes:

- covalent co-ordination to the base pairs

Studies have shown that platinum co-ordinates irreversibly to purines, especially guanines. Evidence shows that the nitrogen (N7) atom of guanine is the preferred site of attack in this co-ordination. The reaction is a two step process. Initial binding leads to monofunctional adducts, followed by closure to form bifunctional lesions[15].

- noncovalent intercalation between the base pairs

Intercalation of a drug into DNA is believed to be the first step in a series of events which eventually leads to DNA damage by other mechanisms. Drugs belonging to the class actinomycin[18] are examples of effective intercalators. A synergistic combination of DNA

recognition (intercalator) and subsequent DNA fixation could broaden the types of active metal complexes which may be effective.

Since intercalation is an important aspect of the studies we have undertaken, this process is discussed in further detail below.

1.2. INTERCALATION

Intercalation into double-stranded DNA is defined as the insertion of planar, aromatic or hetero-aromatic ligands between two stacked base pairs of the double helix[19].

Many intercalators have biological activity and intercalation is now widely accepted as a principle interaction mode for drugs and antibiotics. It was first introduced by Lerman[20] in 1961, as a mode of binding to explain the strong affinity of planar, cationic, heterocyclic dyes to double-stranded DNA.

In the intercalation process, the DNA primary and secondary structures remain largely intact[21]. The tertiary structure (helix) is lengthened as the drug is held perpendicular to the helix axis by noncovalent interactions. As a result some vertical separation of the base pairs occurs. The average separation between adjacent base pairs increases from 3.4 Å to between 7 and 8 Å, and results in distortion of the sugar-phosphate backbone conformation (Figure 1.1). The hydrophobic aromatic stacking interaction between the intercalated molecule and DNA bases stabilises the complex[22].

Intercalation distorts the regular helical structure of DNA and unwinds it at the site of binding. Therefore, this interaction interferes with the action of DNA-binding enzymes such as DNA polymerases (which catalyse the elongation of the DNA chain and correct mistakes by removing mis-matched residues)* and DNA topoisomerases (which alter the degree of supercoiling** in DNA)[19].*

* via hydrolysis of the phosphodiester bonds

** degree to which closed circular DNA is twisted[54]

Figure 1.1: Illustration of a molecule intercalated into double-stranded DNA

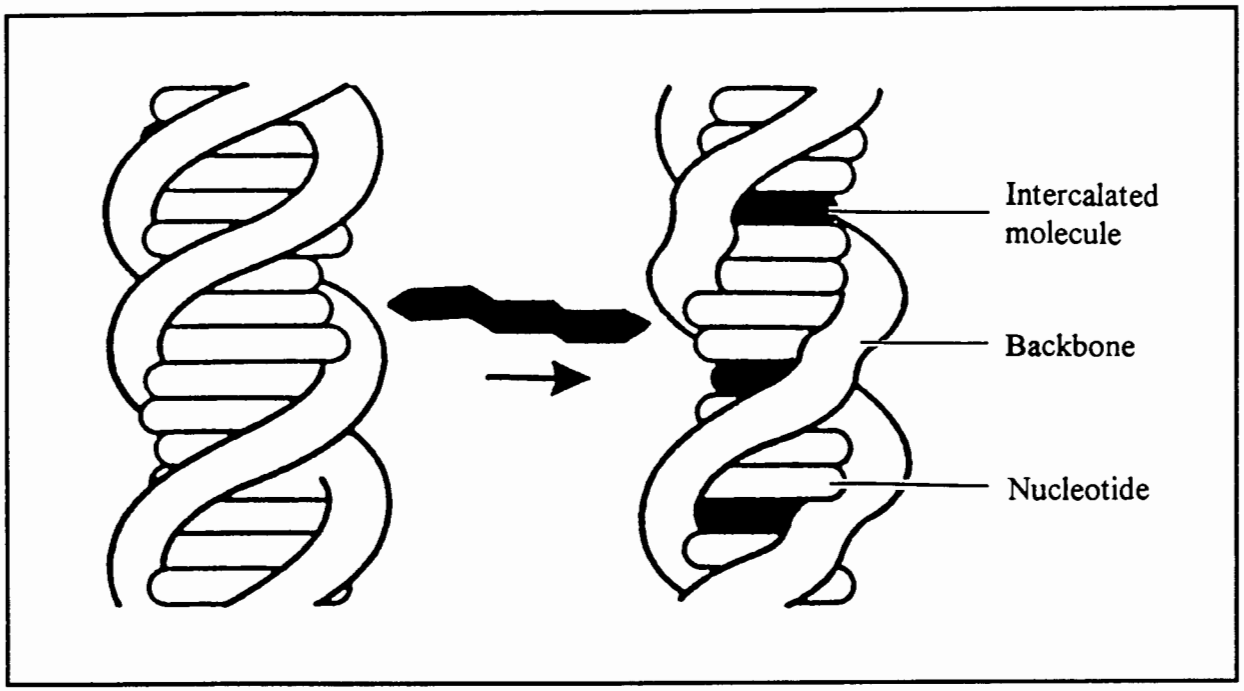

As a result of intercalation, changes in the physical properties of DNA occur. These include increases in viscosity, lowering of sedimentation constants, changes in electrophoretic mobility and hypochromism and red shifts (UV-visible measurements)[21]. The transition melting point of the DNA-helix also increases due to an intercalator-base pair stacking interaction which stabilises the helical over the unwound form.

The tendency of molecules to self-associate in solution is indicative of their ability to intercalate[23]. Aggregation of intercalating dyes is a well-known phenomenon[24,25]. Aggregation is a general term referring to an attractive interaction between molecules which can be ordered or disordered. Stacking is a subset of these interactions and implies an ordered association whereby the molecules lie one above the other.

Many different types of intercalators exist, and these can be classed as aminoacridine dyes, antimicrobial agents (ethidium bromide), organic antibiotics (actinomycin family) and metallointercalators (metalloporphyrins and numerous metal complexes)[26,27]. Classical intercalators are planar aromatic cations having no bulky substituents, while non-classical intercalators can be divided into two classes. These include molecules with non-fused, twisted aromatic systems and terminal cationic functions, and molecules with bulky substituents such as porphyrins [10].

Numerous physiochemical studies have provided information about the structural prerequisites for a typical intercalator[2]. Studies have been undertaken on the potential intercalative behaviour of platinum complexes comprising free pyridine ligands, 1,10-phenanthroline or 2,2'-bipyridyl[28]. The former complex was found not to intercalate into double-stranded DNA due to non-bonded steric repulsions between the adjacent pyridine rings which prevented the complex being coplanar. This suggests that ligand planarity is an important requirement for intercalation.

The relative disposition of the ligands in the co-ordination sphere of the metal complex and how the ligands 'fit' against the DNA minor and major groove are critical[29]. Since DNA is chiral, certain binding sites may favour specific enantiomeric forms of the complex. Studies by Morgan[30] *et al* on the effects of ligand geometry and peripheral charge, verified the need for ligand planarity in intercalating molecules. Wilson *et al* investigated the efficiency of unfused aromatic cations as intercalators[31]. They found that a certain amount of molecular twist could be accommodated in an intercalation ring system while maintaining a relatively high binding constant to DNA.

In a related study on ruthenium(II) mixed-ligand complexes, the effects of hydrophobicity, size, geometry, dipole moment and hydrogen-bonding ability on the intercalation interaction were investigated[32]. The hydrophobic nature of these complexes was found to be an important factor in determining their binding affinity for DNA. Self-association in solution was found to occur with increased hydrophobicity of the complexes. Thus, a reduced binding affinity for DNA could result.

Surprisingly, no additional stabilisation of the DNA-metal complex interaction was found to occur with the presence of potential hydrogen-bonding acceptors. This is in contrast to crystal structure studies of daunorubicin[21] (an anthracycline antibiotic), where hydrogen bonds have been found to make a major contribution to the stability of the DNA-intercalator complex.

Results of the study also highlighted the importance of the complex geometry. Molecular shape was found to be the most important factor, as those complexes in which the van der Waals interactions between DNA and the complex are maximised, displayed the highest binding affinity. Hence, non-covalent intercalators are usually cations with ligands that have extended hydrophobic regions or surfaces. The planar part of the molecule must possess a minimum surface area of 28 $Å^2$ (optimum at three or four rings)[21].

1.3 METAL COMPLEXES AND THEIR INTERACTIONS WITH DNA

Early studies on metallointercalators focused on square-planar complexes with aromatic terpyridyl or phenanthroline ligands[23]. The discovery that [(2,2',2"-terpyridine)PtCl]$^+$ **(A)** (Figure 1.2) caused shifts of the 335 nm band of 4-thiouridine in native *Escherichia coli* tRNA, was the first indication that a platinum complex might bind to a polynucleotide by intercalation[2]. Single-crystal studies of terpyridylplatinum(II) species stacked with nucleotides showed that the entire flat metal complex, and not just the aromatic ligand, intercalates between the base pairs[33,34].

Figure 1.2: Structures of **(A)** chloro(2,2',2"-terpyridine)platinum(II) and **(B)** 2-hydroxyethane-thiolato(2,2',2"-terpyridine)platinum(II)

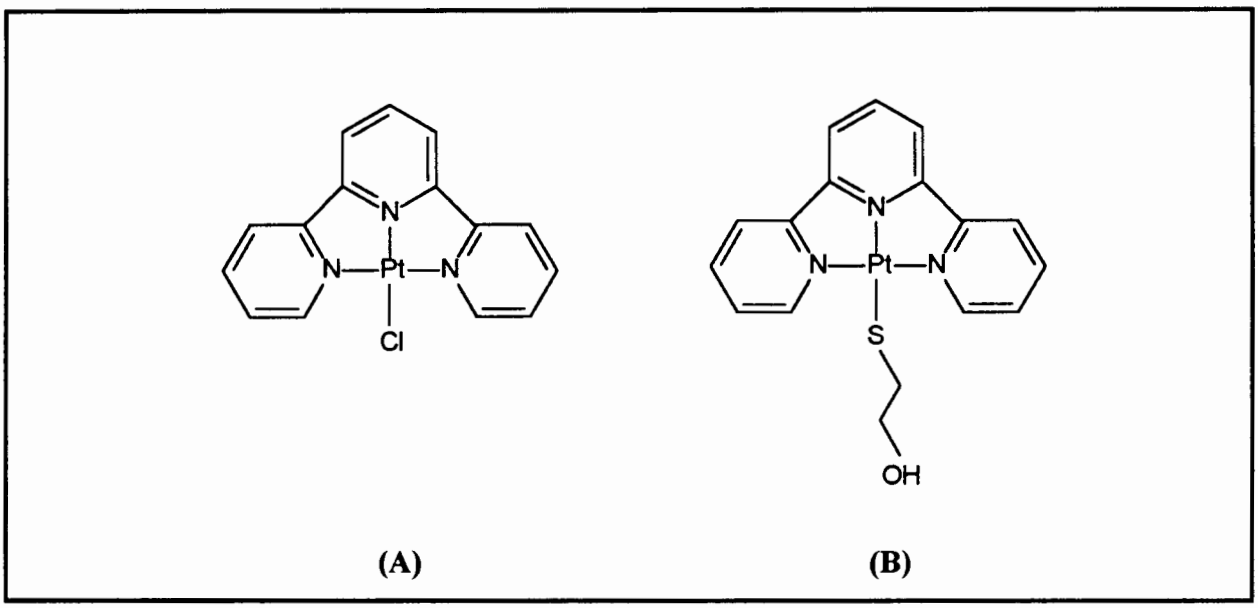

(A) **(B)**

It has been suggested that the presence of the platinum(II) atom enhances the stacking interactions which stabilise intercalation[35]. This is verified by the finding that related complexes chloro(2,2',2"-terpyridine)palladium(II)[36] and bis(9-benzyl-6-mercaptopurine)palladium(II)[37] exhibit close (3.2 - 3.5 Å) intermolecular parallel ring contacts in the solid state. In these complexes the metal ions are proposed to enhance the close-association of adjacent molecules.

Solution studies have shown, that even the simplest intercalators reach saturation point at a maximum of one intercalator per two base-pairs. This has led to the development of the "neighbour exclusion" model to explain the mode of binding by intercalators to DNA[38]. It states that intercalators can at best bind at alternative base-pair sites on DNA, so ensuring a maximum of one

intercalator between every second site. This was shown by Bond *et al* in the interaction of 2-hydroxyethanethiolato(2,2',2"-terpyridine)platinum(II) **(B)** (Figure 1.2) with double-stranded DNA[39].

In an attempt to increase the stability of DNA-metal complex interactions, Srivastava *et al* have extended Lippard's work to synthesise amino acid derivatives of 2,2'-bipyridylplatinum(II)[40] and 2,2'-bipyridylpalladium(II)[41,42]. They have investigated binding studies of these and other mixed-ligand complexes of the type $[M(NN)(AA)]^+$ (where M = Pt or Pd; NN = 2,2'-bipyridyl or 1,10-phenanthroline; and AA = an amino acid anion) to DNA[43,44]. The mode of binding has been found to involve hydrogen bonding interactions of the amino acid moieties.

A very recent study investigated the binding affinity of 2,2'-bipyridylplatinum(II) complexes co-ordinated to different pyridine derivatives, for DNA[45]. The findings suggested that partial intercalation of the bipyridyl moieties occurred with no direct interaction of the pyridine groups. This in contrast to previous findings in which 2,2'-bipyridyl was found to have only a marginal effect at inducing intercalative behaviour[32]. The stability of the DNA-metal complex interaction was found to increase with increasing pK_a of the co-ordinated pyridines, indicating the significant effect of electron density on intercalation.

Chelating ligands like 1,10-phenanthroline and 2,2'-bipyridyl and their metal complexes, are also effective intercalating agents, and their binding to synthetic polynucleotides, DNA and RNA has been extensively studied[46]. Similar diimine ligands have also been used to synthesise chiral metal complexes, which when binding to DNA show enantiomeric selectivity[47]. In many of these cases, co-planarity is not maintained as the complex geometry varies from octahedral tris(1,10-phenanthroline)- to planar or tetrahedral bis(1,10-phenanthroline) metal complexes. Binding and chiral discrimination in these instances, was found to be more dependent on the stereochemistry of the complex, and not on the electronic structure or properties of the metal.

In recent years extensive studies have also been undertaken on the intercalative behaviour of tris-chelates of ruthenium(II) and rhodium(II) with bidentate diimine ligands[26,48]. Selective enantiomeric intercalation of tris(1,10-phenanthroline)ruthenium(II) to double-stranded DNA has been observed[26]. Chiral discrimination was found to be enhanced in the case of tris(4,7-diphenyl-1,10-

phenanthroline)ruthenium(II) isomers, and they have been used as probes to distinguish right- and left- handed DNA helices[48].

Copper phenanthrolines have been found to act as efficient artificial nucleases*, cleaving ribose links in DNA when in the presence of a reducing agent and molecular oxygen[8,49]. Williams *et al* suggested that the copper complex is partially intercalated into the DNA helix, since cleavage preferentially occurs where intercalation is predicted to be favoured[50]. Other studies show that alternative modes of binding also occur. Bis(2,9-dimethyl-1,10-phenanthroline)copper(I) binds externally to DNA while bis(2,9-dimethyl-4,7-diphenyl-1,10-phenanthroline)copper(I) forms bridging structures in which the complex interlinks DNA molecules in solution[29]. Wilson *et al* noted that factors favouring intercalation over groove binding can be extremely subtle[51]. For instance, the introduction of phenyl substituents at the 4,7 positions of 1,10-phenanthroline in bis(1,10-phenanthroline)copper(I) or bis(2,9-dimethyl-1,10-phenanthroline)copper(I) alters the preference from groove binding to intercalation[52].

Numerous metal complexes of 1,10-phenanthroline have been synthesised, and their potential biological uses investigated. Zinc complexes, bis(1,10-phenanthroline)zinc(II), (1,10-phenanthroline)dichlorozinc(II) and octahedral tris(1,10-phenanthroline)zinc(II) have been shown by Barton *et al*, to unwind DNA by intercalation[53]. Using tris(1,10-phenanthroline) metal complexes, a potential stereospecific DNA nicking agent was synthesised with a redox-active metal (a nicking agent causes a single-strand interruption in DNA; no nucleotides are missing)[54]. In addition, low concentrations of tris(1,10-phenanthroline)cobalt(III), was found to cleave DNA when irradiated at 254 nm[55].

The number of studies on metal-complexes with co-ordinated diimine ligands is significant. The high level of recognition of DNA conformation by these chiral inorganic complexes alludes to the powerful applications of stereospecificity in DNA drug design.

* enzymes that catalyse the hydrolysis of polynucleotides

1.4 THE NATURE OF π-π INTERACTIONS

Weak intermolecular 'hydrophobic' or non-covalent interactions, are essential for molecular recognition, but their weak nature makes it difficult to identify specific associated modes of interaction and energies. Attractive interactions involving π-π systems are thought to give rise to a number of observed phenomena, including the well-known porphyrin aggregation[56,57], vertical base-base interactions responsible for stabilising DNA, the packing of aromatic molecules in crystals[58], complexation in host-guest systems[59] and the intercalation of drugs into double-stranded DNA[60]. These π-π or 'stacking' interactions are thought to be stabilised by electrostatic effects, induced dipole effects and dispersive contributions. In addition, solvophobic effects (particularly hydrophobic) which are entropic in origin, can play a significant role in aqueous solutions.

Petsko[61,62] has identified two important geometries for aromatic π-π interactions; an edge-to-face (T-shaped) orientation **(A)** (Figure 1.3) in which positively charged hydrogen atoms on one ring interact with the negatively charged regions on a second ring, and a parallel face-to-face orientation **(B)** (Figure 1.3).

Figure 1.3: Aromatic π-π interactions showing **(A)** face-to-edge and **(B)** face-to-face orientations

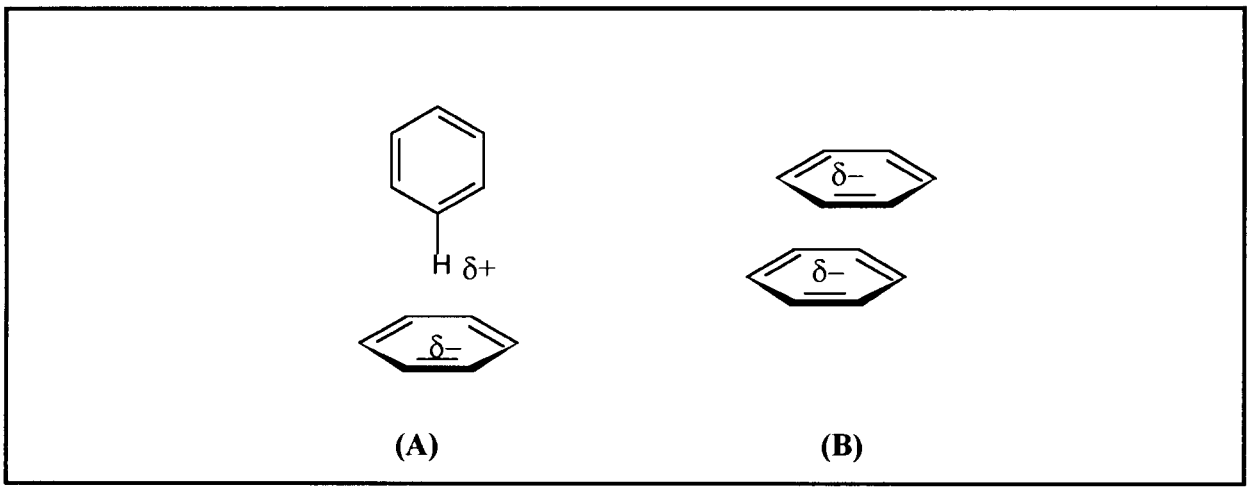

Studies by Jorgensen and Severance[63] on benzene, found that face-to-face stacked structures are net repulsive; structure **(A)** in Figure 1.3 being favoured. However, shifted, stacked structures in which the hydrogens are roughly over the ring centres **(B)**, become more favourable as the arene ring size increases.

By modifying the electronic characteristics of one aromatic component, the geometry of the π-π interaction can be controlled[64,65]. An electrostatic complementarity between partial charges on the rings can result in strong face-to-face stacking, while an absence will favour a weaker edge-to-face geometry.

From their studies on porphyrins, Hunter and Sanders[60] have proposed a model to explain the geometrical requirements for interactions between two π systems. These authors suggest that the geometry of the interaction is controlled by electrostatic interactions, while van der Waals interactions (and solvophobic effects) make the major contribution to the magnitude of the observed interaction.

The overall energy of interaction between two molecules can be represented as

$$E_{TOTAL} = E_{ELECTROSTATIC} + E_{INDUCTION} + E_{DISPERSION} + E_{REPULSION}$$

Electrostatic and van der Waals components are the major contributors to the attractive/repulsive interaction energy. However, the association of two molecules in solution also involves (i) displacement of solvent molecules from the solvation shell of each solvated molecule and (ii) the energy of association of the two molecules. In nonpolar organic solvents, the electrostatic interaction is the dominant contribution to the association energy, since electrostatic interactions with the solvent are negligible. However, both association energies and desolvation energies (entropic effects) are associated with van der Waals interactions.

In general it has been found that van der Waals interactions between two molecules are roughly proportional to the area of π-overlap. However, these interactions do not determine the geometry of the interaction. A geometry of maximum π-π overlap would be observed if van der Waals interactions were the controlling factor for establishing geometry in the stacking interaction. In addition, solvation has the effect of lowering the contribution of van der Waals interactions to the total π-stacking energy.

Porphyrins are known to aggregate in solution[57]. The single porphyrin molecules (monomers) have, in solution, as well as in crystals, been found to adopt a vertically stacked arrangement with their

centres offset so forming a shifted stack. Since van der Waals interactions are believed to be proportional to the area of π-overlap, stacking cannot be explained by van der Waals interactions of maximum π-overlap alone. There is a large electrostatic barrier to maximum π-overlap, therefore by estimating the electrostatic energy for a dimer species the geometry of the stacking interaction can be predicted.

Hunter and Sanders[60] have developed a model of the interaction between two π-systems. A positively charged σ framework is sandwiched between two negatively charged π-electron clouds (Figure 1.4). An attractive interaction between the two π-systems results in repulsion of the two approaching electron clouds. When the separation of the two π-systems is comparable to their thickness, the π-electrons can be considered separately from the σ-framework. A set of point charges is then used to represent the electrostatic charge distribution of the molecule.

Figure 1.4: The interaction between two face-to-face π systems[60]

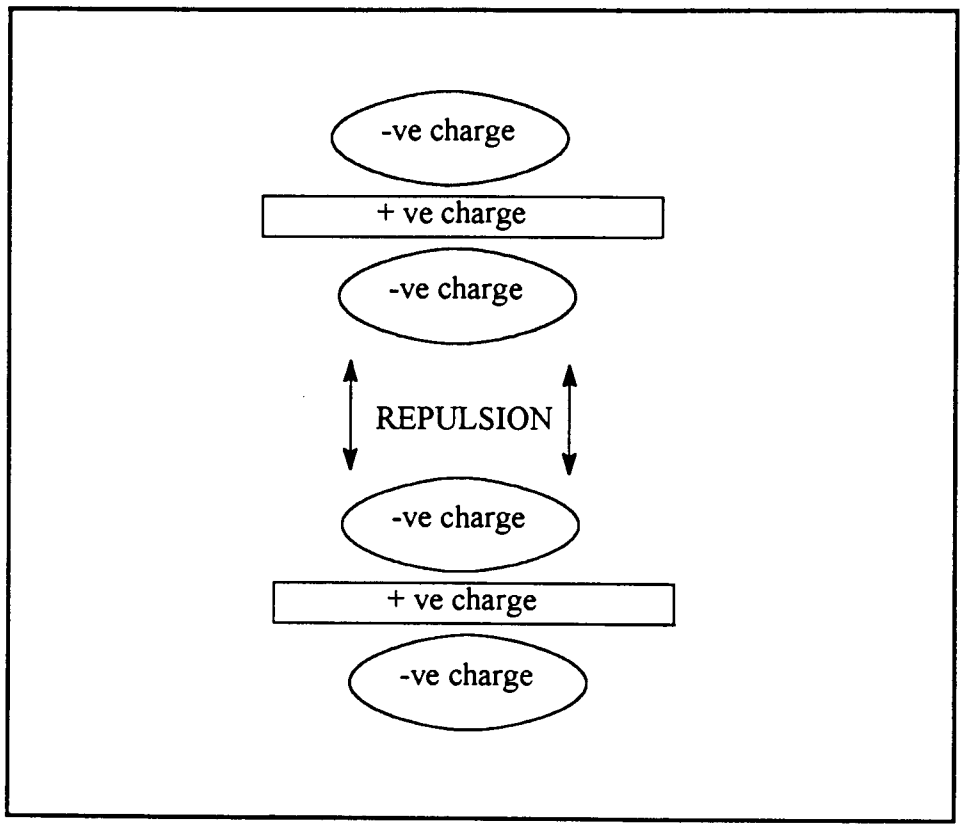

The electrostatic interaction can then be calculated as the sum of the charge-charge interactions between two such π systems. This model can be generalised to explain the presence or absence of attractive π-π interactions in different systems. Essentially, π-π interactions occur when the

favourable interaction between π-electrons of one molecule and the σ-framework of a second, outweigh unfavourable π-electron repulsion contributions.

The Hunter and Sanders[60] model therefore emphasises that the repulsive π-π interactions between arenes in a centrosymmetric stack, can be transformed into attractive interactions. This is achieved by geometric displacement of the ring planes or through charge distribution due to heteroatoms within the ring system.

The electron donor-acceptor (EDA) model has previously been used to describe the strong attraction between π systems[66]. This model suggests that attraction is due to an electronic interaction between an electron donor and electron acceptor. These EDA interactions are the sum of variable electrostatic (coulombic and induced) and higher-order van der Waals (charge transfer and dispersive) effects[59]. The Hunter and Sanders model suggests that this concept can be misleading. A study by Cozzi *et al*, demonstrated the dominance of π-π over charge-transfer effects in the interactions of stacked phenyl rings[67].

'Dimers' of metallated porphyrins were found to have the same geometry as those porphyrins previously discussed, however the magnitude of the interaction was found to differ. The attractive interaction in metallated porphyrins increases because a large positive charge is placed in the central cavity of the porphyrin π-system. This leads to a favourable interaction with the π-electrons of the pyrrole of the adjacent porphyrin. It has been experimentally observed that the greater the net positive charge on the metal, the greater the energy of the π-π interaction[68].

Stacking interactions of (bis((dimethylglyoximato)diphenylborato)iron(II) complexes, ($Fe(dmgBPh_2)_2$), were studied by Stynes[69]. This flexible receptor moves boron-linked phenyl groups in or out of contact with iron-bound axial ligands and the π-π interactions between the two groups were investigated. The author found that the trends in free energies of formation for cases where planar substrates are sandwiched between phenyl groups are consistent with the Hunter and Sanders[60] model. Face to face interactions were found to be repulsive unless strong polarising effects were present. The face-to-face orientation is disfavoured by π-π repulsion, but favoured by van der Waals and solvophobic effects. The presence of strongly polarising atoms has a major

influence on the electrostatic interaction. It seems that π-overlap can be favourable where the atoms at the site of contact are π-deficient.

1.5 *N,N*-DIALKYL-*N'*-ACYLTHIOUREA LIGANDS

1.5.1 Synthesis

The literature reveals that thiourea and its derivatives have played an important role in the early development of platinum chemistry. In the late 1800's, Kurnakow's synthesis of platinum(II) thiourea complexes afforded a large contribution to the knowledge of substitution reactions in square planar complexes[70].

Figure 1.5: Schematic representation of thiourea **(A)** and *N*-acylthiourea **(B)**

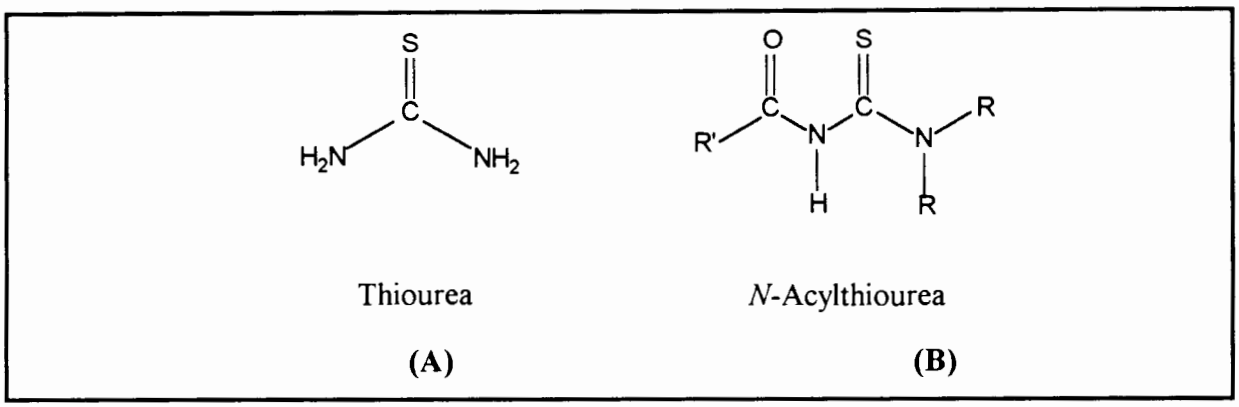

Thiourea **(A)**

N-Acylthiourea **(B)**

Thiourea has an S and N donor ligand and is potentially capable of bonding through both. In an attempt to improve selectivity of thiourea for platinum group metals, various substitutions have been investigated. The introduction of an acyl group (RCO-) on one of the nitrogen atoms was thought to increase the complexation potential of the ligand by the chelate effect[71] (Figure 1.5). After deprotonation of the acyl-substituted nitrogen, *N*-acylthioureas have the potential to act as bidentate S and O donor ligands.

The first reported synthesis of an *N*-acylthiourea was that of an *N'*-substituted-*N*-benzoylthiourea by Douglass and Dains in 1934[72]. The reaction involved the addition of benzoylchloride to a solution of NH_4SCN in acetone followed by the addition of amine. The synthesis required nucleophilic attack of the acyl chloride by thiocyanate and subsequent

thermal isomerisation of the acylthiocyanate intermediate to an acylisothiocyanate. A primary or secondary amine is added in the final step of the reaction. This reagent undergoes nucleophilic addition at the thiocarbonyl carbon of the acylisothiocyanate (Figure 1.6).

Figure 1.6: Reaction scheme for the synthesis of *N*-acylthioureas

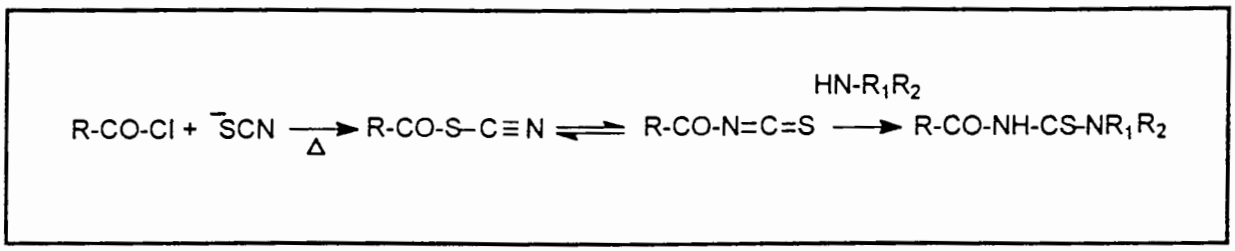

In 1963 Takamizawa *et al*[73], comprehensively investigated the reaction of potassium thiocyanate with an acyl chloride in acetone. They suggested that in acetone, the thiocyanate ion can exist as two tautomeric forms, **(1)** and **(2)** (Figure 1.7).

Figure 1.7: Isomers for the thiocyanate ion found in acetone

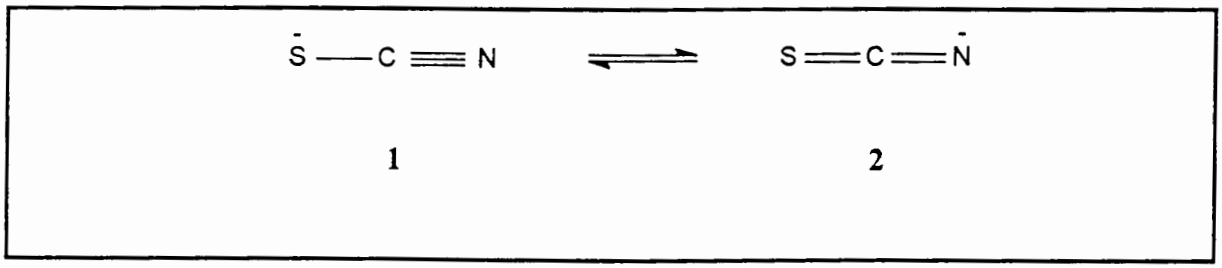

Electrophilic attack by the carbonyl carbon of the acyl chloride is thus possible at both the S and N sites giving rise to acylthiocyanate **(3)** or acylisothiocyanate **(4)** isomers (Figure 1.8).

Figure 1.8: Reaction of thiocyanate with an acyl chloride

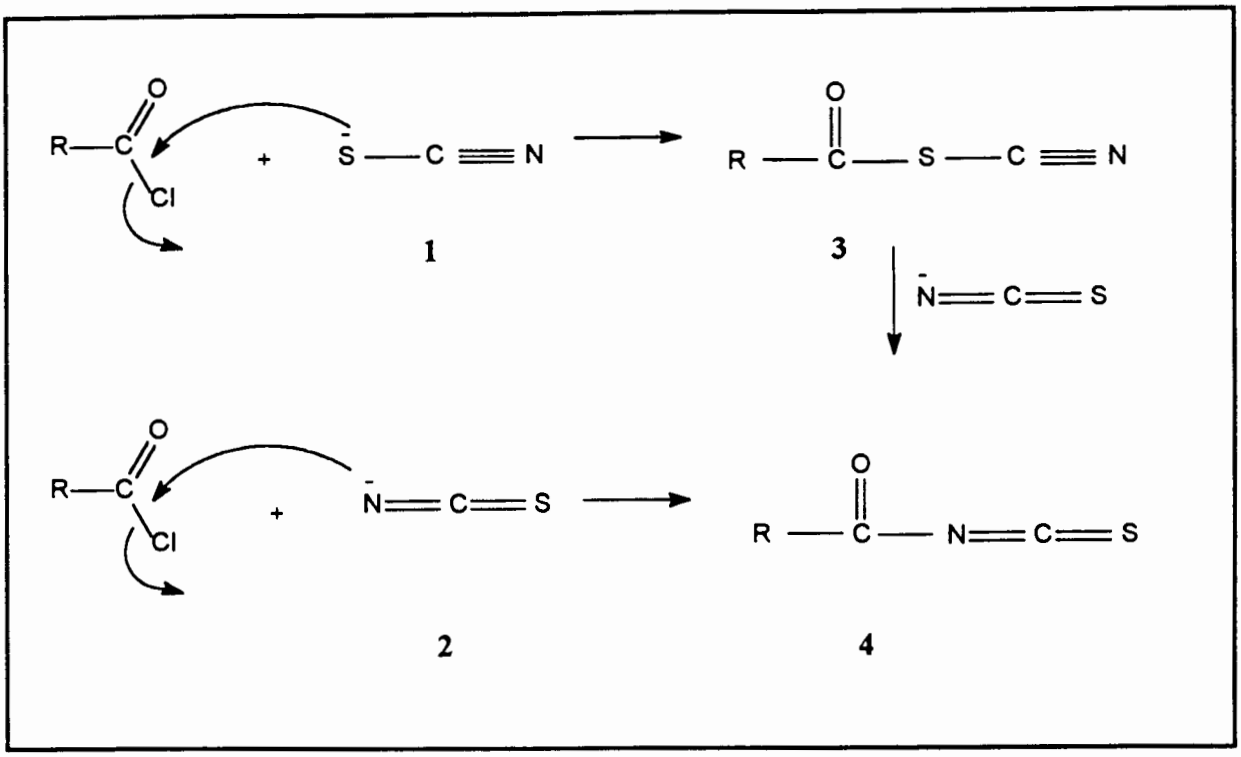

However, they found that the acylthiocyanate **(3)** is apparently less stable and reacts with more isothiocyanate to give the acylisothiocyanate **(4)** exclusively.

The reactions of acylisothiocyanates are many and complex[74]. Nucleophilic substitution of the amine at the carbonyl carbon **(A)** (Figure 1.9), may compete with the required addition to the thiocarbonyl carbon **(B)** (Figure 1.9), of the isothiocyanate moiety of the intermediate. The reaction of acylisothiocyanate with amines has been thoroughly investigated and found to occur smoothly in polar solvents and solvents of low polarity on heating[75]. The mechanism proposed suggests the reaction takes place via an intermediate donor-acceptor complex of the isothiocyanate with the amine (Figure 1.9). The rates of these reactions appear to depend on factors such as the polarity of the solvent, temperature, structure of the acylisothiocyanate intermediate as well as the basicity of the amine.

Figure 1.9: Reaction scheme of acyl isothiocyanates with amines

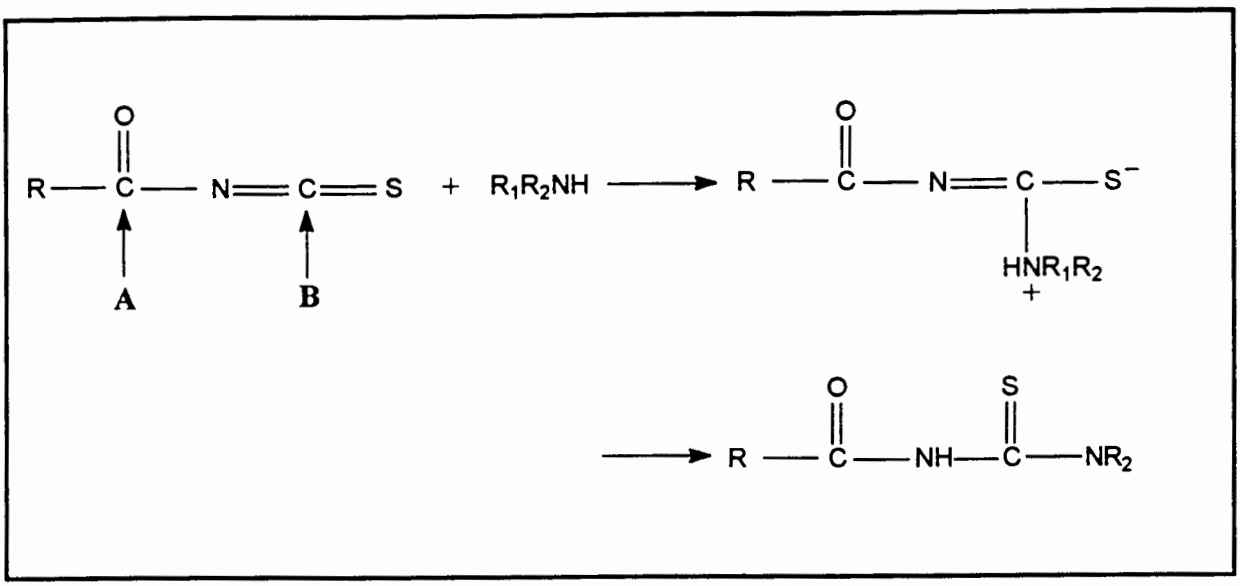

1.5.2 Properties of N-acylthioureas

Since their synthesis, the potential applications of *N*-acylthiourea ligands have been investigated. This has led to the exploitation of their bidentate S and O chelating potential. The biological activity of many *N*-substituted thioureas is well documented with a number of derivatives exhibiting antiviral, antibacterial and fungicidal activities[76].

Simple *N*-acylthioureas have also been found to undergo successive mono- and di-protonation in aqueous sulphuric acid on increasing acid strength[77]. Protonation was shown to occur firstly on the sulphur atom despite the fact that oxygen and sulphur are thought to have approximately equal basicities[77]. Subsequent to protonation, a slow hydrolysis to carboxylic acid and thiourea occurs[78]. In alkaline solutions *N*-acylthioureas readily ionise in solution before being rapidly hydrolysed to thiourea and carboxylic acid[79]. The mechanism of hydrolysis involves the attack by the hydroxide ion on the un-ionised molecule.

The complexation of *N*-acylthioureas with various transition metals has been investigated. Beyer *et al* examined a series of neutral Cu(II), Co(II), Ni(II) and Pd(II) complexes with *N,N*-dialkyl-*N'*-benzoylthioureas[80-82]. However, it is the remarkable selectivity of these ligands for the platinum group metals (PGM's) that has been of particular interest. They have been used to separate PGM's from interfering elements such as copper, iron and nickel, in the form of stable neutral chelates. They have also been used to separate the platinum group metals from each

other. Schuster *et al* have found *N,N*-dialkyl-*N'*-benzoylthioureas to be excellent reagents for pH-selective solvent extractions of PGM's, in which effective separations can be attained by varying the ligand structure and controlling the extraction conditions[83-85]. *N*-substituted-benzoylthioureas, in particular *N,N*-dihexyl-*N'*-benzoylthioureas, have been used to separate gold from PGM's and base metals[86].

The extraction ability of these ligands is significantly influenced by the substituents on the amine moiety of the ligand; with marked differences being observed between diaryl and dialkyl substituents[87]. Pyrene substituted ligands, which form highly fluorescent complexes with a number of heavy metal ions may offer analytical applications for trace analysis of these metals without the necessity of prior separation[88].

Koch *et al* have also investigated the mode of complexation of *N*-acylthiourea ligands with various metals. It has been found that co-ordination of mono-alkyl-substituted ligands to platinum(II), differed from their dialkyl analogues, with the former yielding a mixture of *cis* and *trans* complexes co-ordinated through the sulphur atom[89,90]. On the other hand, *N,N*-di(*n*-butyl)-*N'*-benzoylthiourea and its *para*-benzoyl-substituted analogues, preferentially form *cis* complexes of the type [Pt(L-*S,O*)$_2$] which may be reversibly protonated in solution with HX (X = Cl, Br and I) to yield mixtures of mono and di-protonated complexes[91]. It has also been possible to characterise *trans*-bis(*N,N*-di(*n*-butyl)-*N'*-naphthoylthioureato)platinum(II), as the first example of *trans* chelation of a *N,N*-dialkyl-*N'*-acylthiourea ligand[92]. More recent studies include a crystal structure analysis of *N,N*-di(2-hydroxyethyl)-*N'*-benzoylthiourea and a study of its co-ordination chemistry together with *N*-2-hydroxyethyl-*N'*-benzoylthiourea to Pt(II), Pd(II) and Ni(II)[93].

In summary, largely due to their synthetic versatility, *N*-acylthioureas are ideal donor ligands. Variations of either the acyl- or amine moiety of the ligand is easily possible, yielding a large class of compounds with many potential applications.

1.6 OBJECTIVES

Due to our interest in the design of potential metallointercalators, a series of mixed-ligand platinum(II) complexes was synthesised. The study of the self-association of these mixed-ligand complexes offers the opportunity to predict and explore how factors such as molecular shape and hydrogen-bonding will stabilise small molecules on DNA. By varying ligands and ligand substitutions of the complexes in a systematic fashion and comparing their association constants, we can determine the contributions of the different ligand functionality's and sizes to the association interaction.

Hence, the present aims include:

- synthesis and characterisation of a series of mixed-ligand [Pt(diimine)(*N,N*-di(*n*-butyl)-*N'*-acylthioureato)]$^+PF_6^-$ complexes

- to show these platinum(II) mixed-ligand complexes aggregate in solution with the aid of ^{1}H NMR concentration and temperature dependence studies

- to prove the series of [Pt(diimine)(*N,N*-di(*n*-butyl)-*N'*-acylthioureato)]$^+PF_6^-$ complexes aggregate to form only dimers in solution

- determination of dimerisation constants

- calculation of thermodynamic parameters enthalpy, entropy and Gibbs free energy of association from van't Hoff plots

- investigation of the effect of deuterium oxide on the aggregation of these complexes in acetonitrile-d_3

- proposal of a dimer structure in solution

CHAPTER 2

SYNTHESIS AND CHARACTERISATION

2 SYNTHESIS AND CHARACTERISATION

2.1 SYNTHESIS

A series of [Pt(diimine)(*N*,*N*-di(*n*-butyl)-*N'*-acylthioureato)]$^{+}PF_6^{-}$ complexes has been synthesised and is represented in Figure 2.2. A list of abbreviations is given in Table 2.1, and for the sake of convenience will be used throughout this work.

The preparation of these complexes involves a number of synthetic steps which include

- Pt(diimine)Cl_2 compounds
- *N*,*N*-di(*n*-butyl)-*N'*-acylthiourea ligands
- [Pt(diimine)(*N*,*N*-di(*n*-butyl)-*N'*-acylthioureato)]$^{+}PF_6^{-}$ complexes

A general outline of the synthetic method used is presented in Figure 2.1.

Figure 2.1: Schematic representation of the stepwise preparation of **(A)** Pt(diimine)Cl_2, **(B)** *N,N*-di(*n*-butyl)-*N'*-acylthiourea ligands and **(C)** [Pt(diimine)(*N,N*-di(*n*-butyl)-*N'*-acylthioureato)]$^+PF_6^-$ complexes

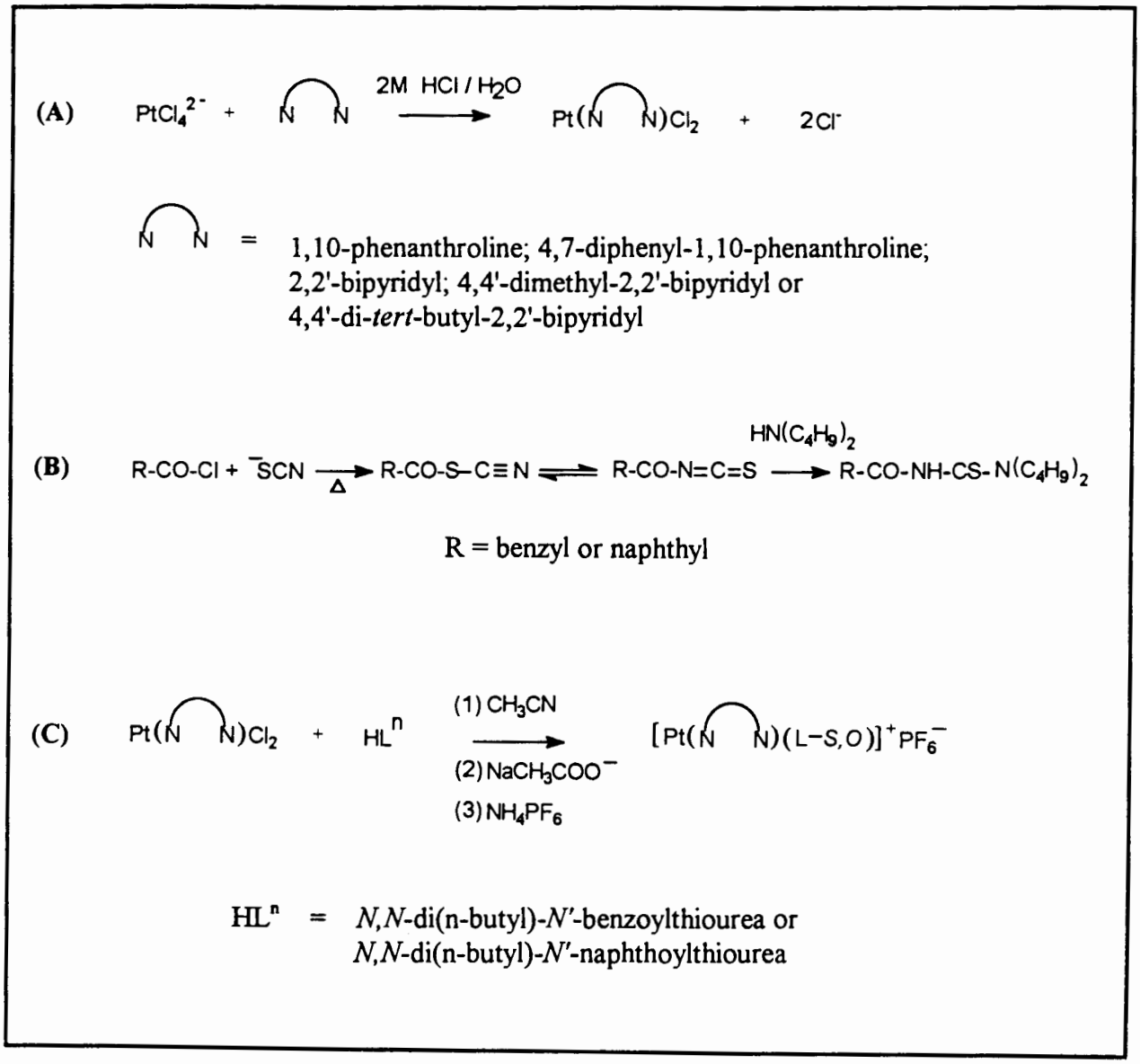

Full details of all synthetic procedures follow in the sections below. The detailed characterisation of these compounds is given in the experimental section (Chapter 5).

Figure 2.2: Schematic representation of [Pt(diimine)(*N,N*-di(*n*-butyl)-*N'*-acylthioureato)]$^{+}PF_6^{-}$ complexes synthesised

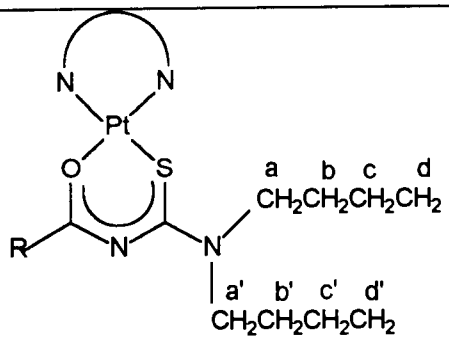

	R =  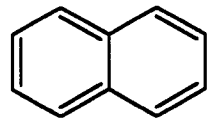
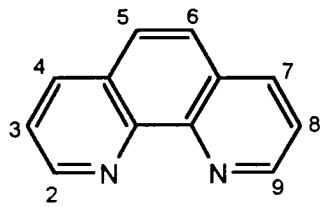	**1** **2**
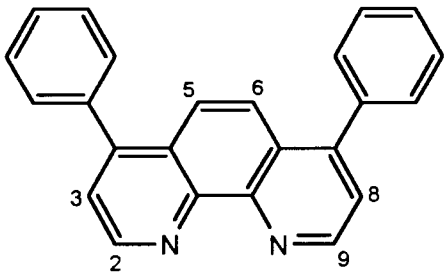	**3** **4**
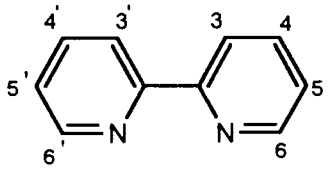	**5** **6**
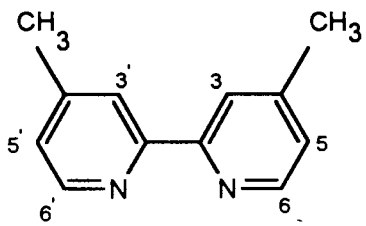	**7** **8**
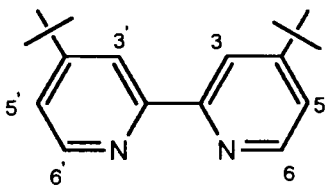	**9** **10**

Table 2.1: [Pt(diimine)(*N,N*-di(*n*-butyl)-*N'*-acylthioureato)]$^+PF_6^-$ complexes synthesised

NUMBER	COMPLEX	
1	[Pt(phen)DiBuBTu]$^+PF_6^-$	1,10-phenanthroline-*N,N*-di(*n*-butyl)-*N'*-benzoylthioureato(*S,O*)platinum(II) hexafluorophosphate
2	[Pt(phen)DiBuNTu]$^+PF_6^-$	1,10-phenanthroline-*N,N*-di(*n*-butyl)-*N'*-naphthoylthioureato(*S,O*)platinum(II) hexafluorophosphate
3	[Pt(4,7-diphenylphen)DiBuBTu]$^+PF_6^-$	4,7-diphenyl-1,10-phenanthroline-*N,N*-di(*n*-butyl)-*N'*-benzoylthioureato(*S,O*)platinum(II) hexafluorophosphate
4	[Pt(4,7-diphenylphen)DiBuNTu]$^+PF_6^-$	4,7-diphenyl-1,10-phenanthroline-*N,N*-di(*n*-butyl)-*N'*-naphthoylthioureato(*S,O*)platinum(II) hexafluorophosphate
5	[Pt(bipy)DiBuBTu]$^+PF_6^-$	2,2'-bipyridyl-*N,N*-di(*n*-butyl)-*N'*-benzoylthioureato(*S,O*)-platinum(II) hexafluorophosphate
6	[Pt(bipy)DiBuNTu]$^+PF_6^-$	2,2'-bipyridyl-*N,N*-di(*n*-butyl)-*N'*-naphthoylthioureato(*S,O*)-platinum(II) hexafluorophosphate
7	[Pt(4,4'-dimethylbipy)DiBuBTu]$^+PF_6^-$	4,4'-dimethyl-2,2'-bipyridyl-*N,N*-di(*n*-butyl)-*N'*-benzoylthioureato(*S,O*)platinum(II) hexafluorophosphate
8	[Pt(4,4'-dimethylbipy)DiBuNTu]$^+PF_6^-$	4,4'-dimethyl-2,2'-bipyridyl-*N,N*-di(*n*-butyl)-*N'*-naphthoylthioureato(*S,O*)platinum(II) hexafluorophosphate
9	[Pt(4,4'-ditbutbipy)DiBuBTu]$^+PF_6^-$	4,4'-di-*tert*-butyl-2,2'-bipyridyl-*N,N*-di(*n*-butyl)-*N'*-benzoylthioureato(*S,O*)platinum(II) hexafluorophosphate
10	[Pt(4,4'-ditbutbipy)DiBuNTu]$^+PF_6^-$	4,4'-di-*tert*-butyl-2,2'-bipyridyl-*N,N*-di(*n*-butyl)-*N'*-naphthoylthioureato(*S,O*)platinum(II) hexafluorophosphate

2.1.1. Synthesis of Pt(diimine)Cl_2

The diimines used in the synthesis of Pt(diimine)Cl_2 include: 1,10-phenanthroline; 4,7-diphenyl-1,10-phenanthroline; 2,2'-bipyridyl; 4,4'-dimethyl-2,2'-bipyridyl and 4,4'-di-*tert*-butyl-

2,2'-bipyridyl (Figure 2.3). The diimines are commercially available except 4,4'-di-*tert*-butyl-2,2'-bipyridyl which was synthesised according to the method of Hadda and Le Bozec[94].

Figure 2.3: Schematic reaction scheme for the synthesis of Pt(diimine)Cl_2

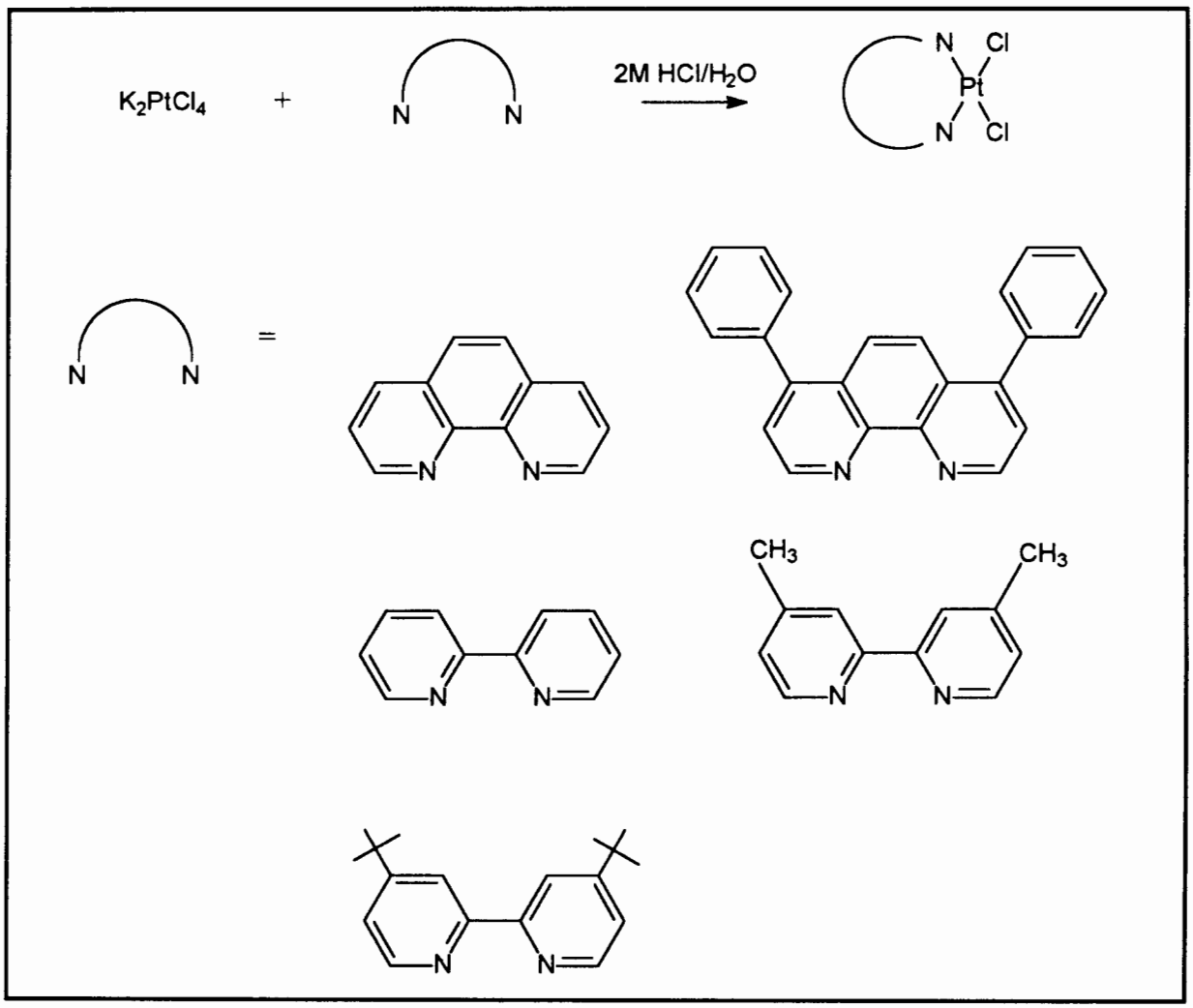

Pt(2,2'-bipyridyl)Cl_2 was synthesised according to the method of Morgan and Burstall[95]. This method was extended to include all the other diimines mentioned above. A method for preparing Pt(1,10-phenanthroline)Cl_2 has also been reported by Palocsay and Rund[96]. The resulting product is a yellow powder with some red crystals present. The existence of a red and yellow form of Pt(bipy)Cl_2 was previously reported by Morgan and Burstall[95]. This was later shown to be different crystalline morphs of the same molecule[97,98]. The red form is perfectly planar, lying on a mirror plane in the crystal[97], and has a linear-chain structure with the molecules stacked in a head to tail fashion with a Pt-Pt distance of 3.45 Å. This favoured bonding is accomplished by σ donation of the nitrogen lone pair electrons, with metal-to-ligand π bonding as a stabilising factor.

In general, many platinum(II) complexes have been found to crystallise in linear-chain stacks[12,99] and can give rise to perturbed absorption if the Pt-Pt spacing is sufficiently short. An attempt was made to determine the crystal structure of the yellow isomer of $Pt(bipy)Cl_2$[100]. Due to the inability of the yellow powder to form suitable crystals for an x-ray crystallographic structure determination, only a partial determination could be completed. Crystal data collected, suggested it to be isomorphous with $Pd(bipy)Cl_2$ as illustrated in Figure 2.4**(B)**. A structure is predicted in which the rings of the bipy moieties are offset by almost 90° to each other, thus allowing for overlap of only one ring from each molecule. The molecules are related by glide planes and the stacking is found to be more efficient in comparison to the 'red' form (Figure 2.4**(A)**). These observations could assist in predicting an 'aggregate' structure of our platinum(II) mixed-ligand complexes.

Figure 2.4: Schematic representation of the dimer structures of **(A)** red form of $Pt(bipy)Cl_2$ and **(B)** $Pd(bipy)Cl_2$ which is isomorphous to $Pt(bipy)Cl_2$

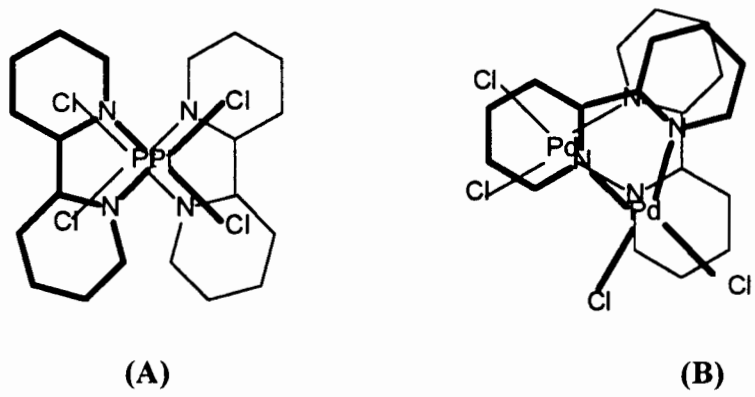

(A) **(B)**

2.1.2 Synthesis of N,N-di(n-butyl)-N'-acylthiourea ligands

N,N-Di(*n*-butyl)-*N'*-benzoylthiourea and *N,N*-di(*n*-butyl)-*N'*-naphthoylthiourea were synthesised according to the method of Douglass and Dains[72] to give white crystalline products. The general method of synthesis is summarised in Figure 2.5.

Figure 2.5: Schematic reaction scheme for the synthesis of *N,N*-di(*n*-butyl)-*N'*-acylthiourea ligands

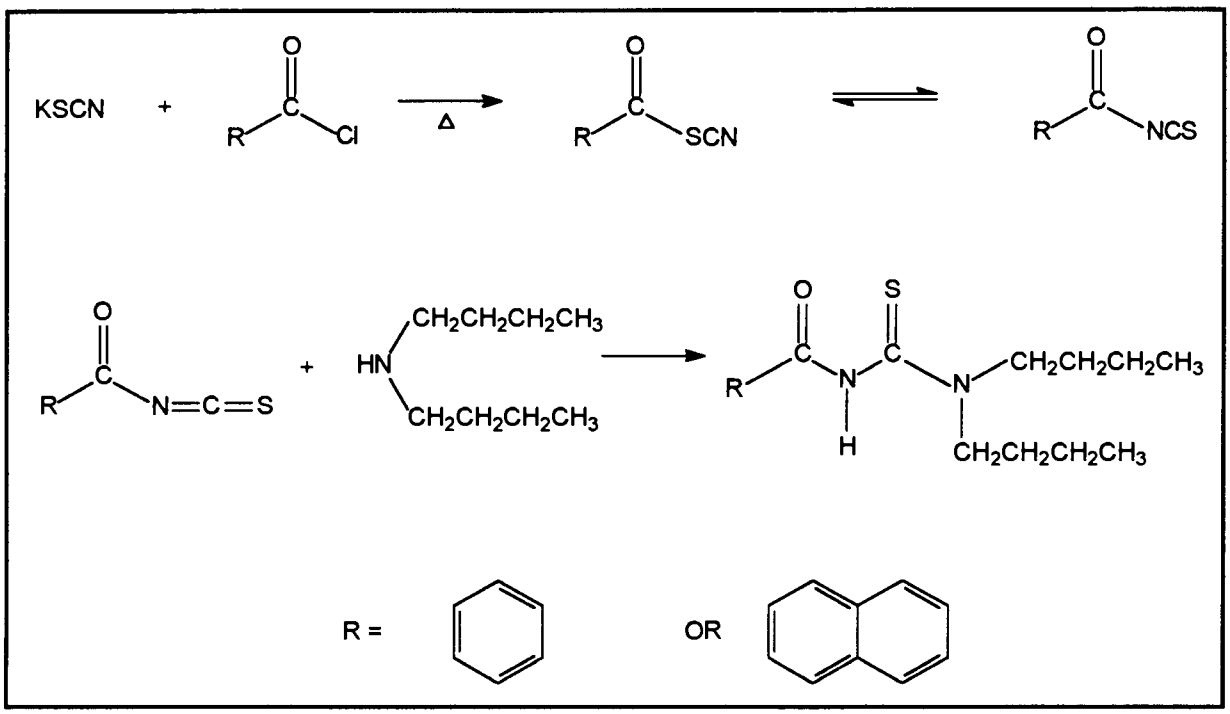

Our interest in *N*-acylthiourea compounds is due to their relative ease of synthesis and synthetic versatility. Since their discovery, interest in these deceptively simple molecules has grown. From early use as biological reagents[76,101] and in platinum group metal extractions[84], their applications have expanded to include liquid crystals[102] and potential polymer supports[103].

2.1.3 Synthesis of [Pt(diimine)(N,N-di(n-butyl)-N'-acylthioureato)]$^+PF_6^-$ complexes

The platinum complexes were all synthesised according to the experimental method outlined in Chapter 5 to form yellow powders. A general method is outlined in Figure 2.6.

Figure 2.6: Schematic reaction scheme for the synthesis of [Pt(diimine)(*N,N*-di(*n*-butyl)-*N'*-acylthioureato)]$^{+}PF_6^{-}$ complexes

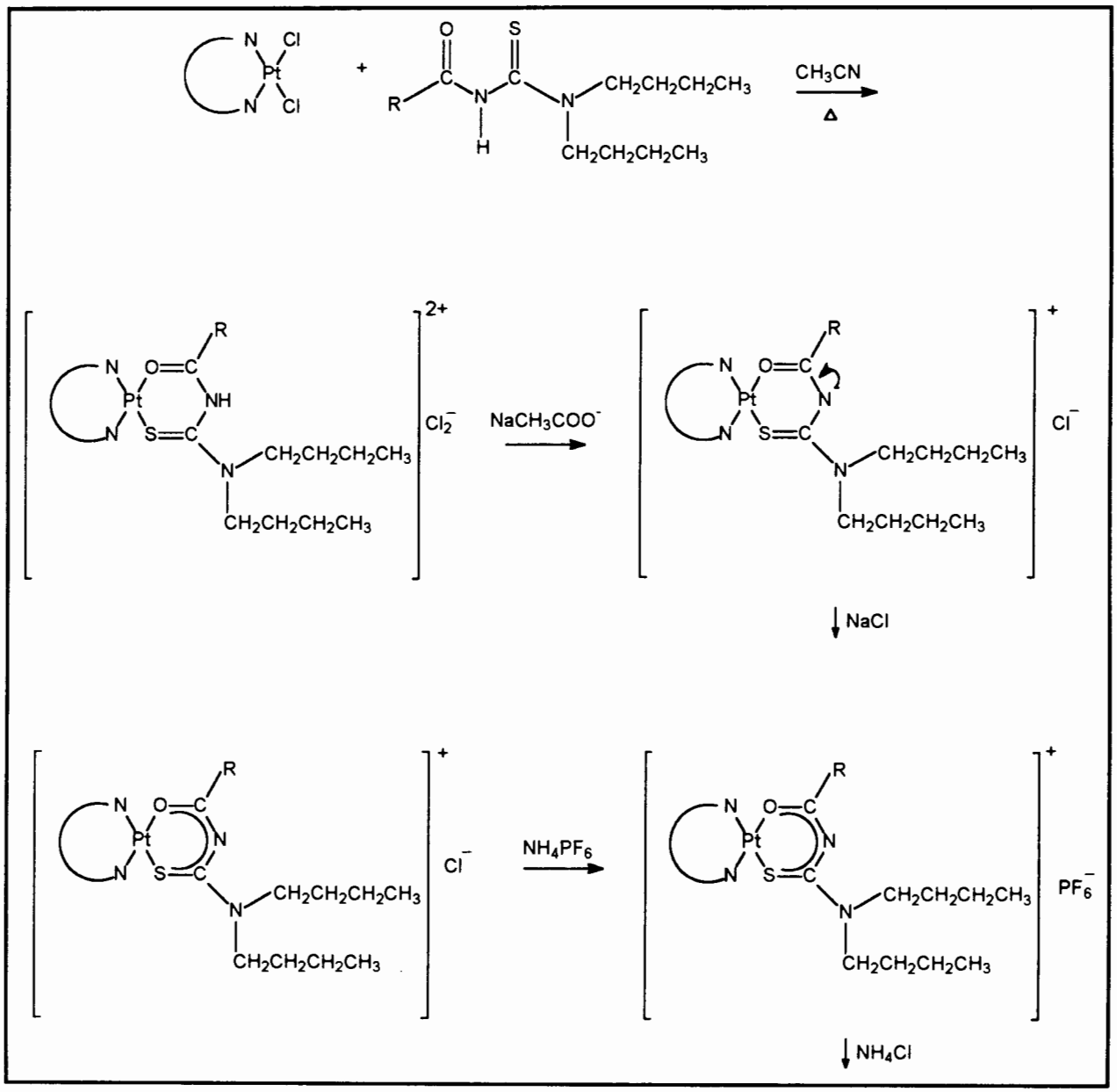

Several attempts were made to grow crystals but this was not achieved. As observed previously[100], attempts at growing suitable Pt(bipy)Cl_2 crystals (yellow form) proved to be unsuccessful. It may be possible that the nature of intermolecular stacking interactions result in microcrystalline powder formation, so that large crystals do not readily form.

In general, stable oxidation states for platinum ions are II and IV, but complexes in which platinum has an oxidation state of I, III or O are also found[12]. Usually, platinum(II) complexes

are square planar and form stable four-co-ordinate complexes with polarisable ligands; platinum(II) being classified as a 'soft' (class b) metal[104].

N-acylthiourea ligands incorporate a 'soft' sulphur donor and a 'hard' oxygen donor atom. The chelate effect[105] in which complexes with bidentate ligands exhibit a greater stability in comparison to their non-chelated analogues is of great importance in this co-ordination chemistry. Therefore, complexes of 'hard' oxygen donors and 'soft' metals, can be stabilised by incorporation into bidentate ligands with other 'soft' donor atoms such as nitrogen or sulphur. Hence, *N*-acylthioureas are found to bind strongly and fairly selectively to the platinum group metals.

Diimine ligands (for example 2,2'-bipyridyl and 1,10-phenanthroline) with their relatively 'soft' nitrogen donor atoms form stable complexes due to their ability to act as σ-bases as well as π-acids[105]. The σ-bonds appear to be stabilised by the ability of the ligand to form π bonds with full metal d orbitals and their vacant π* orbitals.

The reaction of Pt(diimine)Cl_2 with *N,N*-di(*n*-butyl)-*N'*-acylthiourea is expected to proceed by co-ordination of the sulphur atom to platinum, with the subsequent loss of a chloride ion. This is followed by co-ordination to oxygen due to the chelate effect. Addition of the mild base, sodium acetate, results in deprotonation of the amide nitrogen. This results in delocalisation of the negative charge, and renders the carboxy oxygen atom more nucleophilic toward the platinum(II) centre. Finally, ammonium hexafluorophosphate is added to convert the product to a hexafluorophosphate salt to aid in the isolation of the complex.

Pt(phen)Cl_2 and Pt(4,7-diphenylphen)Cl_2 were only sparingly soluble in acetonitrile, so reactions were left overnight in some instances to ensure the complete displacement of the two chloride ions from the platinum(II) co-ordination sphere by the *N,N*-di(*n*-butyl)-*N'*-acylthiourea ligand. By comparison, Pt(bipy)Cl_2, Pt(4,4'-dimethylbipy)Cl_2 and Pt(4,4'-dit-butbipy)Cl_2 were readily soluble in acetonitrile on heating. All of the mixed-ligand platinum(II) complexes were found to be reasonably soluble in acetonitrile, however substantial differences are observed in the degree of solubility, $[Pt(bipy)DiBuBTu]^+PF_6^-$ being most soluble and $[Pt(phen)DiBuNTu]^+PF_6^-$ least soluble.

2.2 CHARACTERISATION

2.2.1 Synthesis of Diimines

4,4'-di-*tert*-butyl-2,2'-bipyridyl was synthesised according to the method of Hadda and Le Bozec[94] from 4-*tert*-butyl-pyridine. This method is an adaptation of the synthesis of 4,4',4"-trialkyl-2,2':6',2"-terpyridyls by Rosevear and Sasse[106].

Palladium (10% on charcoal) was degassed in a schlenk flask overnight. 4-*Tert*-butyl-pyridine was heated under reflux in the presence of the palladium catalyst. The mixture was left to stir under an inert atmosphere (nitrogen) for six days. After addition of tetrahydrofuran, the catalyst was removed by filtration. Neutral alumina was then added to the solution followed by complete evaporation of the solvent. A mixture of 4,4',4"-tri-*tert*-butyl-2,2'-bipyridyl and 4,4'-di-*tert*-butyl-2,2'-bipyridyl was obtained. However, they were readily separated by sublimation of the more volatile 4,4'-di-*tert*-butyl-2,2'-bipyridyl. Additional purification of the product was carried out by recrystallisation from ethanol/water mixtures.

The compound was characterised by mass spectrometry, ^{1}H NMR, ^{13}C NMR and C, H and N elemental analysis. The ^{1}H NMR spectrum compares favourably with that reported previously[94]. Details of the procedure and analytical data of 4,4'-di-*tert*-butyl-2,2'-bipyridyl are described in Chapter 5.

The five Pt(diimine)Cl_2 compounds were synthesised in good yields (75-100 %) and characterised by C, H and N elemental analysis. The melting points of these compounds are usually very high (greater than 335 °C) and therefore cannot be used for characterisation purposes.

2.2.2 Synthesis of N,N-di(n-butyl)-N'-acylthiourea ligands

The two *N,N*-di(*n*-butyl)-*N'*-acylthiourea compounds were successfully recrystallised from ethanol and their structures confirmed by ^{1}H and ^{13}C NMR spectroscopy ($CDCl_3$). C, H, N

and S elemental analysis was found to be consistent with calculated values, and melting points corresponded to literature values.

NMR Spectroscopy

The assignment of the ^{1}H and ^{13}C NMR spectra are straightforward, with the ^{13}C NMR shifts being comparable to those previously reported by Koch *et al* for dialkyl-*N'*-benzoyl-thiourea[107,92]. The thiocarbonyl peak at 179.72 ppm and the carbonyl peak at 163.57 ppm for *N,N*-di(*n*-butyl)-*N'*-benzoylthiourea, are characteristic of the ^{13}C NMR spectrum of *N,N*-di(*n*-butyl)-*N'*-acylthioureas.

The ^{1}H NMR spectrum of a typical *N,N*-di(*n*-butyl)-*N'*-acylthiourea ligand is characterised by a single N-H peak in the region 8-9 ppm. The $H_{2''}$,$H_{6''}$ protons of *N,N*-di(*n*-butyl)-*N'*-benzoylthiourea were observed as a doublet at 7.84 ppm. The $H_{4''}$ and $H_{3''}$,$H_{5''}$ protons were observed as two sets of triplets at 7.58 and 7.47 ppm respectively. The $H_{8''}$ proton of *N,N*-di(*n*-butyl)-*N'*-naphthoylthiourea occurs furthest downfield as a doublet at 8.47 ppm. The $H_{2''}$, $H_{4''}$ and $H_{5''}$ protons were all observed as doublets at 8.00, 7.91 and 7.77 ppm respectively. The $H_{3''}$, $H_{6''}$ and $H_{7''}$ protons were observed as a broad multiplet in the range 7.46 - 7.66 ppm.

What is also of interest is the observation of two sets of resonances for the protons on the dialkyl chain. This is due to restricted rotation around the C-N bond[108] between the thiocarbonyl group and nitrogen atom, which has significant double bond character as shown schematically in the resonance structure **(B)** of Figure 2.7. Hence, in the lowest energy configuration, protons H_a and $H_{a'}$ are in different chemical environments and thus have different chemical shifts. In the absence of restricted rotation the chemical shifts would be approximately the same due to free internal rotation about the C-N bond. A high C-N energy barrier to rotation at room temperature, results in a low exchange frequency. Hence, the residence time of the protons in the two non-equivalent environments is relatively long on the NMR time scale. A similar situation pertains to resonances of the $H_{b'}$, H_b, $H_{c'}$, H_c and $H_{d'}$, H_d protons. This is also reflected in the ^{13}C NMR spectra, where C_a and $C_{a'}$ signals at 53.11 and 53.28 ppm are observed for *N,N*-di(*n*-butyl)-*N'*-benzoylthiourea.

Figure 2.7: Resonance structures of a thio-amidic C-N bond

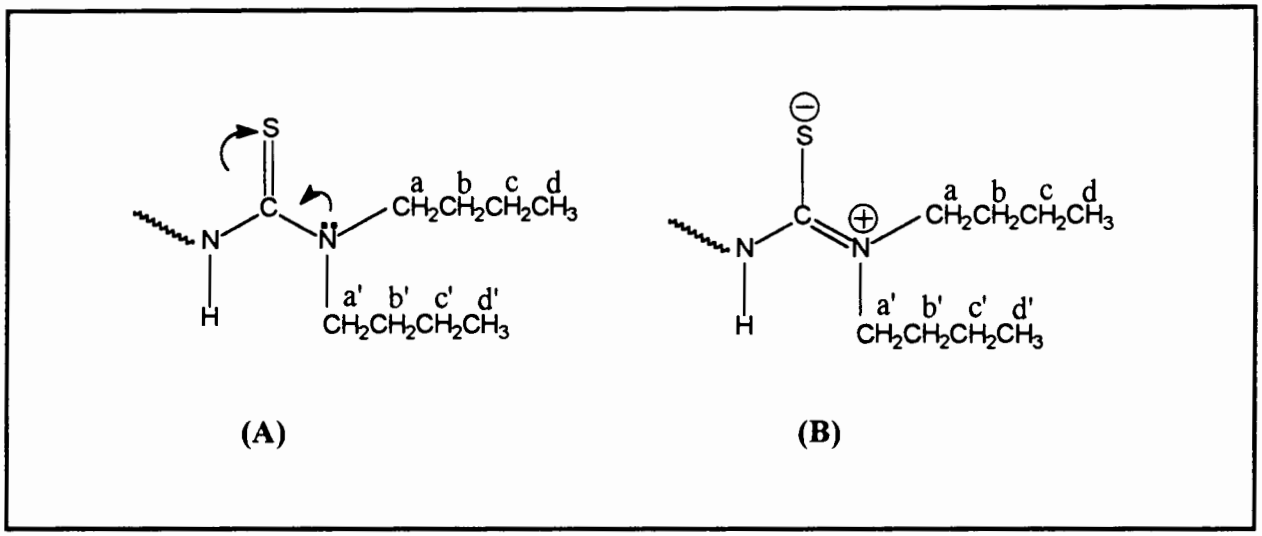

Due to restricted rotation, $^4J(^{195}Pt\text{-}^{13}C)$ coupling satellites have previously been observed for $C_{a'}$ of the butyl residue of *cis*-bis(*N,N*-di(*n*-butyl)-*N'*-benzoylthiourea)platinum(II)[107]. This was not observed for C_a. Since $C_{a'}$ is placed in a 'W' configuration with respect to the ^{195}Pt atom, it allows for long-range coupling to be transmitted through the electronic framework of the molecule. This gives additional support to the assignments of $H_{a'}$ and H_a.

2.2.3 Synthesis of [Pt(diimine)(N,N-di(n-butyl)-N'-acylthioureato)]$^+PF_6^-$ complexes

Ten different [Pt(diimine)(*N,N*-di(*n*-butyl)-*N'*-acylthioureato)]$^+PF_6^-$ complexes were synthesised by systematically changing the diimine moiety of the complex (Table 2.2). They were satisfactorily characterised by C, H, N and S elemental analysis and ^1H NMR spectroscopy (acetonitrile-d_3). The C, H, N and S elemental analysis and characterisation data for these complexes are presented in Table 2.2. This data shows that these complexes could be prepared with satisfactory purity. Additional purity could be achieved by repeated recrystallisations from acetonitrile and diethyl ether mixtures.

In general, the melting points of complexes with *N,N*-di(*n*-butyl)-*N'*-naphthoylthiourea ligands were found to be lower than those with *N,N*-di(*n*-butyl)-*N'*-benzoylthiourea ligands. The higher melting points of the latter complexes could suggest optimal packing of the benzyl complexes in the solid state.

Table 2.2: [Pt(diimine)(*N,N*-di(*n*-butyl)-*N'*-acylthioureato)]$^+PF_6^-$ complex characterisation data

	COMPLEX	YIELD %	MPT °C	CALCULATED				OBSERVED			
				%C	%H	%N	%S	%C	%H	%N	%S
1	[Pt(phen)DiBuBTu]$^+PF_6^-$	80.3	270-272	41.4	3.9	6.9	-	41.1	3.8	6.9	-
2	[Pt(phen)DiBuNTu]$^+PF_6^-$	76.3	182-185	44.6	3.9	6.5	3.7	43.3	3.7	6.4	3.5
3	[Pt(4,7-diphenylphen)DiBuBTu]$^+PF_6^-$	50.3	280-283	49.8	4.1	5.8	-	48.5	3.8	6.0	-
4	[Pt(4,7-diphenylphen)DiBuNTu]$^+PF_6^-$	34.0	236-238	52.1	4.1	5.5	-	51.2	3.9	5.7	-
5	[Pt(bipy)DiBuBTu]$^+PF_6^-$	78.6	250-253	39.6	4.0	7.1	4.1	39.1	3.9	6.8	3.7
6	[Pt(bipy)DiBuNTu]$^+PF_6^-$	73.8	132-135	43.0	4.0	6.7	3.8	42.3	3.9	6.7	3.8
7	[Pt(4,4'-dimethylbipy)DiBuBTu]$^+PF_6^-$	83.4	272-275	41.2	4.3	6.9	3.9	40.3	4.3	6.5	3.7
8	[Pt(4,4'-dimethylbipy)DiBuNTu]$^+PF_6^-$	76.7	206-209	44.4	4.3	6.5	3.7	44.9	4.2	6.4	3.5
9	[Pt(4,4'-ditbutbipy)DiBuBTu]$^+PF_6^-$	71.6	263-265	45.4	5.3	6.2	3.6	45.4	5.3	6.1	3.4
10	[Pt(4,4'-ditbutbipy)DiBuNTu]$^+PF_6^-$	84.1	212-215	48.0	5.2	5.9	3.4	47.2	5.2	5.9	3.2

NMR Spectroscopy

The chemical shift assignments were established with the aid of 2D-COSY NMR experiments. The ^1H NMR spectra of these complexes are characterised by the loss of the N-H resonance, which is convincing evidence that the *N,N*-di(*n*-butyl)-*N'*-acylthiourea ligand has co-ordinated to platinum in a bidentate fashion.

The structures of two of the platinum(II) complexes synthesised, namely [Pt(phen)DiBuBTu]$^+PF_6^-$ and [Pt(4,4'-ditbutbipy)DiBuNTu]$^+PF_6^-$, with the numbering of all the proton positions used in the NMR study, are presented in Figure 2.8.

Figure 2.8: The numbering scheme of **(A)** [Pt(phen)DiBuBTu]$^+PF_6^-$ and **(B)** [Pt(4,4'-ditbutbipy)-DiBuNTu]$^+PF_6^-$

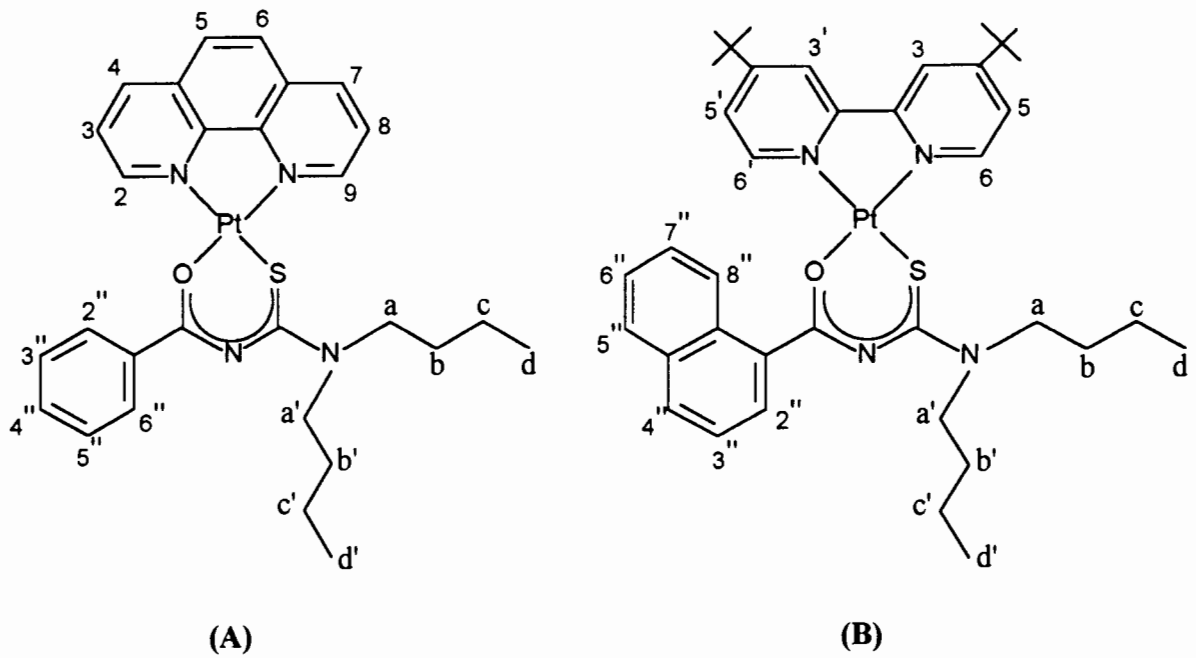

The ^{1}H NMR spectrum of the aromatic region of [Pt(phen)DiBuBTu]$^+PF_6^-$ is illustrated in Figure 2.9, showing the assignments determined for the phenanthroline ligand and the benzyl moiety of *N,N*-di(*n*-butyl)-*N'*-benzoylthiourea. Since H_2 and H_9 in the above complex cannot be unambiguously distinguished, the assignments are based on the following reasoning. The proton opposite the sulphur atom is numbered H_2 and therefore the proton opposite the oxygen atom will be H_9. Since the Pt-S bond is likely to be "stronger" than the Pt-O bond, the shift of the H_2 resonance is probably greater than the corresponding H_9 chemical shift. Hence, H_2 will be more deshielded. On this basis, we will always refer to the proton opposite the sulphur atom as H_2.

The ^{1}H NMR spectrum of the aromatic region of [Pt(4,4'-ditbutbipy)DiBuNTu]$^+PF_6^-$ is represented in Figure 2.10. The assignments of the 4,4'-di-*tert*-butyl-2,2'-bipyridyl ligand protons and the protons of the naphthyl moiety of the *N,N*-di(*n*-butyl)-*N'*-naphthoylthiourea ligand are shown. The same reasoning applied to distinguish between H_2 and H_9 of [Pt(phen)-DiBuBTu]$^+PF_6^-$, was used to assign $H_{6'}$ and H_6 of [Pt(4,4'-ditbutbipy)DiBuNTu]$^+PF_6^-$. The proton opposite the Pt-S bond is therefore assigned to $H_{6'}$.

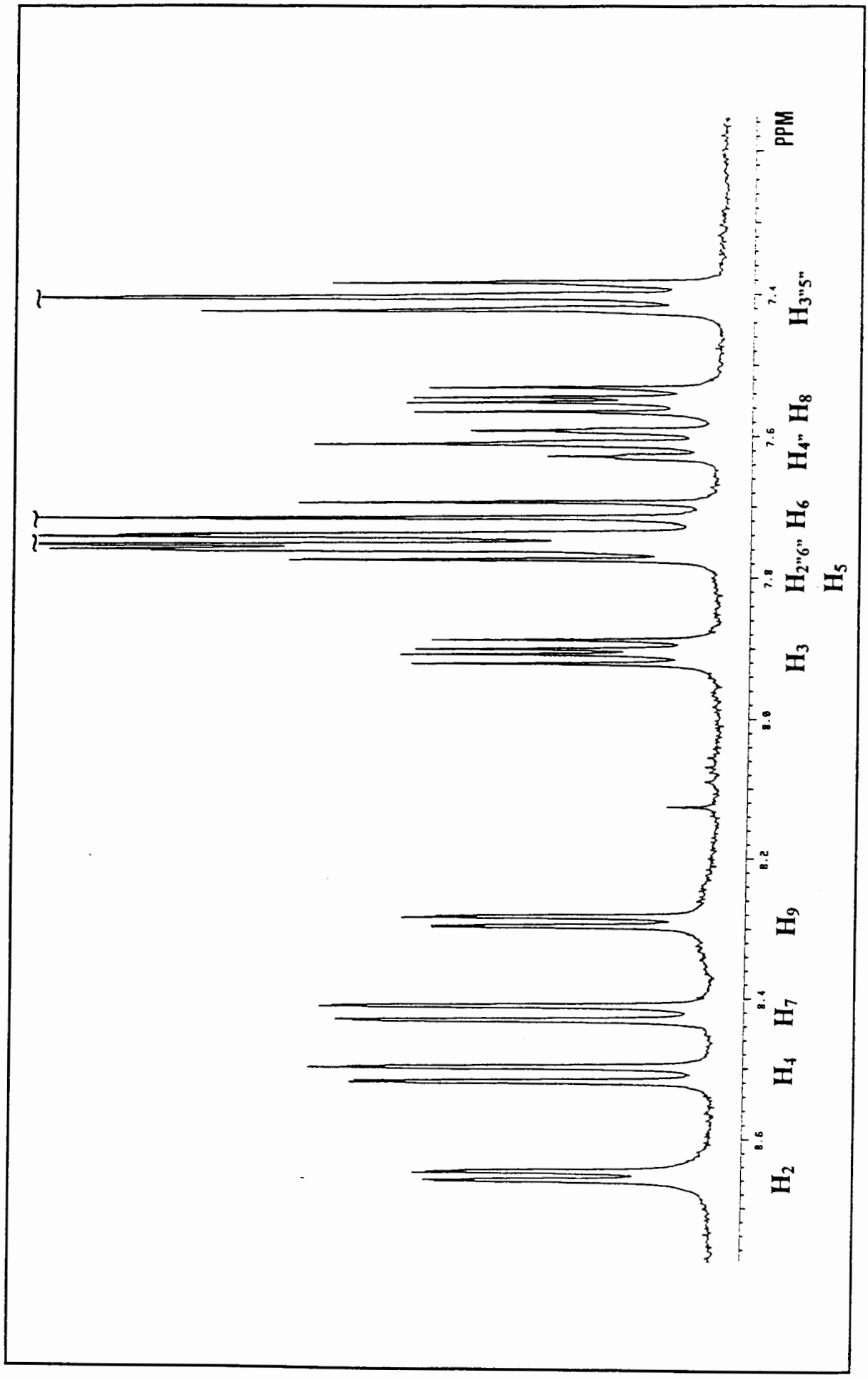

Figure 2.9: ^{1}H NMR spectrum of the aromatic region of [Pt(phen)DiBuBTu]$^{+}PF_6^{-}$ in acetonitrile-d_3 (at 25 °C)

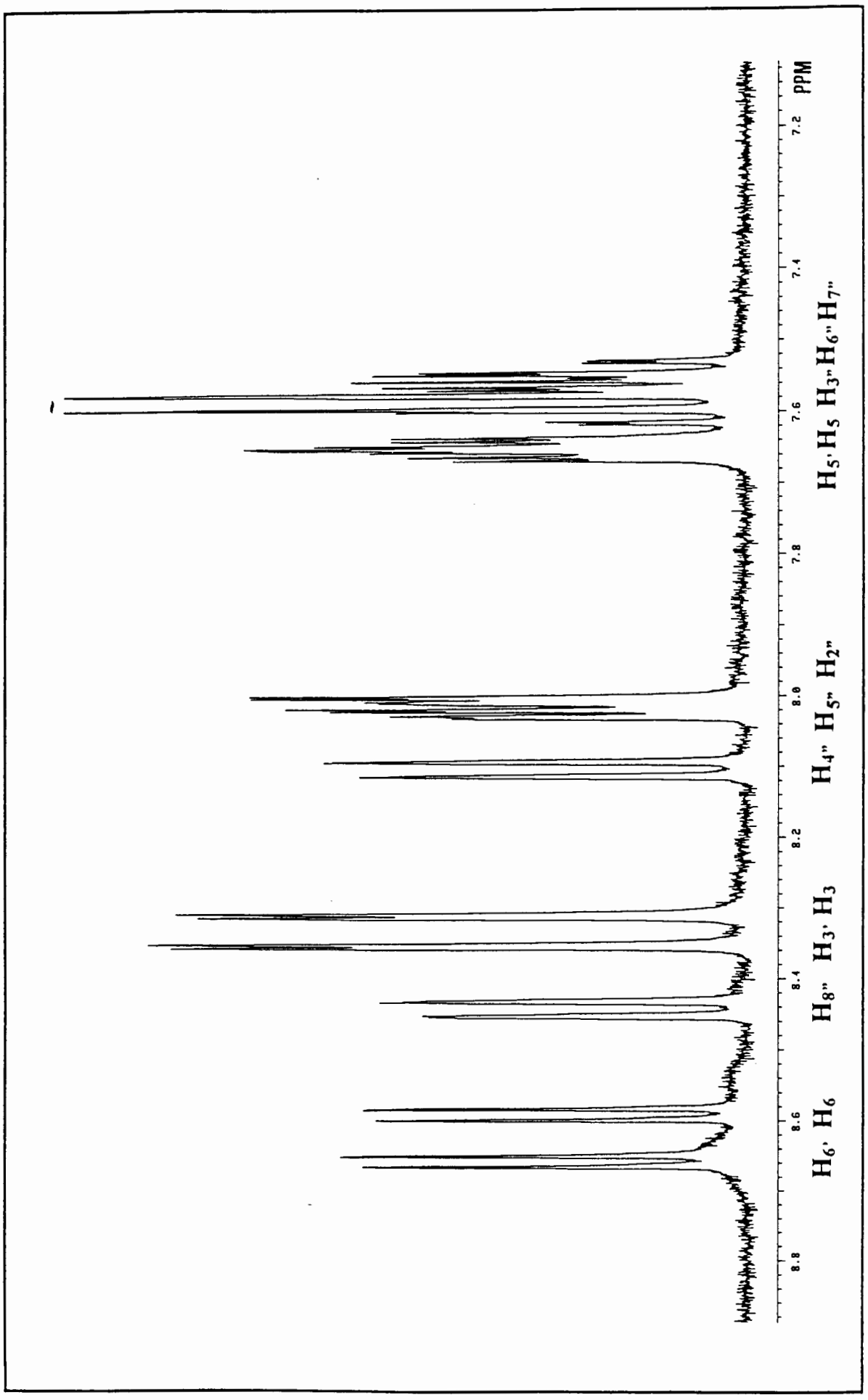

Figure 2.10: ^{1}H NMR spectrum of the aromatic region of [Pt(4,4'-ditbutbipy)DiBuNTu]$^+PF_6^-$ in acetonitrile-d_3 (at 25 °C)

In the case of [Pt(phen)DiBuBTu]$^+PF_6^-$, [Pt(phen)DiBuNTu]$^+PF_6^-$, [Pt(4,7-diphenylphen)-DiBuBTu]$^+PF_6^-$ and [Pt(4,7-diphenylphen)DiBuNTu]$^+PF_6^-$ no distinction can be made between the H_2 and H_9 protons. However, H_2 is assigned as occurring furthest downfield. Similarly, for the bipyridyl complexes, no distinction can be made between $H_{6'}$ and H_6, and $H_{6'}$ is assigned as occurring furthest downfield. The chemical shift data and assignments from the concentration dependence studies for the protons of [Pt(phen)DiBuBTu]$^+PF_6^-$, [Pt(phen)DiBuNTu]$^+PF_6^-$, [Pt(4,7-diphenylphen)DiBuBTu]$^+PF_6^-$, [Pt(4,7-diphenylphen)DiBuNTu]$^+PF_6^-$, [Pt(4,4'-dimethyl-bipy)DiBuBTu]$^+PF_6^-$, [Pt(4,4'-dimethylbipy)DiBuNTu]$^+PF_6^-$, [Pt(4,4'-ditbutbipy)DiBuBTu]$^+PF_6^-$, [Pt(4,4'-ditbutbipy)DiBuNTu]$^+PF_6$ and [Pt(bipy)DiBuBTu]$^+PF_6$ are represented in Tables 7.2.1 - 7.2.9 (Chapter 7 - Appendix 2).

The non-equivalence of the ^1H NMR resonances of the butyl fragments in the *N*-acylthiourea ligands is also observed in the ^1H NMR spectra of the platinum complexes (Figure 2.11). This shows that a degree of double bond character of these C-N linkages persists in the complexes, as was previously found by Koch *et al* in their studies on platinum complexes of the type *cis*-[Pt(L-*S,O*)$_2$][91] (where L-*S,O* represents a deprotonated chelating ligand co-ordinated to platinum through both the S- and O-atom).

Figure 2.11: ^{1}H NMR spectrum of [Pt(phen)DiBuBTu]$^{+}PF_6^{-}$ in the region 1-4 ppm illustrating the separate resonances for the butyl fragments in the *N*-acylthiourea ligand

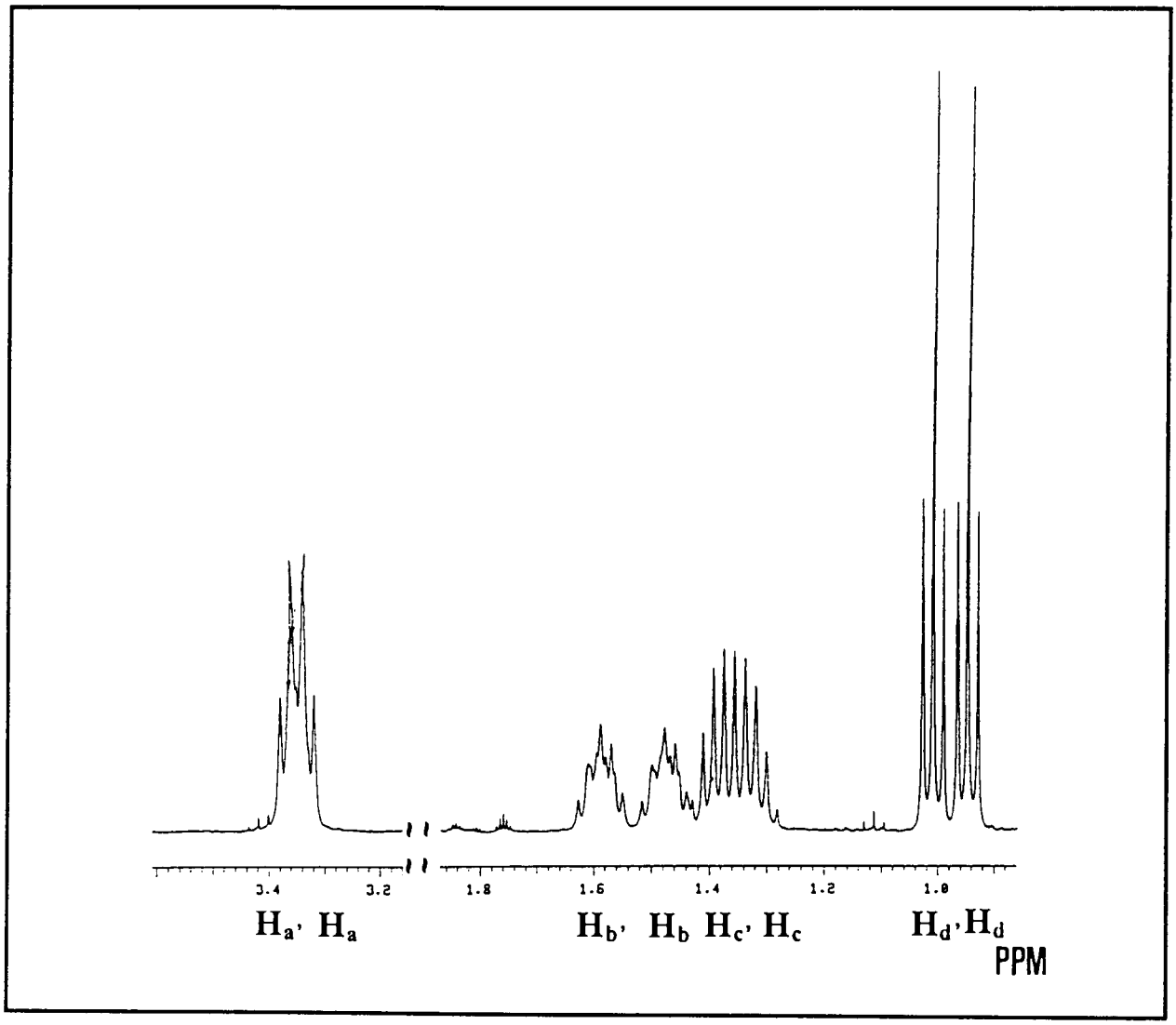

CHAPTER 3

RESULTS AND DISCUSSION

3 RESULTS AND DISCUSSION

3.1 INTRODUCTION AND METHODOLOGY

^{1}H NMR spectroscopy has previously been used to study and quantify self-aggregation of various molecules in solution[109-115]. From these studies, the nature of self-association can be elucidated and predictions made about the structure of the 'aggregate' in solution. NMR spectroscopic methods have a number of advantages over other methods such as UV-visible or fluorescence techniques. NMR data reveals more detailed structural information so enabling the use of a number of chemical shift variables to be used in the calculation of aggregation constants. Moreover, chemical shifts are not affected by the presence of minor impurities[116].

Previous studies on self-aggregation in aqueous solutions have determined that some metal complexes having aromatic ligands tend to associate significantly to form large aggregates (for example 2-hydroxyethanethiolato(2,2',2"-terpyridine)platinum(II) complexes[23]). The extent of such interactions is dependent on the molecule's hydrophobicity, and can be decreased by the addition of organic solvents[117]. It is generally observed that the addition of organic solvents to aqueous solutions reduces stacking and hydrophobic interactions[117,118]. In this work on platinum(II) complexes, self-aggregation was studied in a non-aqueous system. This prevented formation of excessively large aggregates, hence facilitating the study of self-association at a fundamental level.

Using ^{1}H NMR spectroscopy, the following studies were undertaken on the self-association of [Pt(diimine)(*N,N*-di(*n*-butyl)-*N'*-acylthioureato)]$^+PF_6^-$ complexes in solution:

- The effect of complex concentration on the proton chemical shifts was investigated. ^{1}H NMR Spectra for each complex were recorded over a concentration range of 10^{-4} to 10^{-2} mol dm^{-3}.

- The effect of temperature on the proton chemical shifts was investigated. For each complex, ^{1}H NMR spectra were recorded at 5 °C intervals over a temperature range

25 -55 °C. These temperature arrayed experiments were carried out at several different complex concentrations.

- The ^{1}H NMR chemical shifts observed in the concentration and temperature dependence studies were used to calculate dimerisation constants for each [Pt(diimine)(*N,N*-di(*n*-butyl)-*N'*-acylthioureato]$^+PF_6^-$ complex using an appropriate computer program.

- Association constants determined from temperature dependence studies were used to construct van't Hoff plots from which the thermodynamic parameters ΔG, ΔH and ΔS of association could be estimated.

- Positive fast atom bombardment {(+)FAB} mass spectra for selected platinum complexes were run to verify the existence of 'aggregate' species.

3.1.1 Concentration Dependence

The concentration dependence of proton chemical shifts is indicative of self-aggregation. Upfield shifts with increasing concentration can only be interpreted in terms of molecular association where aromatic rings are vertically stacked, or where π-complexation results in a face-to-edge arrangement of aromatic molecules.

A single set of resonances is observed for both the monomer and the 'aggregate' species, irrespective of concentration. The observed ^{1}H NMR peaks are sharp. This indicates that the rate of exchange between the monomeric and 'aggregate' species is rapid on the NMR time scale at room temperature. The chemical shift of a selected proton (δ_{obs}) on the platinum(II) complex thus represents a weighted average of that proton's chemical shifts in two possible environments - the chemical shift of the monomer and the chemical shift in the aggregate environment.

The upfield movement of proton chemical shifts with increasing concentration is well-known for aromatic systems and can be attributed to anisotropic shielding effects of one complex molecule upon its neighbour[110,108]. Due to the mobile π-electrons, a large diamagnetic current is induced in the plane of the ring by an external, perpendicular magnetic field *Bo*. This ring current gives rise to

a smaller, secondary magnetic field which can be approximated by the field of a dipole opposed to *Bo* and centred in the middle of the ring. As the concentration of the complex is increased, the average distance between the aromatic rings decreases. As a result, the protons of one aromatic ring are increasingly exposed to the secondary magnetic field produced by the ring current of an adjacent molecule[108].

As a general trend for our platinum(II) complexes studied, the most deshielded protons of the 'monomeric' form, experienced the largest upfield change in chemical shift as a function of concentration increases. For all complexes, the deshielded diimine protons nearest to the platinum atom experienced the largest changes in their chemical shifts.

Finally, it was also found that the chemical shifts of these complexes are strongly dependent on solvent. This was first noticed in acetonitrile-d_3, when traces of water were found to cause substantial shifts in proton resonance signals, compared to those found in anhydrous acetonitrile-d_3. The H_2 resonance of $[Pt(phen)DiBuBTu]^+PF_6^-$, typically found at 8.94 ppm in anhydrous acetonitrile-d_3, was shifted to 9.11 ppm in acetonitrile-d_3 which had adsorbed some water (at the same complex concentration). Since this complex is not readily soluble in water, it is reasonable to speculate that a hydrophobic effect results in greater aggregation as the amount of water in acetonitrile-d_3 increases. An experiment was undertaken to investigate this phenomenon more thoroughly. This emphasises the necessity for thoroughly dry complexes and solutions when undertaking these NMR studies.

3.1.2 Temperature Dependence

To further elucidate the nature of the aggregation interaction of these complexes, a temperature dependence study was carried out at fixed complex concentrations. ^1H NMR Spectra were recorded at 5 °C intervals over a temperature range 25-55 °C. A general trend of downfield shift of the proton resonances with increasing temperature, was found.

From linear van't Hoff plots, an equilibrium system is implied, and this yields estimates of ΔH, ΔS and ΔG values for the association and dissociation of molecular aggregates.

3.1.3 Estimation of Dimerisation Constants

The concentration and temperature dependence of the chemical shifts of the diimine protons supports the theory that these platinum(II) complexes are associating in solution. In view of the difficulties associated with characterising higher order aggregates, it is convenient to study the process of aggregation from the fundamental level of the dimeric aggregate. Hence, we initially assumed the existence of only dimers in solution and adopted the method carried out by Horman and Deux[119] for the determination of dimerisation constants. It is reasonable to conclude that if the data fits the dimerisation model, that only dimers and not higher aggregates are found in solution. Conversely, if the data does not fit the model, it is reasonable to assume higher order species exist in the solution.

The dimerisation reaction can be represented as follows:

$$2[\text{Pt(diimine)(L-}S,O\text{)}]^{+}PF_6^{-} \overset{K^D}{\rightleftharpoons} \{[\text{Pt(diimine)(L-}S,O\text{)}]_2\}^{2+}(PF_6^{-})_2 \qquad \text{(Equation 1)}$$

(where diimine = 1,10-phenanthroline; 4,7-diphenyl-1,10-phenanthroline; 2,2'-bipyridyl; 4,4'-dimethyl-2,2'-bipyridyl or 4,4'-di-*tert*-butyl-2,2'-bipyridyl and L-*S,O* = *N,N*-di(*n*-butyl)-*N'*-benzoylthiourea or *N,N*-di(*n*-butyl)-*N'*-naphthoylthiourea ligands which are deprotonated and co-ordinated to Pt through both the S and O atom).

Previous methods for determining association constants (K^D) have required the direct measurement of δ_o, the intrinsic chemical shift of the monomer, in order to determine the dimerisation-induced chemical shift displacements ($\delta_o - \delta_i$). However, the true value of δ_o cannot be measured directly because even at low concentrations, some complex monomers associate forming dimeric species. Thus, in previous NMR studies, δ_o has been estimated by manual extrapolation of chemical shift *vs.* concentration curves to zero concentration[109,114]. From this, approximate K^D values have been calculated. The method developed by Horman and Deux[119], which is detailed below, overcomes these problems by estimating δ_o (monomer), K^D and δ_∞ (dimer) and optimising these values simultaneously using linear regression of the chemical shift *vs.* concentration data.

The association constant, K^D, for the formation of a dimer M_2 (where M_2 = {[Pt(diimine)-

$(L\text{-}S,O)]_2\}^{2+}(PF_6^-)_2$) according to Equation 1, is related to the equilibrium concentrations of M (where M = [Pt(diimine)(L-*S,O*)]$^+PF_6^-$) by the law of mass action expression

$$K^D = [M_2]/[M]^2 \qquad \text{(Equation 2)}$$

Equation 2 can be written as

$$K^D = [M_2]/([M]_o - 2[M_2])^2 \qquad \text{(Equation 3)}$$

($[M_2]$ = dimer concentration, $[M]_o$ = nominal concentration of M)

Re-arrangement gives

$$1/(2K^D[M]_o) = 2[M_2]/[M]_o + [M]_o/2[M_2] - 2 \qquad \text{(Equation 4)}$$

where $2[M_2]/[M]_o$ is the fraction of M present as M_2.

Replacing $2[M_2]/[M]_o$ by x and $1/(2K^D[M]_o)$ by y, results in the equation of a hyperbola:

$$y = x + 1/x - 2 \qquad \text{(Equation 5)}$$

For a given y_i (calculated for a given K^D at concentration $[M_i]_o$) the above equation is satisfied by x_i and $1/x_i$. The value of x_i ($0 < x_i < 1$) is given by:

$$x_i = (1+y_i/2) - [(1+y_i/2)^2 - 1]^{1/2} \qquad \text{(Equation 6)}$$

The fraction x_i is related to the measured chemical shift δ_i

$$x_i = (\delta_o-\delta_i) / (\delta_o-\delta_\infty) \qquad \text{(Equation 7)}$$

(δ_o = intrinsic chemical shift of the monomer, δ_∞ = intrinsic chemical shift of the dimer)

or

$$\delta_i = \delta_o - x_i (\delta_o-\delta_\infty) \qquad \text{(Equation 8)}$$

This equation should be a straight line, relating chemical shift (δ_i) to the fraction of dimer present (x_i), (slope = $-(\delta_o - \delta_\infty)$ and intercept is δ_o). For a series of solutions of varying concentrations of M, a set of x_i values corresponding to different values of $[M_i]_o$, is calculated according to Equation 6 for each K^D. The optimum K^D value is defined as the value which gives the best straight line fit for δ_i *vs.* x_i. Standard statistical linear regression procedures are used to determine this, and to find optimal values of K^D, δ_o and $(\delta_o - \delta_\infty)$.

The dispersion of experimental points is reflected by a standard deviation $s(\delta_o)$. The lower and upper limits on δ_o are given by $\delta_o - t.s(\delta_o)$ and $\delta_o + t.s(\delta_o)$ respectively (where t represents the student's coefficient appropriate for the number of experimental points used and the level of significance desired). Since the intercept value is δ_o, the limits on $(\delta_o - \delta_\infty)$ and K^D are obtained by determining the value of K^D which constrains the plot of δ_i *vs.* x_i to pass through the lower and upper limits of δ_o.

A computer program has been written to perform this calculation[120]. Concentration $[M_i]_o$ and corresponding chemical shift values (δ_i's) are entered. A K^D value is estimated ($=K_{first}$) and a set of x_i values for each $[M_i]_o$ concentration is calculated (Equation 6). A linear regression calculation for $\delta_i = \delta_o - x_i (\delta_o - \delta_\infty)$ is performed. For the line obtained, a mean square deviation of experimental chemical shift is computed (relative standard deviation). Using an iterative calculation, K^D is systematically varied until a minimum relative standard deviation is found (see Appendix 7.1, Chapter 7 for a flow chart of the steps used in the computer program).

3.1.4 Sources of Error in Determining Dimerisation Constants

Previous methods employing manual extrapolation of δ_o values have assumed no error in measuring this quantity and used it as a reference point in determining $(\delta_o - \delta_i)$ and other parameters[109,114]. However, studies carried out by Horman and Dreux[119] on the dimerisation of caffeine determined average errors in measuring chemical shifts to be 0.06 Hz (maximum errors being 0.3 Hz). These errors cannot be ignored, as a large error in K^D is induced by a minor error in δ_o. The error in K^D increases markedly as the chemical shift difference of the monomer relative to the dimer $(\delta_o - \delta_\infty)$,

becomes smaller. Although average errors in δ_i were found to be small (better than 0.1 Hz), they still resulted in a large range of possible K^D values.

The above reasons, emphasise the necessity of carefully prepared experimental solutions and their measurement. Precision can be improved by employing a wide concentration range. This ensures that the error in δ_i is small compared to the total δ_i range measured. Errors may also be reduced by using a larger number of data points. If the range of δ_i is limited due to low K^D or $(\delta_o - \delta_i)$ values, or limited solubility, improved accuracy can only be achieved by an increase in the number of data points. When the range of concentrations over which the ^1H NMR studies were carried out was limited, the quality of the results determined was found to decline.

3.2 RESULTS

3.2 1 Concentration Dependence

Concentration dependence studies were undertaken to ascertain the effects of association on the chemical shifts of the various protons, and to determine the extent of intermolecular association of the complexes. A concentration dependence was observed in the ^1H NMR spectra of all the platinum(II) complexes studied. The magnitude of this dependence varied for the different complexes, being quite pronounced in some instances. Full details of all ^1H NMR assignments are found in Appendix 7.2 (Chapter 7).

The diimine protons of the mixed-ligand platinum(II) complexes, exhibited the most significant upfield resonance shifts with increasing concentration of the complex in acetonitrile-d_3. To illustrate these findings, the results of the study on $[Pt(phen)DiBuBTu]^+PF_6^-$ will be discussed below. The structure, together with the numbering of the protons used in this study, is illustrated in Figure 3.1.

The ^1H NMR chemical shift changes for the diimine protons of $[Pt(phen)DiBuBTu]^+PF_6^-$ are given in Table 3.1 (over the specified concentration range). This clearly demonstrates the large concentration induced shifts experienced by these protons; the magnitude of which ranged from 0.464 ppm for H_3 to 0.883 ppm for H_2.

Figure 3.1: Schematic representation of $[Pt(phen)DiBuBTu]^+PF_6^-$ showing the numbering of the protons

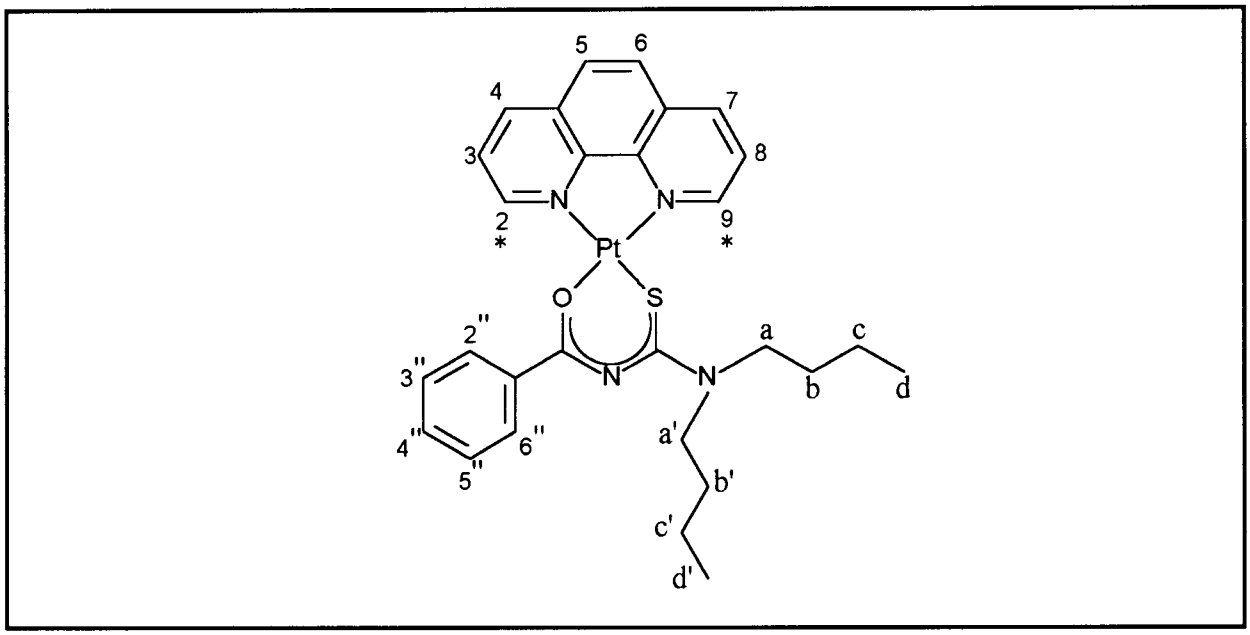

Table 3.1: ^1H NMR Chemical shift data of the diimine protons of $[Pt(phen)DiBuBTu]^+PF_6^-$ as determined by concentration dependence studies over the range $2.699x10^{-3}$ - $2.970x10^{-2}$ mol dm^{-3}

CONC mol dm^{-3}	^1H NMR CHEMICAL SHIFTS ppm							
	H_{2*}	H_3	H_4	H_5	H_6	H_7	H_8	H_{9*}
$2.699x10^{-3}$ [a]	9.106	8.143	8.765	8.066	7.984	8.672	7.793	8.715
$2.970x10^{-2}$ [b]	8.223	7.679	8.242	7.480	7.429	8.177	7.324	7.914
Δδ	**0.883**	**0.464**	**0.523**	**0.586**	**0.555**	**0.495**	**0.469**	**0.801**

a: Cmin = lowest concentration at which ^1H chemical shift data is measured
b: Cmax = highest concentration at which ^1H chemical shift data is measured
Δδ: chemical shift difference δ(Cmin) -δ(Cmax)

By comparison, the proton chemical shifts of the benzyl or naphthyl group on the *N,N*-di(*n*-butyl)-*N'*-acylthiourea moiety of the complex, did not appear to undergo significant changes (Table 3.2). A variation in the magnitude of the resonance shifts with distance from the platinum atom was observed. For this reason, attention is focused on the diimine protons of the complexes and the effects of concentration and temperature changes to their proton resonance shifts investigated.

Table 3.2: ^{1}H NMR Chemical shift data of the *N,N*-di(*n*-butyl)-*N'*-benzoylthiourea protons of [Pt(phen)DiBuBTu]$^+$PF$_6^-$ as determined by concentration dependence studies over the range 2.699x10^{-3} - 2.970x10^{-2} mol dm^{-3}

CONC mol dm^{-3}	^{1}H NMR CHEMICAL SHIFTS ppm										
	$H_{2"6"}$	$H_{3"5"}$	$H_{4"}$	$H_{a'}$	H_a	$H_{b'}$	H_b	$H_{c'}$	H_c	$H_{d'}$	H_d
2.699x10^{-3} [a]	8.058	7.502	7.657	3.750	3.750	1.826	1.688	1.510	1.412	1.067	1.067
2.970x10^{-2} [b]	7.445	7.287	7.537	3.360	3.339	1.588	1.477	1.383	1.327	1.008	1.008
Δδ	**0.613**	**0.215**	**0.120**	**0.390**	**0.411**	**0.238**	**0.211**	**0.127**	**0.085**	**0.059**	**0.059**

a: Cmin = lowest concentration at which ^{1}H chemical shift data is measured
b: Cmax = highest concentration at which ^{1}H chemical shift data is measured
Δδ: chemical shift difference δ(Cmin) -δ(Cmax)

A detailed account of the ^{1}H NMR assignments for all the platinum(II) complexes, is presented in Chapter 2 and Chapter 5. A summary of their structures, with the numbering of the protons used throughout this study, is given in Figure 2.2 (pg. 22). In addition, a list of abbreviations is presented in Table 2.1 (pg. 23) for easy reference. Hence, no further discussion of ^{1}H NMR assignments or structures is made here.

3.2.1.1 The effect of increased complex concentration on ^{1}H NMR chemical shifts of [Pt(phen)DiBuBTu]$^+$PF$_6^-$, [Pt(phen)DiBuNTu]$^+$PF$_6^-$, [Pt(4,7-diphenylphen)-DiBuBTu]$^+$PF$_6^-$ and [Pt(4,7-diphenylphen)DiBuNTu]$^+$PF$_6^-$

The concentration dependence of the ^{1}H NMR chemical shifts of [Pt(phen)DiBuBTu]$^+$PF$_6^-$ is clearly demonstrated by the upfield shift of the diimine proton resonances with increasing concentration (Figure 3.2).

This dependence can be represented by plotting chemical shift (δ_{obs}) for the diimine protons (H_2, H_3, H_4, H_5, H_6, H_7, H_8 and H_9) *vs.* concentration, as illustrated in Figure 3.3 for [Pt(phen)-DiBuBTu]$^+$PF$_6^-$ and Figure 3.4 for [Pt(phen)DiBuNTu]$^+$PF$_6^-$. Similar chemical shift *vs.* concentration curves for [Pt(4,7-diphenylphen)DiBuBTu]$^+$PF$_6^-$ and [Pt(4,7-diphenylphen)-DiBuNTu]$^+$PF$_6^-$ are represented in Figure 3.5 and Figure 3.6 respectively.

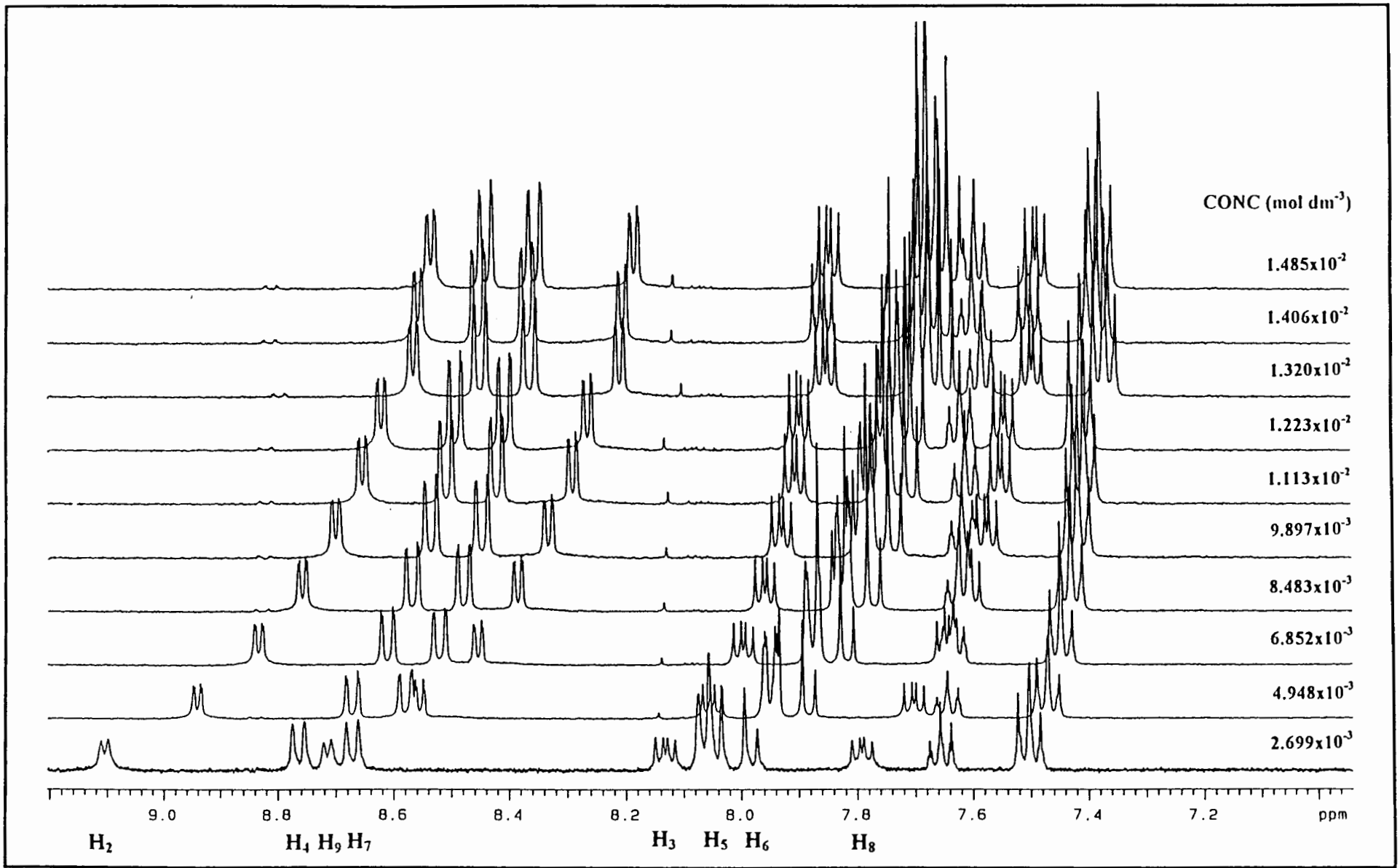

Figure 3.2: ^{1}H NMR spectra of the aromatic region of $[Pt(phen)DiBuBTu]^{+}PF_6^{-}$ in acetonitrile-d_3 over the concentration range $2.699x10^{-3}$ to $1.485x10^{-2}$ mol dm^{-3}

Figure 3.3: Graphical representation of chemical shift (ppm) *vs.* concentration (mol dm^{-3}) for $[Pt(phen)DiBuBTu]^{+}PF_6^{-}$ illustrating the upfield chemical shift of the diimine proton resonances

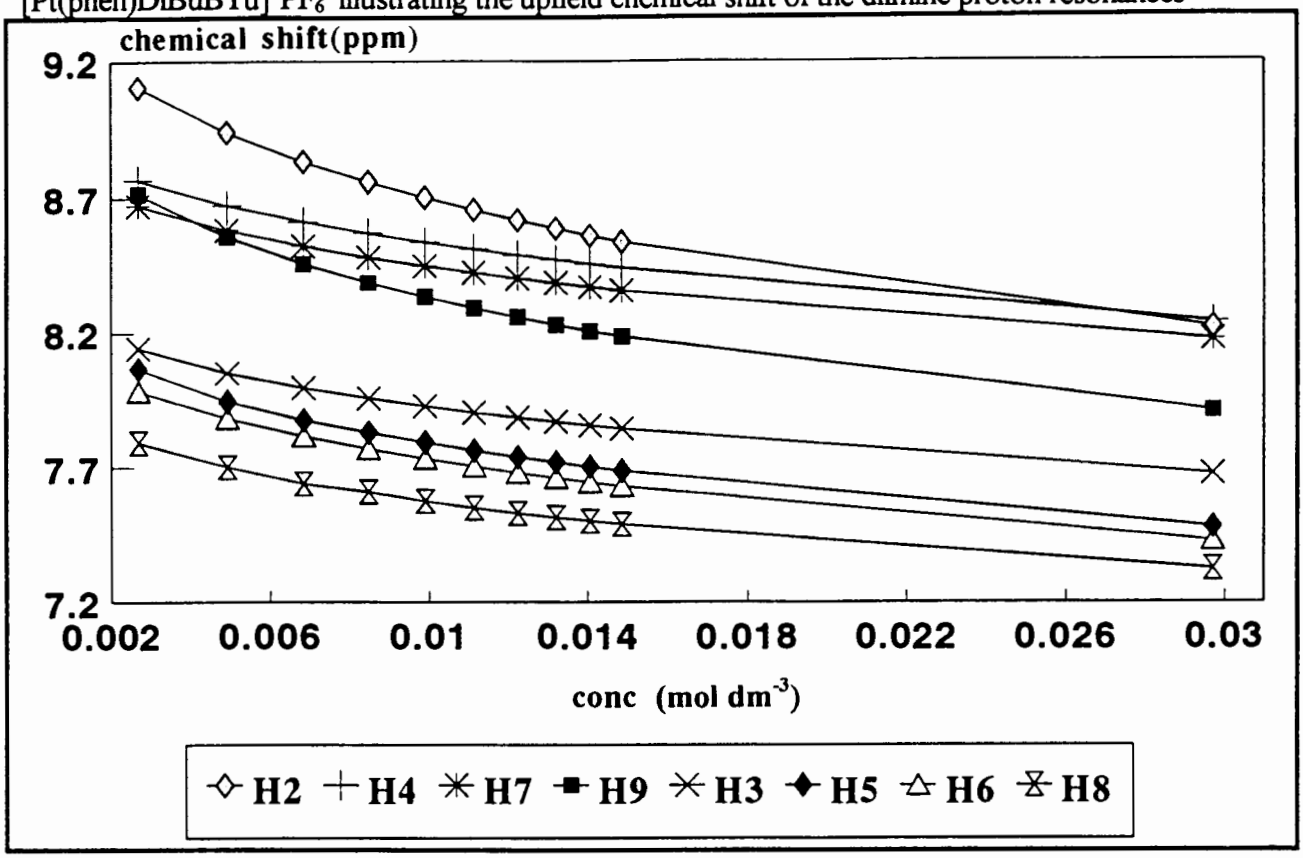

Figure 3.4: Graphical representation of chemical shift (ppm) *vs.* concentration (mol dm^{-3}) for $[Pt(phen)DiBuNTu]^{+}PF_6^{-}$ illustrating the upfield chemical shift of the diimine proton resonances

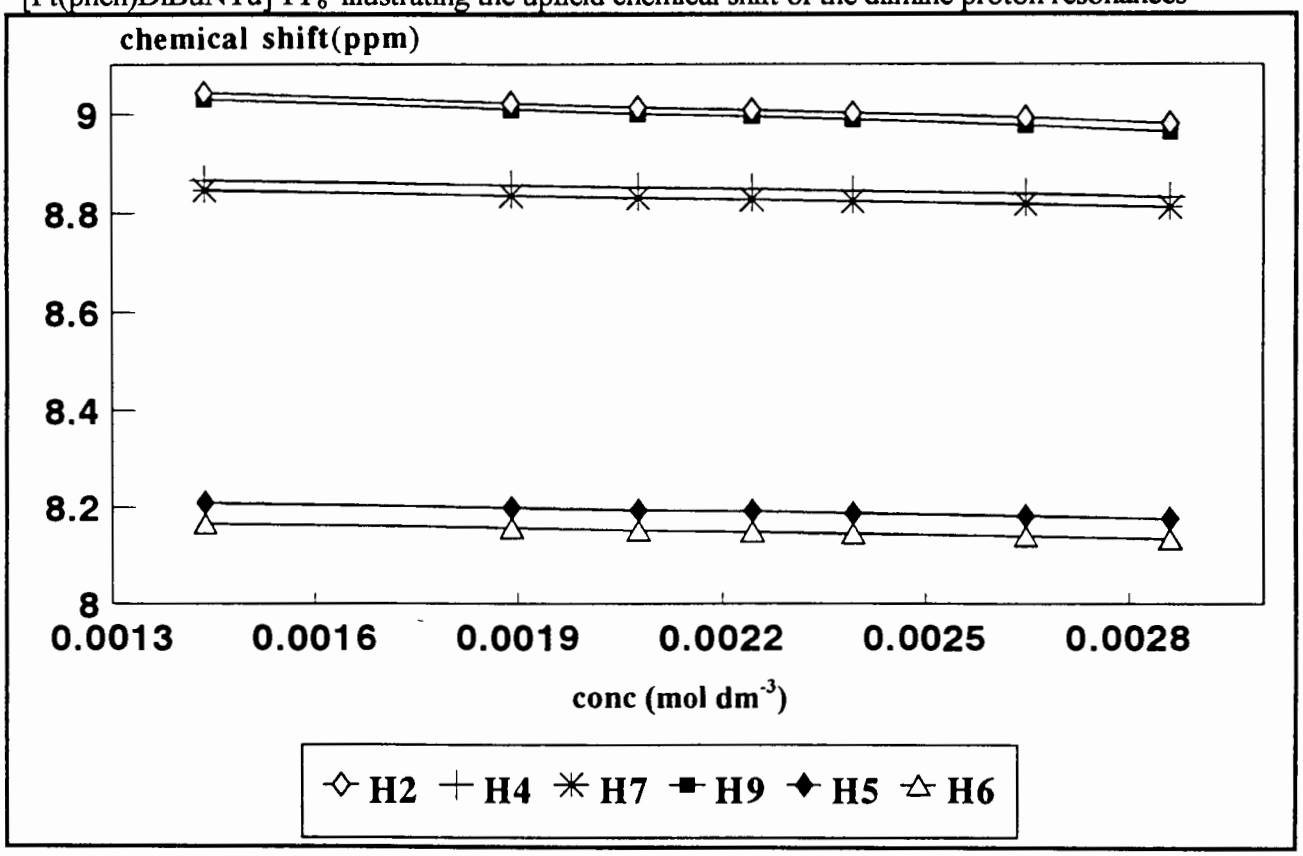

Figure 3.5: Graphical representation of chemical shift (ppm) *vs.* concentration (mol dm^{-3}) for [Pt(4,7-diphenylphen)DiBuBTu]$^{+}PF_6^{-}$ illustrating the upfield chemical shift of the diimine proton resonances

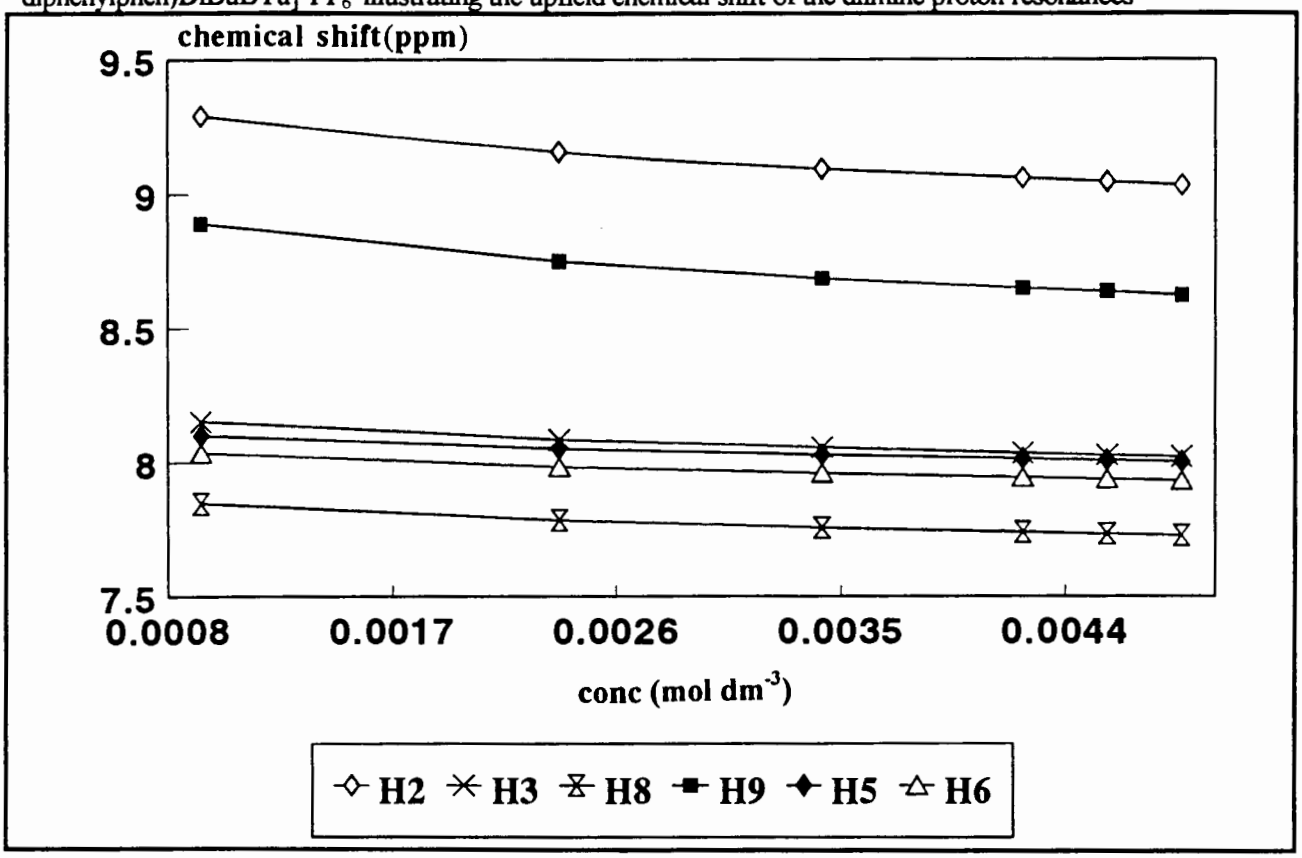

Figure 3.6: Graphical representation of chemical shift (ppm) *vs.* concentration (mol dm^{-3}) for [Pt(4,7-diphenylphen)DiBuNTu]$^{+}PF_6^{-}$ illustrating the upfield chemical shift of the diimine proton resonances

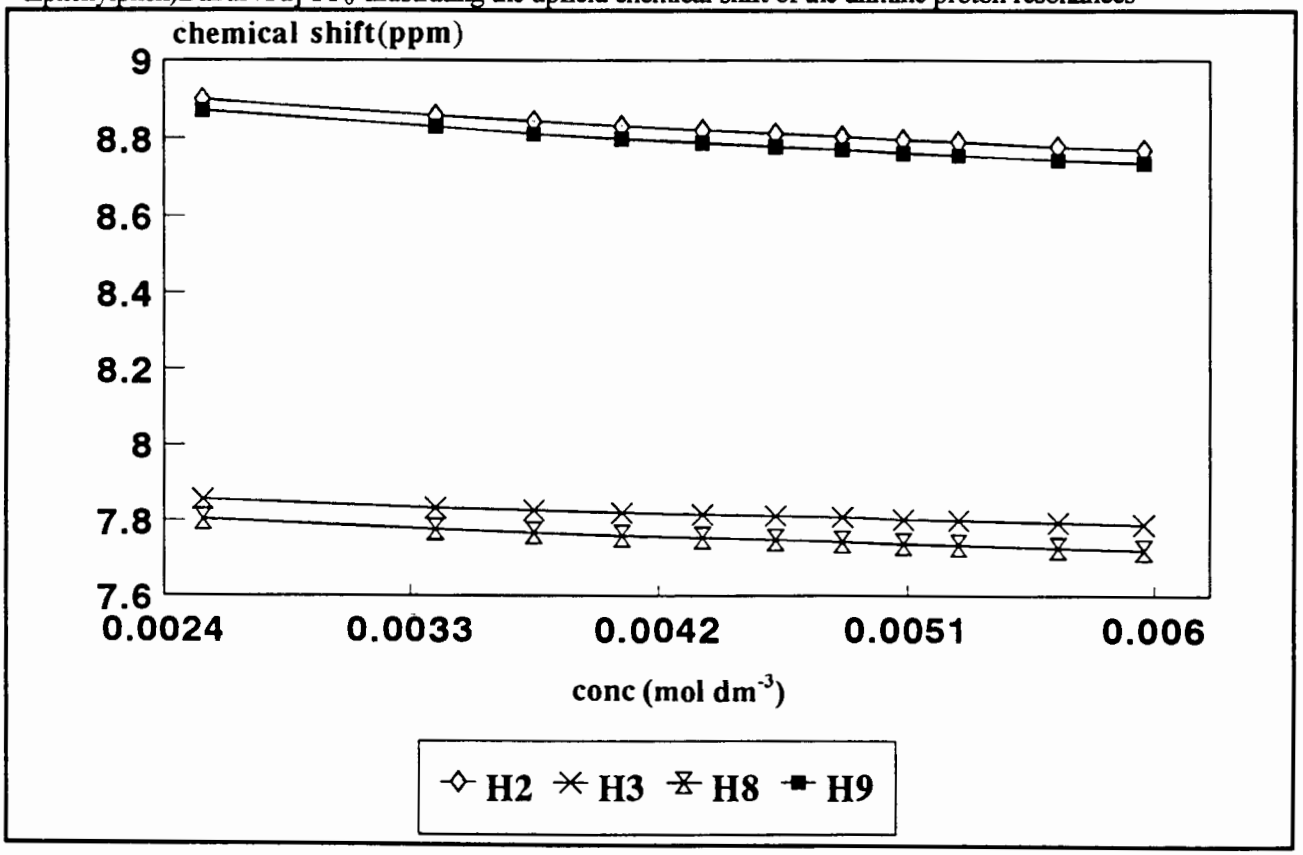

For [Pt(phen)DiBuBTu]$^{+}PF_6^{-}$, [Pt(4,7-diphenylphen)DiBuBTu]$^{+}PF_6^{-}$, and [Pt(4,7-diphenylphen)DiBuNTu]$^{+}PF_6^{-}$ the H_2 and H_9 protons experienced noticeably larger concentration induced chemical shifts, compared with the other diimine protons. In each case, these shifts were of nearly equal magnitude as indicated by the shape of the chemical shift *vs.* concentration curves. Matching trends were also seen for the H_4, H_7; H_3, H_8 and H_5, H_6 protons of all complexes.

The concentration induced chemical shifts of the diimine protons of [Pt(phen)DiBuBTu]$^{+}PF_6^{-}$, [Pt(phen)DiBuNTu]$^{+}PF_6^{-}$, [Pt(4,7-diphenylphen)DiBuBTu]$^{+}PF_6^{-}$ and [Pt(4,7-diphenylphen)-DiBuNTu]$^{+}PF_6^{-}$ are summarised in Table 3.3 (over the specified concentration ranges). The chemical shift changes ($\Delta\delta$, Table 3.3) are dependent on the concentration level of the complex in solution. As the complex becomes less soluble, different relative trends are expected. To facilitate comparison of concentration effects on the different complexes, ^{1}H NMR experiments should ideally be undertaken over identical concentration ranges. Due to solubility differences, this was not always possible.

However, studies were carried out by Horman and Deux[119] to check the intra-experimental reproducibility of complex parameters determined from ^{1}H NMR data. They divided a series of data points into subsets and calculated K^D for each group. In each case the calculated value compared favourably with the overall K^D value calculated for the complete data set. This indicates that K^D is not affected by concentration, and suggests that comparison of K^D's for different complexes is valid even if the values were not determined over identical concentration ranges.

[Pt(phen)DiBuNTu]$^{+}PF_6^{-}$ did not appear to exhibit a significant concentration dependence. Due to the poor solubility of this complex in acetonitrile-d_3 (less than 5 mg/ml), the concentration study could only be carried out over a very small range. Corresponding resonance shifts were thus too small to be of major significance.

Table 3.3: ^{1}H NMR Chemical shift data showing the overall upfield chemical shifts with increased concentration (in acetonitrile-d_3 at 25 °C)

COMPLEX	^{1}H NMR CHEMICAL SHIFTS (ppm)							
	H_2	H_3	H_4	H_5	H_6	H_7	H_8	H_9
	Cmin[a] Cmax[b]	Cmin Cmax	Cmin Cmax	Cmin Cmax	Cmin Cmax	Cmin Cmax	Cmin Cmax	Cmin Cmax
(a) $[Pt(phen)DiBuBTu]^+PF_6^-$ [d]	9.106 8.223	8.143 7.679	8.765 8.242	8.066 7.480	7.984 7.429	8.672 8.177	7.793 7.324	8.715 7.914
$\Delta\delta$[c]	**0.883**	**0.464**	**0.523**	**0.586**	**0.555**	**0.501**	**0.469**	**0.801**
(b) $[Pt(phen)DiBuNTu]^+PF_6^-$ [e]	9.043 8.981	*h*	8.867 8.832	8.209 8.176	8.166 8.134	8.847 8.812	*h*	9.030 8.964
$\Delta\delta$[c]	**0.062**		**0.035**	**0.033**	**0.032**	**0.035**		**0.066**
(c) $[Pt(4,7\text{-diphenylphen})DiBuBTu]^+PF_6^-$ [f]	9.292 9.037	8.153 8.025		8.100 8.006	8.036 7.935		7.847 7.729	8.891 8.612
$\Delta\delta$[c]	**0.272**	**0.128**		**0.094**	**0.101**		**0.118**	**0.279**
(d) $[Pt(4,7\text{-diphenylphen})DiBuNTu]^+PF_6^-$ [g]	8.900 8.769	7.856 7.789		*h*	*h*		7.804 7.722	8.871 8.735
$\Delta\delta$[c]	**0.131**	**0.067**					**0.082**	**0.136**

a: Cmin = lowest concentration at which ^{1}H chemical shift data is measured
b: Cmax = highest concentration at which ^{1}H chemical shift data is measured
c: $\Delta\delta$ = chemical shift difference δ(Cmin) - δ(Cmax)
d: $[Pt(phen)DiBuBTu]^+PF_6^-$: Cmin = 2.699×10^{-3} mol dm^{-3} Cmax = 2.970×10^{-2} mol dm^{-3}
e: $[Pt(phen)DiBuNTu]^+PF_6^-$: Cmin = 1.438×10^{-3} mol dm^{-3} Cmax = 2.861×10^{-3} mol dm^{-3}
f: $[Pt(4,7\text{-diphenylphen})DiBuBTu]^+PF_6^-$: Cmin = 9.336×10^{-4} mol dm^{-3} Cmax = 4.865×10^{-3} mol dm^{-3}
g: $[Pt(4,7\text{-diphenylphen})DiBuNTu]^+PF_6^-$: Cmin = 2.543×10^{-3} mol dm^{-3} Cmax = 5.962×10^{-3} mol dm^{-3}
h: due to overlapping peaks accurate assignment is not possible

3.2.1.2 The effect of increased complex concentration on ^1H NMR chemical shifts of [Pt(bipy)DiBuBTu]$^+PF_6^-$, [Pt(4,4'-dimethylbipy)DiBuBTu]$^+PF_6^-$, [Pt(4,4'-dimethylbipy)DiBuNTu]$^+PF_6^-$, [Pt(4,4'-ditbutbipyDiBuBTu]$^+PF_6^-$ and [Pt(4,4'-ditbutbipy) DiBuNTu]$^+PF_6^-$

The effect of systematically increasing the electron density of the diimine ligand on aggregation, was investigated. For this purpose, electron donating substituents were introduced on the aromatic 2,2'-bipyridyl moiety. A comparison was then made of three [Pt(diimine)(*N,N*-di(*n*-butyl)-*N'*-benzoylthioureato)]$^+PF_6^-$ complexes, where only the substituents at the 4',4 position on the bipyridyl moiety of the complex differed. The three substituents were a proton-, a methyl- and a tertiary butyl group. Studies on the corresponding *N,N*-di(*n*-butyl)-*N'*-naphthoylthiourea complexes were also undertaken.

The concentration induced chemical shifts of the diimine protons of [Pt(bipy)DiBuBTu]$^+PF_6^-$, [Pt(4,4'-dimethylbipy)DiBuBTu]$^+PF_6^-$, [Pt(4,4'-dimethylbipy)DiBuNTu]$^+PF_6^-$, [Pt(4,4'-ditbutbipy)-DiBuBTu]$^+PF_6^-$ and [Pt(4,4'-ditbutbipy)DiBuNTu]$^+PF_6^-$ are illustrated by plots of chemical shift *vs.* concentration in Figure 3.7 to Figure 3.11 respectively.

In all five complexes, the proton resonances of $H_{6'}$ and H_6 experienced the largest upfield shift. Here too, the changes were of similar magnitude (similarly $H_{5'}$ and H_5). The overall upfield chemical shift of the diimine resonances of [Pt(bipy)DiBuBTu]$^+PF_6^-$, [Pt(4,4'-dimethylbipy)DiBuNTu]$^+PF_6^-$, [Pt(4,4'-ditbutbipy)DiBuBTu]$^+PF_6^-$ and [Pt(4,4'-ditbutbipy)DiBuNTu]$^+PF_6^-$ are represented in Table 3.4 (over the specified concentration ranges).

Figure 3.7: Graphical representation of chemical shift (ppm) *vs.* concentration (mol dm^{-3}) for $[Pt(bipy)DiBuBTu]^{+}PF_6^{-}$ illustrating the upfield chemical shift of the diimine proton resonances

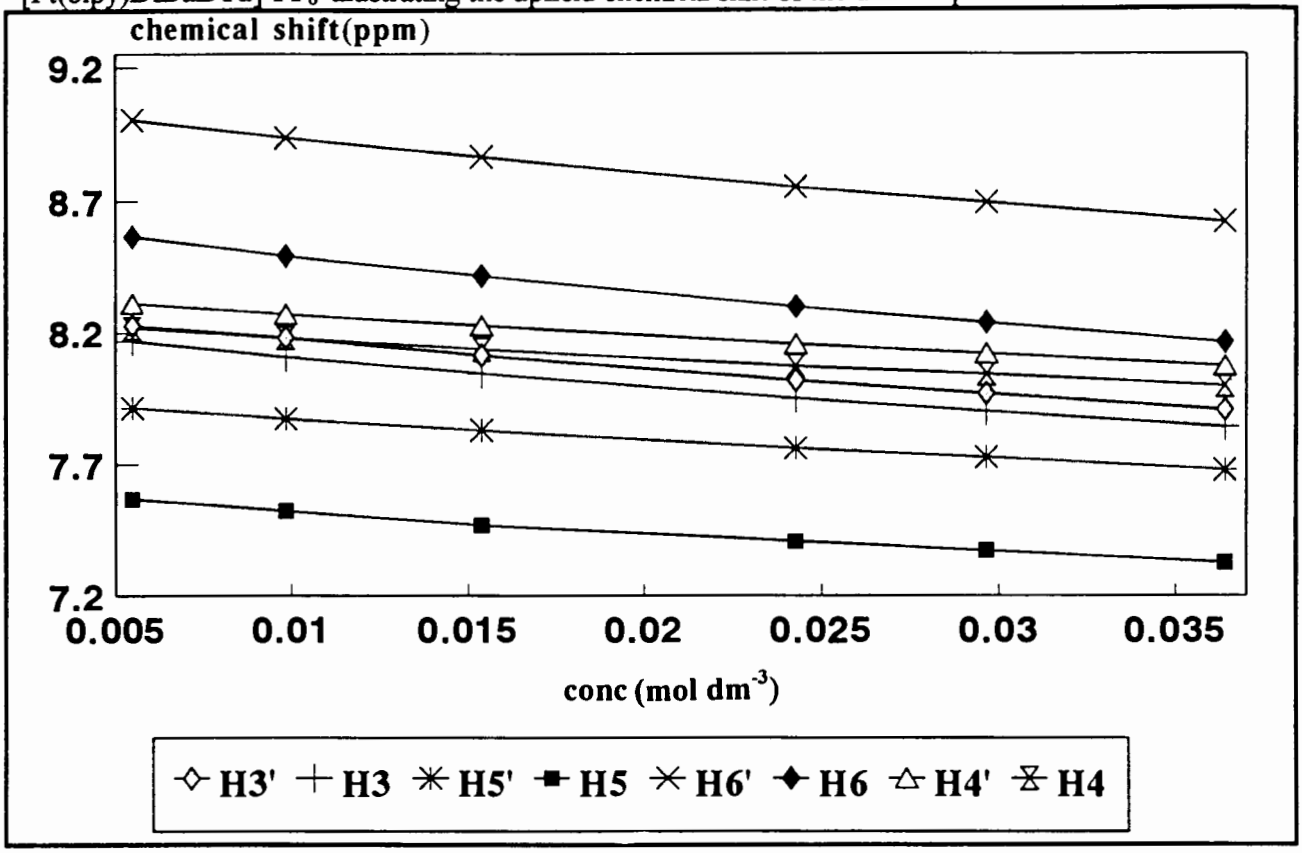

Figure 3.8: Graphical representation of chemical shift (ppm) *vs.* concentration (mol dm^{-3}) for [Pt(4,4'-dimethylbipy)DiBuBTu]$^{+}PF_6^{-}$ illustrating the upfield chemical shift of the diimine proton resonances

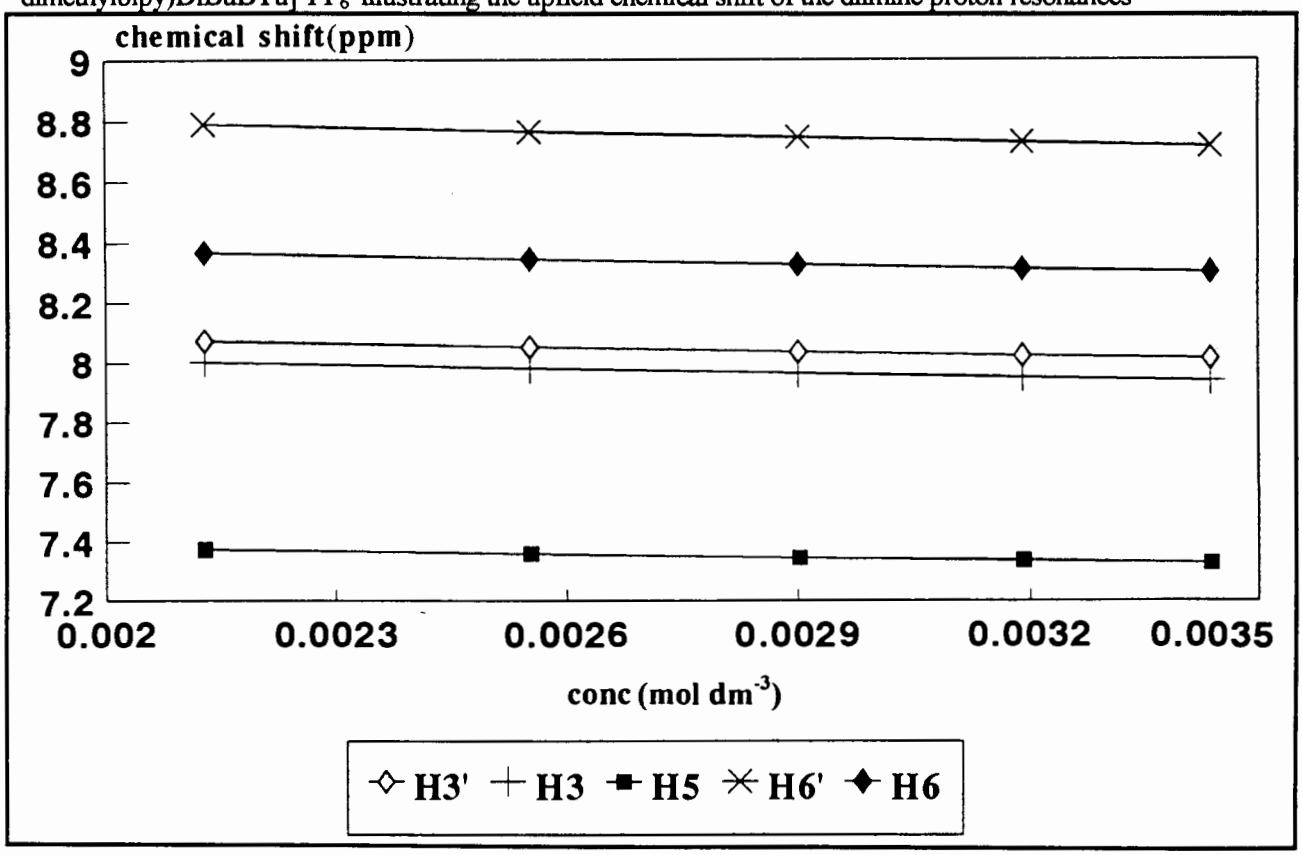

Figure 3.9: Graphical representation of chemical shift (ppm) *vs.* concentration (mol dm^{-3}) for [Pt(4,4'-dimethylbipy)DiBuNTu]$^{+}PF_6^{-}$ illustrating the upfield chemical shift of the diimine proton resonances

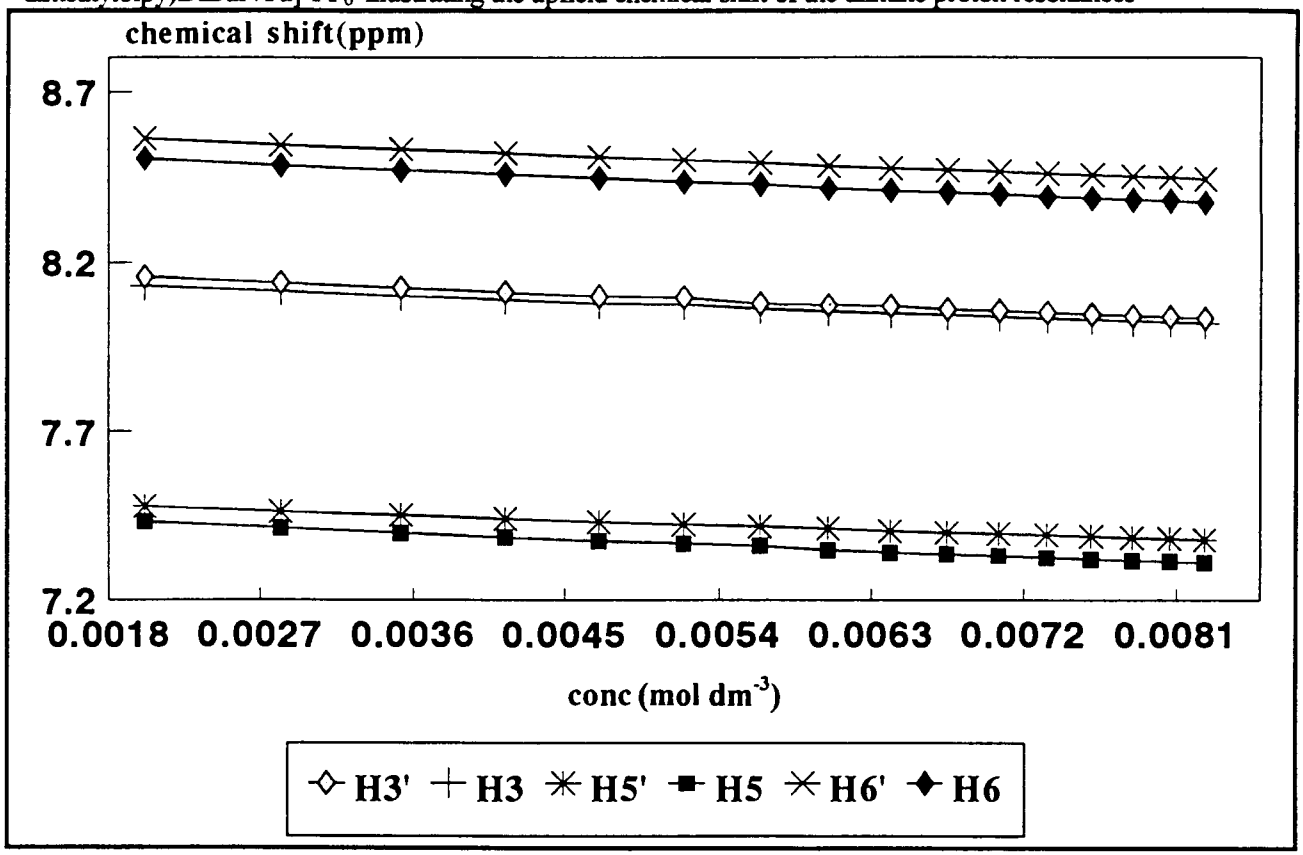

Figure 3.10: Graphical representation of chemical shift (ppm) *vs.* concentration (mol dm^{-3}) for [Pt(4,4'-dit-butbipy)DiBuBTu]$^{+}PF_6^{-}$ illustrating the upfield chemical shift of the diimine proton resonances

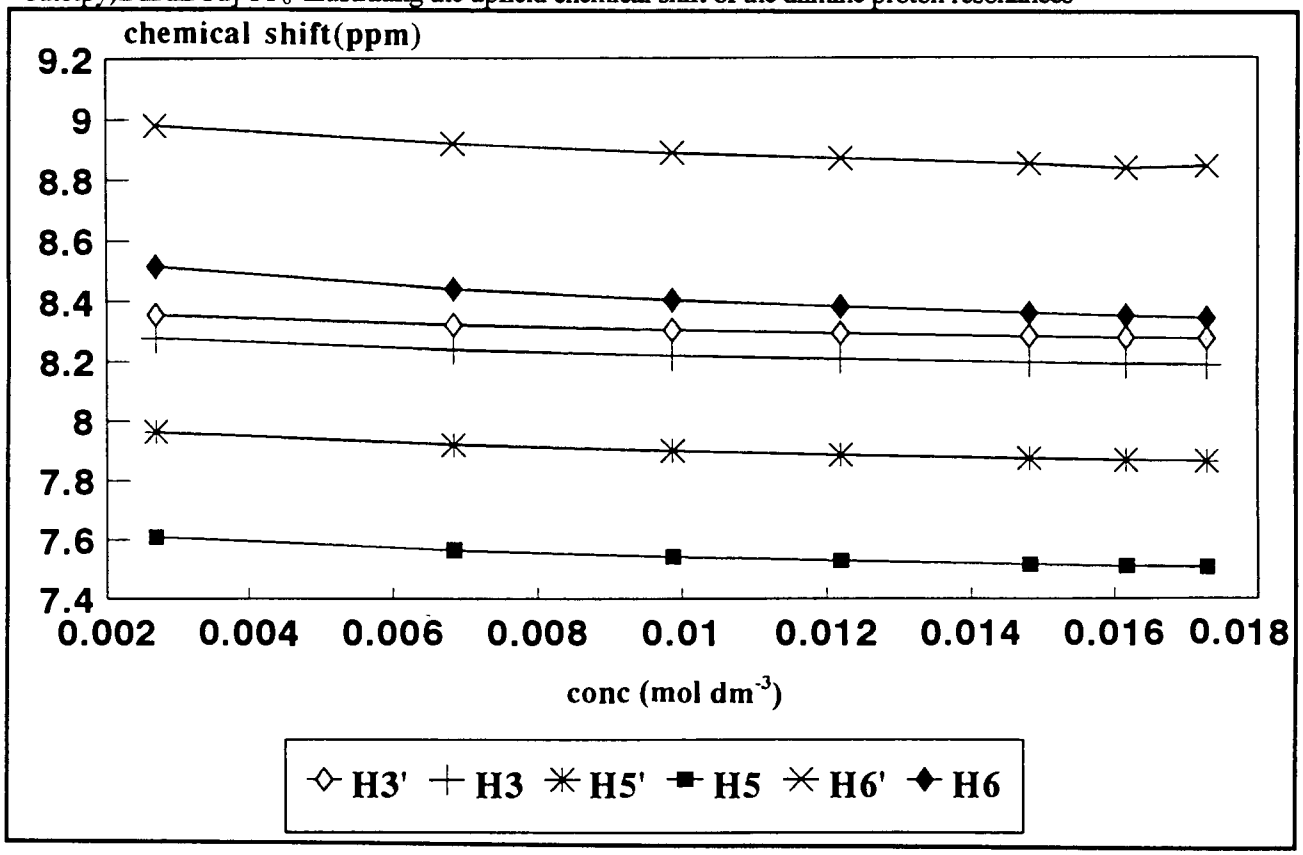

Figure 3.11: Graphical representation of chemical shift (ppm) *vs.* concentration (mol dm^{-3}) for [Pt(4,4'-dit-butbipy)DiBuNTu]$^{+}PF_6^{-}$ illustrating the upfield chemical shift of the diimine proton resonances

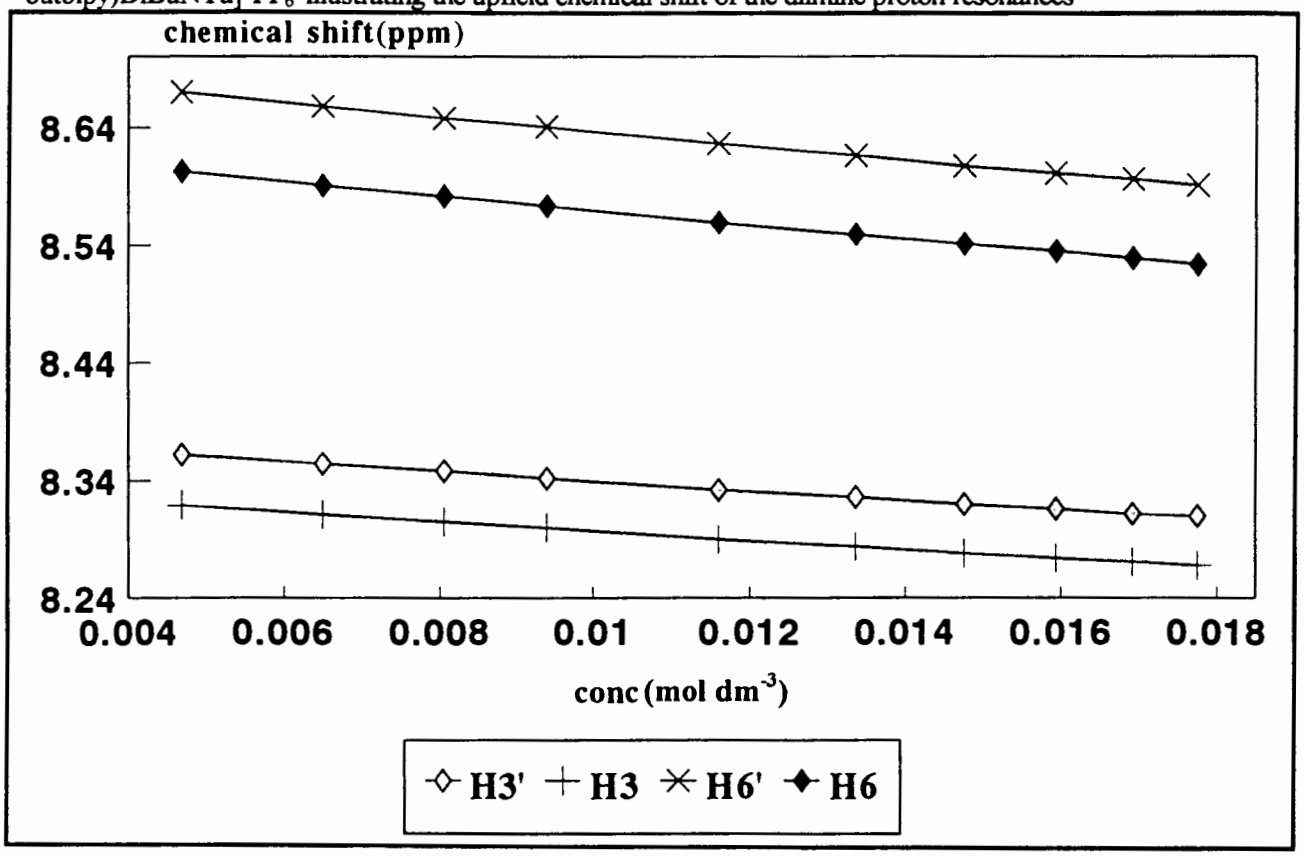

Table 3.4: ^{1}H NMR Chemical shift data showing the overall upfield chemical shifts with increased concentration (in acetonitrile-d_3 at 25 °C)

COMPLEX	^{1}H NMR CHEMICAL SHIFTS (ppm)											
	$H_{3'}$		H_3		$H_{4'}$		H_4		$H_{5'}$		H_5		$H_{6'}$		H_6	
	Cmin[a]	Cmax[b]	Cmin	Cmax	Cmin	Cmax	Cmin	Cmax	Cmin	Cmax	Cmin	Cmax	Cmin	Cmax	Cmin	Cmax
(a) $[Pt(bipy)DiBuBTu]^+PF_6^-$ [d]	8.226	7.909	8.167	7.844	8.311	8.076	8.217	8.001	7.914	7.680	7.568	7.327	9.005	8.623	8.566	8.166
$\Delta\delta$[c]	**0.317**		**0.323**		**0.235**		**0.216**		**0.234**		**0.241**		**0.382**		**0.400**	
(b) $[Pt(4,4'\text{-dimethylbipy})DiBuNTu]^+PF_6^-$ [e]	8.157	8.035	8.130	8.020					7.477	7.378	7.432	7.310	8.564	8.444	8.505	8.376
$\Delta\delta$[c]	**0.122**		**0.110**						**0.099**		**0.122**		**0.120**		**0.129**	
(c) $[Pt(4,4'\text{-ditbutbipy})DiBuBTu]^+PF_6^-$ [f]	8.355	8.273	8.278	8.185					7.964	7.863	7.610	7.507	8.980	8.836	8.515	8.340
$\Delta\delta$[c]	**0.082**		**0.093**						**0.101**		**0.103**		**0.144**		**0.175**	
(d) $[Pt(4,4'\text{-ditbutbipy})DiBuNTu]^+PF_6^-$ [g]	8.362	8.310	8.319	8.268					*h*		*h*		8.670	8.592	8.603	8.525
$\Delta\delta$[c]	**0.052**		**0.051**										**0.078**		**0.078**	

a: Cmin = lowest concentration at which ^{1}H chemical shift data is measured
b: Cmax = highest concentration at which ^{1}H chemical shift data is measured
c: $\Delta\delta$ = chemical shift difference δ(Cmin) - δ(Cmax)
d: $[Pt(bipy)DiBuBTu]^+PF_6^-$: Cmin = 5.484×10^{-3} mol dm^{-3} Cmax = 3.639×10^{-2} mol dm^{-3}
e: $[Pt(4,4'\text{-dimethylbipy})DiBuNTu]^+PF_6^-$: Cmin = 2.014×10^{-3} mol dm^{-3} Cmax = 8.266×10^{-3} mol dm^{-3}
f: $[Pt(4,4'\text{-ditbutbipy})DiBuBTu]^+PF_6^-$: Cmin = 2.695×10^{-3} mol dm^{-3} Cmax = 1.729×10^{-3} mol dm^{-3}
g: $[Pt(4,4'\text{-ditbutbipy})DiBuNTu]^+PF_6^-$: Cmin = 4.697×10^{-3} mol dm^{-3} Cmax = 1.774×10^{-2} mol dm^{-3}
h: due to overlapping peaks accurate assignment is not possible

3.2.2 Calculation of K^D

The chemical shift data obtained in the concentration dependence studies were used to determine association constants using the method outlined by Horman and Deux[119]. Dimerisation constants (K^D) were calculated for the diimine protons in each complex. An average K^D for each complex could then be estimated. The plot of observed chemical shift (δ_i) *vs.* x_i (the fraction of dimer present) for $[Pt(phen)DiBuBTu]^+PF_6^-$ is illustrated in Figure 3.12.

Figure 3.12: Graphical representation of chemical shift (ppm) *vs.* fraction of dimer present (x_i) for $[Pt(phen)DiBuBTu]^+PF_6^-$ (at 25 °C)

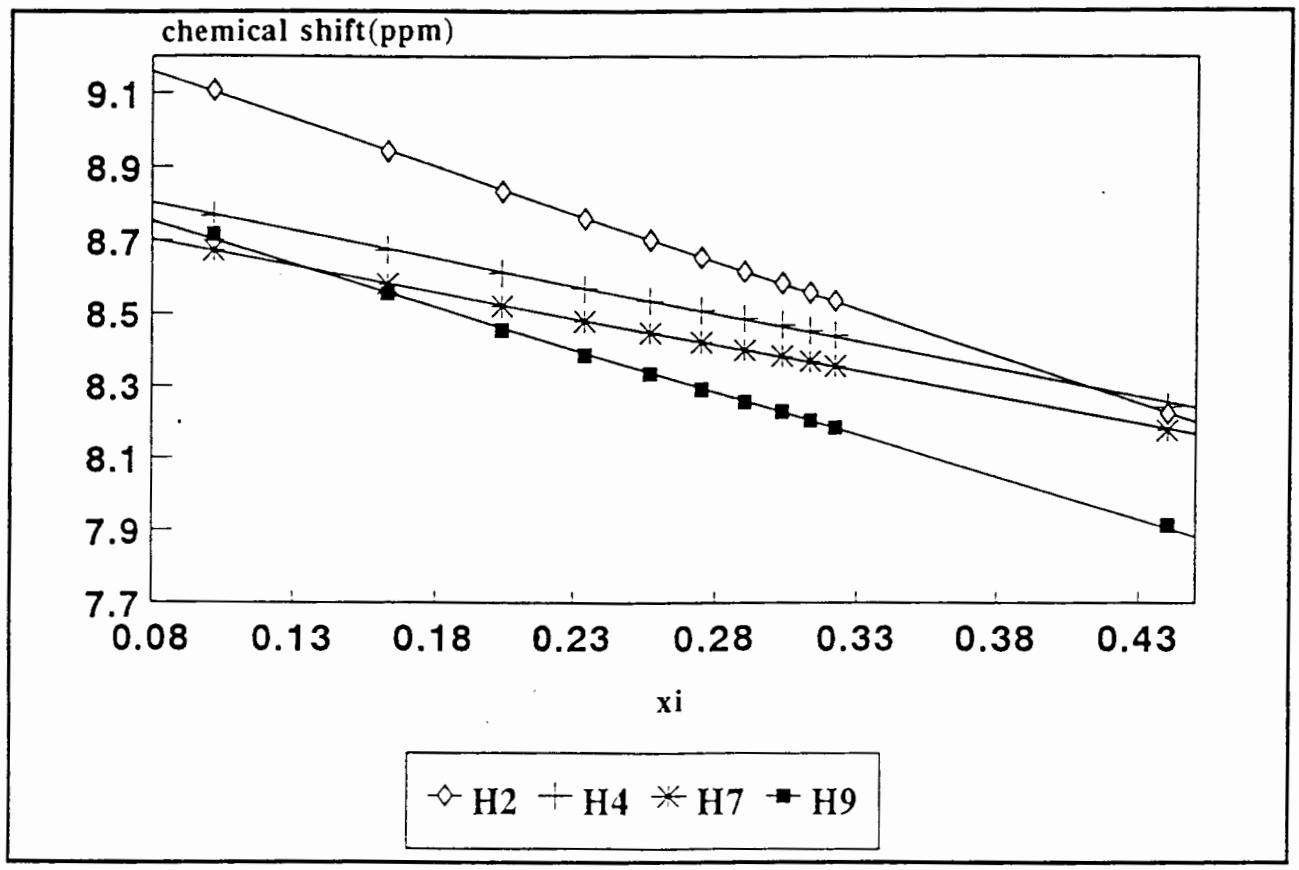

Since K^D is used to a calculate a set of x_i values, plots of δ_i *vs.* x_i will only be linear if the determined value of K^D is correct.

$$\delta_i = \delta_o - x_i (\delta_o - \delta_\infty) \qquad \text{(Equation 8)}$$

Thus, the linearity demonstrated by the platinum(II) complexes, suggests that the dimerisation model can be used to explain the form of association occurring. Additional trimeric and higher aggregates are therefore not expected to be present in significant amounts. The optimum value of K^D is defined as the value which gives the best straight line fit for δ_i *vs.* x_i. This is determined by standard statistical linear regression procedures. Optimum values of δ_o and $(\delta_o - \delta_i)$ are determined simultaneously with K^D.

Previous studies have illustrated how a minor error in δ_o induces a significantly large error in K^D. This error increases markedly as the overall chemical shift changes, $(\delta_o-\delta_\infty)$ becomes smaller[119]. The best estimate of K^D will therefore be obtained from those protons for which $(\delta_o-\delta_\infty)$ is largest.

3.2.2.1 Dimerisation constants for [Pt(phen)DiBuBTu]$^+PF_6^-$, [Pt(4,7-diphenylphen)-DiBuBTu]$^+PF_6^-$ and [Pt(4,7-diphenylphen)DiBuNTu]$^+PF_6^-$

The calculated dimerisation constants for [Pt(phen)DiBuBTu]$^+PF_6^-$, [Pt(4,7-diphenylphen)-DiBuBTu]$^+PF_6^-$ and [Pt(4,7-diphenylphen)DiBuNTu]$^+PF_6$ are given in Table 3.5, Table 3.6 and Table 3.7 respectively. Optimum values for δ_o (the intrinsic chemical shift of the monomer) and $(\delta_o - \delta_\infty)$ are also given together with their lower and upper limits (within 95% confidence limits).

Table 3.5: Comparison of complex parameters for the formation of [Pt(phen)DiBuBTu]$^+PF_6^-$ dimers in acetonitrile-d_3 at 25 °C (optimum parameters within 95% confidence limits)

H	**min < K^D < max** **$dm^3\ mol^{-1}$**	**min < δ_o < max** **ppm**	**min < -(δ_o-δ_∞) < max** **ppm**
2	22.85 < 23.55 < 24.26	9.363 < 9.369 < 9.375	-2.623 < -2.602 < -2.582*
3	21.71 < 23.47 < 25.30	8.269 < 8.276 < 8.284	-1.383 < -1.354 < -1.328
4	16.82 < 17.91 < 19.05	8.890 < 8.896 < 8.903	-1.696 < -1.660 < -1.628
5	22.03 < 24.19 < 26.46	8.223 < 8.236 < 8.248	-1.734 < -1.691 < -1.654
6	19.94 < 20.75 < 21.58	8.133 < 8.137 < 8.142	-1.711 < -1.691 < -1.671
7	21.35 < 22.28 < 23.23	8.809 < 8.814 < 8.818	-1.495 < -1.477 < -1.460
8	21.79 < 24.78 < 27.98	7.920 < 7.934 < 7.947	-1.402 < -1.355 < -1.316
9	28.40 < 29.31 < 30.23	8.979 < 8.985 < 8.991	-2.257 < -2.242 < -2.227*
	AVE K^D	23.3 ± (3.3)	

Table 3.6: Comparison of complex parameters for the formation of [Pt(4,7-diphenylphen)-DiBuBTu]$^+PF_6^-$ dimers in acetonitrile-d_3 at 25 °C (optimum parameters within 95% confidence limits)

H	min < K^D < max $dm^3\ mol^{-1}$	min < δ_o < max ppm	min < $-(\delta_o-\delta_\infty)$ < max ppm
2	114.1 < 120.3 < 126.5	9.449 < 9.453 < 9.458	-1.027 < -1.014 < -1.003*
3	102.9 < 108.9 < 115.1	8.228 < 8.230 < 8.233	-0.532 < -0.524 < -0.517
5	84.29 < 92.99 < 102.0	8.150 < 8.152 < 8.155	-0.411 < -0.399 < -0.389
6	88.48 < 95.93 < 103.6	8.091 < 8.093 < 8.095	-0.435 < -0.425 < -0.416
8	117.7 < 123.6 < 129.6	7.921 < 7.923 < 7.925	-0.473 < -0.467 < -0.463
9	135.6 < 142.8 < 150.1	9.067 < 9.072 < 9.077	-1.016 < -1.006 < -0.998*
	AVE K^D	114 ± (19)	

Table 3.7: Comparison of complex parameters for the formation of [Pt(4,7-diphenylphen)-DiBuNTu]$^+PF_6^-$ dimers in acetonitrile-d_3 at 25 °C (optimum parameters within 95% confidence limits)

H	min < K^D < max $dm^3\ mol^{-1}$	min < δ_o < max ppm	min < $-(\delta_o-\delta_\infty)$ < max ppm
2	52.85 < 55.74 < 58.68	9.089 < 9.093 < 9.098	-1.058 < -1.034 < -1.020*
3	50.25 < 57.36 < 64.79	7.948 < 7.954 < 7.959	-0.536 < -0.516 < -0.501
8	66.53 < 71.57 < 76.73	7.933 < 7.937 < 7.941	-0.613 < -0.604 < -0.596
9	65.53 < 69.16 < 72.86	9.089 < 9.094 < 9.099	-1.042 < -1.029 < -1.018*
	AVE K^D	63 ± (8)	

H_5 and H_6 - due to overlapping, accurate assignment of peaks is not possible

The close agreement of the observed shift trends of protons H_2 and H_9, for [Pt(phen)DiBuBTu]$^+PF_6^-$, [Pt(4,7-diphenylphen)DiBuBTu]$^+PF_6^-$ and [Pt(4,7-diphenylphen)-DiBuNTu]$^+PF_6^-$ are shown in plots of chemical shift *vs.* concentration (Figure 3.3, Figure 3.5 and Figure 3.6). This indicates that these protons are in similar magnetic environments (similarly for H_4, H_7 and H_3, H_8). This is also seen in the similarity of their respective $(\delta_o-\delta_\infty)$ values (Table 3.5, 3.6 and 3.7).

Association constants determined for the protons on the diimine moiety of [Pt(phen)DiBuBTu]$^+PF_6^-$ are given in Table 3.5 together with their lower and upper limits (within 95% confidence limits). Good agreement is found between all the values determined. Furthermore, the error associated with each K^D is relatively small being lowest for H_2. This is consistent with the results of Horman and Dreux[119] who found that the larger the chemical shift difference, $(\delta_o-\delta_\infty)$, the smaller the error associated with K^D.

Association constants for [Pt(4,7-diphenylphen)DiBuBTu]$^+PF_6^-$ and [Pt(4,7-diphenylphen)DiBuNTu]$^+PF_6^-$ are given in Tables 3.6 and 3.7 respectively. The errors associated with K^D for both these complexes are larger than those associated with [Pt(phen)DiBuBTu]$^+PF_6^-$. Due to the lower $(\delta_o-\delta_\infty)$ values of the former complex, larger errors are expected.

3.2.2.2 Dimerisation constants for [Pt(bipy)DiBuBTu]$^+PF_6^-$, [Pt(4,4'-dimethylbipy)-DiBuNTu]$^+PF_6^-$, [Pt(4,4'-ditbutbipy)DiBuBTu]$^+PF_6^-$ and [Pt(4,4'-ditbutbipy)-DiBuNTu]$^+PF_6^-$

The calculated dimerisation constants for the diimine protons of [Pt(bipy)DiBuBTu]$^+PF_6^-$, [Pt(4,4'-dimethylbipy)DiBuNTu]$^+PF_6^-$, [Pt(4,4'-ditbutbipy)DiBuBTu]$^+PF_6^-$ and [Pt(4,4'-ditbutbipy)-DiBuNTu]$^+PF_6^-$ are given in Tables 3.8 to Table 3.11. Optimum values for δ_o and $(\delta_o-\delta_\infty)$ are given, together with their lower and upper limits (within 95% confidence limits).

Table 3.8: Comparison of complex parameters for the formation of $[Pt(bipy)DiBuBTu]^+PF_6^-$ dimers in acetonitrile-d_3 at 25 °C (optimum parameters within 95% confidence limits)

H	min < K^D < max $dm^3\ mol^{-1}$	min < δ_o < max ppm	min < $-(\delta_o-\delta_\infty)$ < max ppm
3'	2.399 < 2.659 < 2.924	8.315 < 8.312 < 8.317	-2.845 < -3.061 < -2.663
3	2.546 < 2.969 < 3.406	8.241 < 8.245 < 8.249	-3.406 < -2.593 < -2.367
4'	1.568 < 1.998 < 2.447	8.360 < 8.363 < 8.366	-3.030 < -2.509 < -2.160
4	1.877 < 2.517 < 3.196	8.263 < 8.268 < 8.272	-2.416 < -1.943 < -1.648
5'	1.616 < 2.500 < 3.459	7.961 < 7.968 < 7.974	-2.923 < -2.101 < -1.683
5	2.847 < 4.083 < 5.432	7.626 < 7.631 < 7.640	-1.974 < -1.562 < -1.326
6'	1.930 < 2.299 < 2.680	9.088 < 9.092 < 9.097	-4.193 < -3.679 < -3.296*
6	2.534 < 2.923 < 3.325	8.658 < 8.663 < 8.667	-3.587 < -3.246 < -2.978*
	AVE K^D	2.7 ± (0.6)	

Table 3.9: Comparison of complex parameters for the formation of $[Pt(4,4'\text{-dimethylbipy})\text{-}DiBuNTu]^+PF_6^-$ dimers in acetonitrile-d_3 at 25 °C (optimum parameters within 95% confidence limits)

H	min < K^D < max $dm^3\ mol^{-1}$	min < δ_o < max ppm	min < $-(\delta_o-\delta_\infty)$ < max ppm
3'	5.811 < 8.451 < 11.25	8.208 < 8.206 < 8.211	-2.067 < -1.549 < -1.266
3	4.459 < 6.297 < 8.217	8.169 < 8.172 < 8.175	-2.320 < -1.751 < -1.428
5'	5.568 < 6.567 < 7.589	7.514 < 7.515 < 7.516	-1.732 < -1.519 < -1.359
5	6.156 < 7.930 < 9.775	7.478 < 7.480 < 7.483	-1.976 < -1.626 < -1.397
6'	5.209 < 6.323 < 7.466	8.608 < 8.610 < 8.611	-2.214 < -1.895 < -1.666*
6	3.368 < 4.543 < 5.754	8.550 < 8.552 < 8.554	-3.481 < -2.694 < -2.218*
	AVE K^D	6.7 ± (1.4)	

Table 3.10: Comparison of complex parameters for the formation of [Pt(4,4'-ditbutbipy)-DiBuBTu]$^{+}PF_6^{-}$ dimers in acetonitrile-d_3 at 25°C (optimum parameters within 95% confidence limits)

H	min < K^D < max $dm^3\ mol^{-1}$	min < δ_o < max ppm	min < -(δ_o-δ_∞) < max ppm
3'	21.86 < 23.01 < 24.18	8.388 < 8.389 < 8.390	-0.346 < -0.340 < -0.334
3	28.41 < 28.97 < 29.54	8.320 < 8.321 < 8.321	-0.358 < -0.356 < -0.354
5'	29.28 < 30.45 < 31.64	8.011 < 8.012 < 8.013	-0.385 < -0.381 < -0.377
5	30.61 < 31.43 < 32.26	7.659 < 7.660 < 7.660	-0.388 < -0.385 < -0.383
6'	25.69 < 26.24 < 26.79	9.043 < 9.043 < 9.044	-0.571 < -0.568 < -0.564*
6	27.38 < 27.87 < 28.37	8.593 < 8.594 < 8.595	-0.679 < -0.676 < -0.672*
	AVE K^D	28.0 ± (3.1)	

Table 3.11: Comparison of complex parameters for the formation of [Pt(4,4'-ditbutbipy)-DiBuNTu]$^{+}PF_6^{-}$ dimers in acetonitrile-d_3 at 25°C (optimum parameters with 95% confidence limits)

H	min < K^D < max $dm^3\ mol^{-1}$	min < δ_o < max ppm	min < -(δ_o-δ_∞) < max ppm
3'	2.905 < 2.217 < 3.617	8.385 < 8.384 < 8.386	-0.878 < -1.093 < -0.741
3	2.544 < 1.913 < 3.196	8.341 < 8.340 < 8.342	-0.949 < -1.203 < -0.792
6'	1.911 < 1.496 < 2.335	8.702 < 8.701 < 8.703	-1.827 < -2.258 < -1.544*
6	1.583 < 1.255 < 1.918	8.634 < 8.633 < 8.635	-2.143 < -2.634 < -1.815*
	AVE K^D	1.7 ± (0.4)	

An average association constant for [Pt(4,4'-dimethylbipy)DiBuBTu]$^{+}PF_6^{-}$ could not be accurately determined. Due to the poor solubility of the complex in acetonitrile-d_3, the K^D values of the diimine protons occurred over a large range. However, when taking into consideration these results together with the observed trends of the other bipyridyl-type complexes, a value of between 40-50 $dm^3\ mol^{-1}$ is estimated.

3.2.2.3 Observed vs. Calculated shifts

To further test the validity of the dimerisation model, calculated chemical shift values were compared with experimentally observed values. The concentration curves for the diimine protons of the platinum(II) complexes were analysed in terms of a monomer-dimer equilibrium in which the calculated chemical shift (δ_{obs}) at any concentration (a) is given by[121,122]

$$\delta_{obs} = \delta_o + (\delta_\infty - \delta_o)\,[(1 + 8aK^D)^{1/2} - 1]^2 / 8aK^D \qquad \text{(Equation 9)}$$

where K^D is the association constant at 25 °C and ($\delta_\infty - \delta_o$) is the dimerisation shift (δ_o is the intrinsic chemical shift of the monomer and δ_∞ is the intrinsic chemical shift of the dimer). The calculated concentration curves of H_2, H_4, H_7 and H_9 of [Pt(phen)DiBuBTu]$^+PF_6^-$ are given together with the observed curves in Figure 3.13. The excellent agreement between the observed and calculated proton chemical shifts was observed for the diimine protons of all complexes studied.

Figure 3.13: Graphical representation of chemical shift (ppm) *vs.* concentration (mol dm^{-3}) for [Pt(phen)DiBuBTu]$^+PF_6^-$ illustrating the excellent agreement between observed and calculated chemical shift values

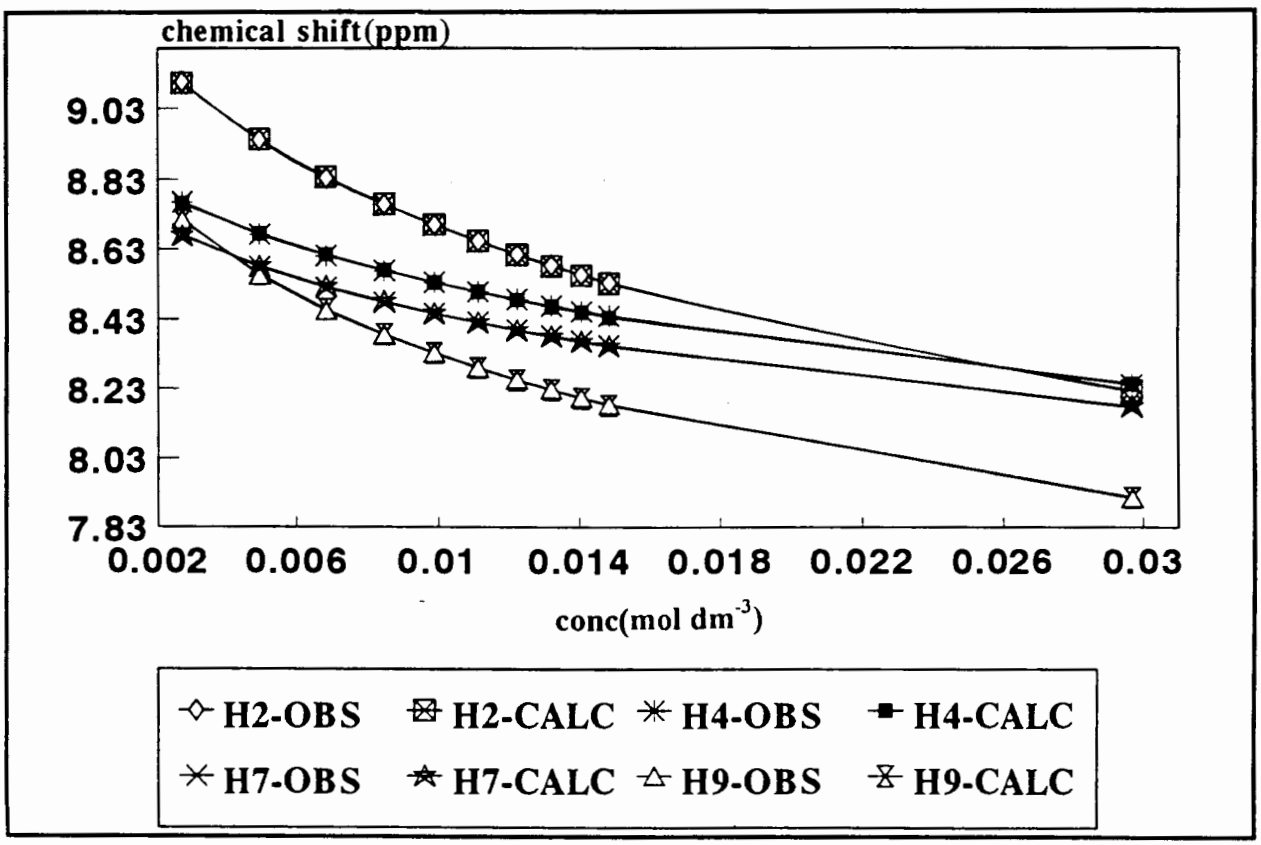

3.2.3 Temperature Dependence

All the complexes studied exhibit a general trend of downfield shift with increasing temperature. This is illustrated for [Pt(phen)DiBuBTu]$^{+}PF_6^{-}$ in Figure 3.14, which shows a plot of chemical shift *vs.* temperature. As an example, the experimental temperature dependencies of the diimine protons of [Pt(phen)DiBuBTu]$^{+}PF_6^{-}$ in acetonitrile-d_3 are summarised in Figure 3.15 which shows the ^1H NMR spectra over the temperature range 25-55 °C. Disaggregation of the complexes occurred with increasing temperature which is reflected in downfield shifts as more monomer is formed. Those protons which experienced the largest temperature induced chemical shifts, were those most affected by self-association (i.e. protons on the diimine moiety of the complex).

Figure 3.14: Graphical representation of chemical shift (ppm) *vs.* temperature (K) for [Pt(phen)-DiBuBTu]$^{+}PF_6^{-}$ illustrating the downfield shift of the diimine proton resonances with increasing temperature (at fixed complex concentration)

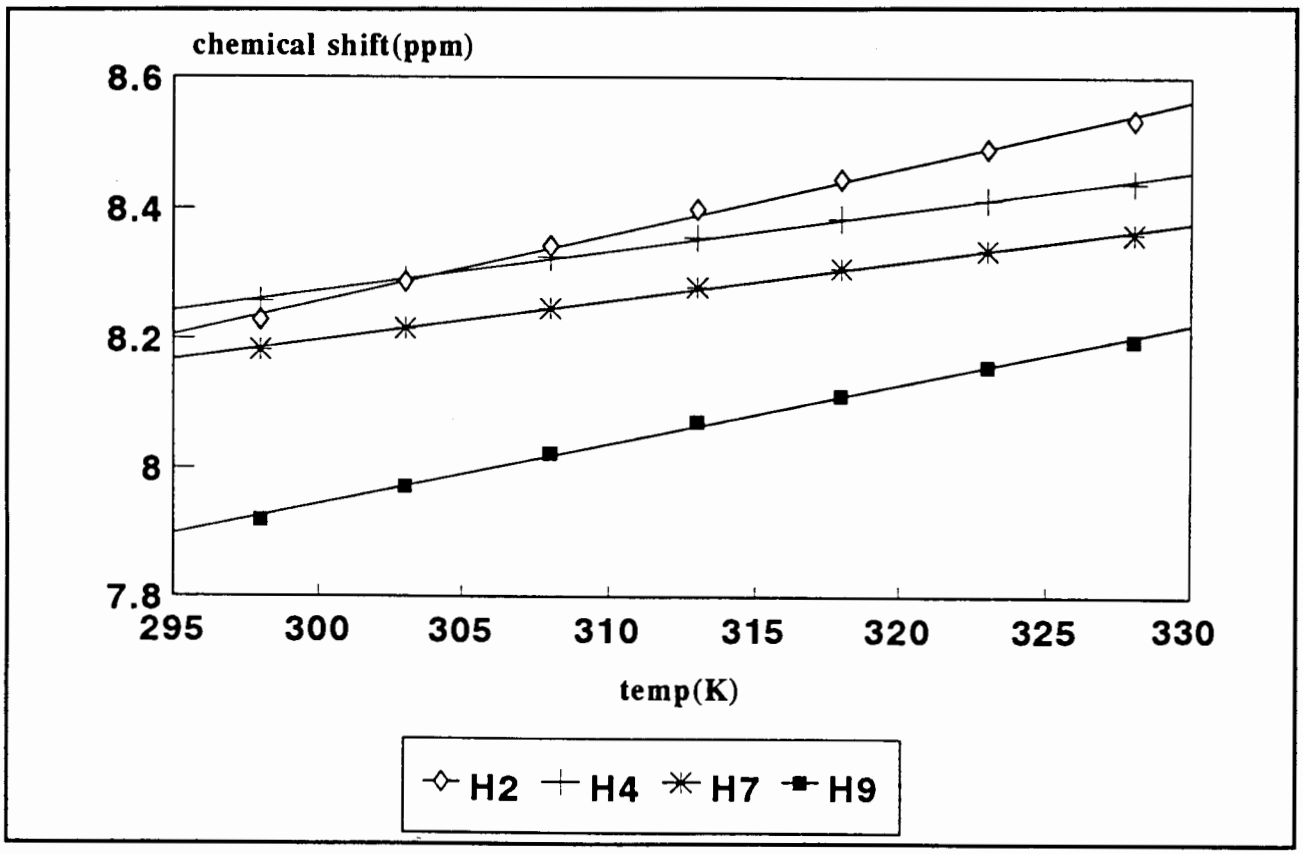

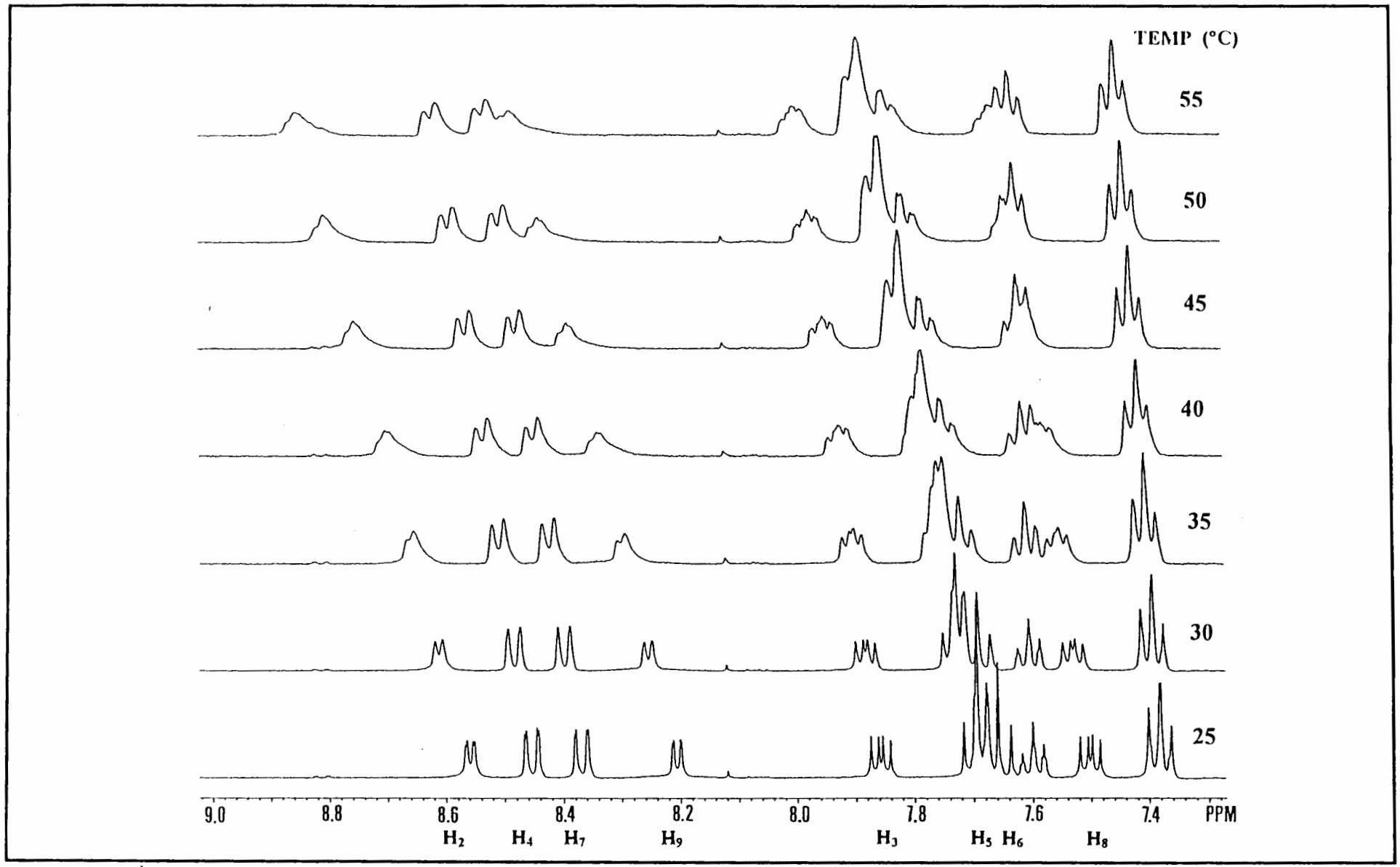

Figure 3.15: ^{1}H NMR spectra of the aromatic region of [Pt(phen)DiBuBTu]$^{+}PF_6^{-}$ in acetonitrile-d_3 in the temperature range 25-55 °C

The dimerisation reaction is as follows:

$$2[Pt(diimine)(L\text{-}S,O)]^{+}PF_6^{-} \overset{K^D}{\rightleftharpoons} \{[Pt(diimine)(L\text{-}S,O)]_2\}^{2+}(PF_6^{-})_2 \qquad \text{(Equation 1)}$$

At low temperatures sharp peaks are observed. This is indicative of a fast rate of exchange between the monomer and dimer species. However, as illustrated in Figure 3.15, at higher temperatures some of the peaks, particularly those of the diimine moiety, become broader. The reasons for this are not clear, but it is suggested that some form of conformational change occurs. Increased temperatures have been observed to cause changes in nucleoside dimer conformations[114]. In this regard it may be significant that complexes with *N,N*-di(*n*-butyl)-*N'*-naphthoylthiourea ligands appear to be more affected by an increase in temperature. This is manifested by significantly greater broadening of the ^{1}H NMR peaks in comparison to complexes with *N,N*-di(*n*-butyl)-*N'*-benzoylthiourea ligands.

The temperature induced chemical shifts for the diimine protons of all the platinum(II) complexes studied, are found in Appendix 7.3 (Chapter 7).

3.2.3.1 The effect of temperature on the ^{1}H NMR chemical shifts of [Pt(phen)DiBuBTu]$^+$PF$_6^-$, [Pt(phen)DiBuNTu]$^+$PF$_6^-$, [Pt(4,7-diphenylphen)DiBuBTu]$^+$PF$_6^-$ and [Pt(4,7-diphenylphen)DiBuNTu]$^+$PF$_6^-$

The effect of temperature on the ^{1}H NMR chemical shifts of [Pt(phen)DiBuBTu]$^+$PF$_6^-$, [Pt(phen)-DiBuNTu]$^+$PF$_6^-$, [Pt(4,7-diphenylphen)DiBuBTu]$^+$PF$_6^-$ and [Pt(4,7-diphenylphen)DiBuNTu]$^+$PF$_6^-$ was investigated. The temperature induced chemical shifts of the diimine protons of [Pt(phen)DiBuBTu]$^+$PF$_6^-$ are represented Figure 3.14, which clearly demonstrates the downfield shift of the proton resonances. As was observed in the concentration study, H_2 and H_9 of [Pt(phen)DiBuBTu]$^+$PF$_6^-$, experienced larger induced chemical shifts in comparison to those experienced by the other diimine protons. This was generally observed in studies on all four complexes. The overall temperature effects on the chemical shifts of the above platinum(II) complexes varies greatly, as can be seen in Table 3.12.

Table 3.12: ^{1}H NMR Chemical shift data showing the overall downfield chemical shifts over the temperature range 25-55 °C (in acetonitrile -d_3 at fixed complex concentration)

COMPLEX	^{1}H NMR CHEMICAL SHIFTS (ppm)							
	H_2	H_3	H_4	H_5	H_6	H_7	H_8	H_9
	T_{25}^a T_{55}^b	T_{25}^a T_{55}^b	T_{25}^a T_{55}^b	T_{25}^a T_{55}^b	T_{25}^a T_{55}^b	T_{25}^a T_{55}^b	T_{25}^a T_{55}^b	T_{25}^a T_{55}^b
(a) $[Pt(phen)DiBuBTu]^+PF_6^-$ [d]	8.228 8.535	7.683 7.837	8.257 8.439	7.486 *h*	7.435 *h*	8.182 8.361	7.328 7.499	7.919 8.197
$\Delta\delta^c$	**0.307**	**0.154**	**0.182**			**0.179**	**0.171**	**0.278**
(b) $[Pt(phen)DiBuNTu]^+PF_6^-$ [e]	8.983 *h*	*h*	8.832 8.864	8.176 8.205	8.134 8.165	8.812 8.845	*h*	8.964 *h*
$\Delta\delta^c$			**0.032**	**0.029**	**0.031**	**0.033**		
(c) $[Pt(4,7\text{-diphenylphen})DiBuBTu]^+PF_6^-$ [f]	9.012 9.199	8.012 8.099		7.997 8.070	7.925 8.002		7.717 7.801	8.604 8.798
$\Delta\delta^c$	**0.187**	**0.087**		**0.073**	**0.077**		**0.084**	**0.194**
(d) $[Pt(4,7\text{-diphenylphen})DiBuNTu]^+PF_6^-$ [g]	8.801 8.934	7.806 7.877		*h*	*h*		7.743 7.839	8.768 8.920
$\Delta\delta^c$	**0.133**	**0.071**					**0.096**	**0.152**

a: T_{25} = lowest temperature at which ^1H chemical shift data is measured is 25 °C
b: T_{55} = highest temperature at which ^1H chemical shift data is measured is 55 °C
c: $\Delta\delta$ = chemical shift difference $\delta(T_{55}) - \delta(T_{25})$
d: $[Pt(phen)DiBuBTu]^+PF_6^-$: concentration = $2.970x10^{-2}$ mol dm^{-3}
e: $[Pt(phen)DiBuNTu]^+PF_6^-$: concentration = $2.861x10^{-3}$ mol dm^{-3}
f: $[Pt(4,7\text{-diphenylphen})DiBuBTu]^+PF_6^-$: concentration = $6.102x10^{-3}$ mol dm^{-3}
g: $[Pt(4,7\text{-diphenylphen})DiBuNTu]^+PF_6^-$: concentration = $5.304x10^{-3}$ mol dm^{-3}
h: due to overlapping peaks accurate assignment is not possible

Table 3.13: ^{1}H NMR Chemical shift data showing the overall downfield chemical shifts over the temperature range 25 - 55 °C (in acetonitrile -d_3 at fixed complex concentration)

COMPLEX	^{1}H NMR CHEMICAL SHIFTS (ppm)											
	$H_{3'}$		H_3		$H_{4'}$		H_4		$H_{5'}$		H_5		$H_{6'}$		H_6	
	T_{25}^a	T_{55}^b	T_{25}^a	T_{55}^b	T_{25}^a	T_{55}^b	T_{25}^a	T_{55}^b	T_{25}^a	T_{55}^b	T_{25}^a	T_{55}^b	T_{25}^a	T_{55}^b	T_{25}^a	T_{55}^b
(a) $[Pt(bipy)DiBuBTu]^+PF_6^-$ [d]	8.213	*g*	8.146	*g*	8.292	8.355	8.202	*g*	7.897	7.952	7.550	*g*	8.982	9.087	8.543	8.633
$\Delta\delta^c$					**0.063**				**0.055**				**0.105**		**0.090**	
(b) $[Pt(4,4'\text{-dimethylbipy})DiBuNTu]^+PF_6^-$ [e]	8.055	8.095	8.038	8.075					*g*		*g*		8.465	8.539	8.398	8.485
$\Delta\delta^c$	**0.040**		**0.037**										**0.074**		**0.087**	
(c) $[Pt(4,4'\text{-ditbutbipy})DiBuBTu]^+PF_6^-$ [f]	8.267	8.303	8.178	8.221					7.858	*g*	7.505	*g*	8.834	8.920	8.342	8.451
$\Delta\delta^c$	**0.036**		**0.043**										**0.086**		**0.109**	

a: T_{25} = lowest temperature at which ^1H chemical shift data is measured is 25 °C
b: T_{55} = Highest temperature at which ^1H chemical shift data is measured is 55 °C
c: $\Delta\delta$ = chemical shift difference $\delta(T_{55}) - \delta(T_{25})$
d: $[Pt(bipy)DiBuBTu]^+PF_6^-$: concentration = $7.463x10^{-3}$ mol dm^{-3}
e: $[Pt(4,4'\text{-dimethylbipy})DiBuNTu]^+PF_6^-$: concentration = $7.785x10^{-3}$ mol dm^{-3}
f: $[Pt(4,4'\text{-ditbutbipy})DiBuBTu]^+PF_6^-$: concentration = $1.747x10^{-2}$ mol dm^{-3}
g: due to overlapping peaks accurate assignment is not possible

3.2.3.2 The effect of temperature on the ^1H NMR chemical shifts of [Pt(bipy)DiBuBTu]$^+PF_6^-$, [Pt(4,4'-dimethylbipy)DiBuNTu]$^+PF_6^-$ and [Pt(4,4'-ditbutbipy)DiBuBTu]$^+PF_6^-$

The temperature related chemical shifts observed for the diimine protons of [Pt(bipy)DiBuBTu]$^+PF_6^-$, [Pt(4,4'-dimethylbipy)DiBuNTu]$^+PF_6^-$ and [Pt(4,4'-ditbutbipy)-DiBuBTu]$^+PF_6^-$ were small, as summarised in Table 3.13. This implies that significant dissociation of the 'dimer" did not occur.

3.2.4 Calculation of K^D

Temperature effects on the dimerisation constant, K^D, were determined by measuring the change in downfield shifts of the protons with increasing temperature. For each complex, a series of temperature arrayed experiments was carried out at different concentrations of the complex in acetonitrile-d_3 (ranging from five to eight). Association constants could thus be determined for a range of temperatures (25-55 °C, at 5 °C intervals).

As mentioned previously, significant line broadening was observed at higher temperatures. This caused large errors in δ_i measurements, and hence large errors in K^D were found. This also resulted in variation of the K^D values at higher temperatures. The dissociation constant is related to the fraction of dimers present in solution and Figure 3.16 illustrates the deviation from linearity at high temperatures.

Figure 3.16: Graphical representation of chemical shift (ppm) *vs.* fraction of dimer present (x_i) for [Pt(phen)DiBuBTu]$^+PF_6^-$ at various temperatures

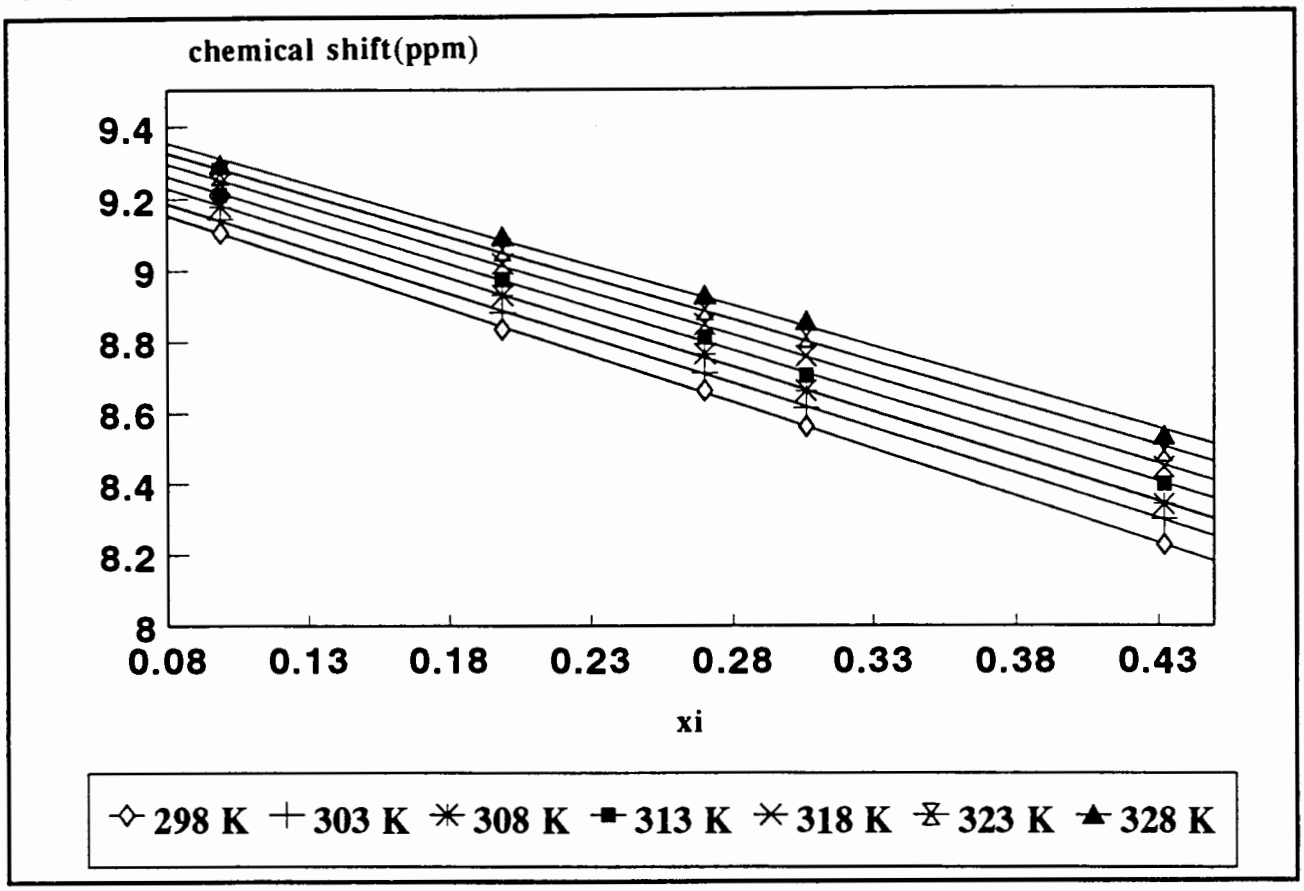

The difference between resonance shifts of protons at high (55 °C) and low (25 °C) temperatures ($\delta(T_{55}) - \delta(T_{25})$) decreased, as the concentration of the complex in the solution decreased. This suggests that the degree of dissociation is greatest when a large fraction of dimers is present in the solution. At lower concentrations fewer dimers are present. An increase in temperature thus results in a smaller downfield chemical shift.

3.2.4.1 Dimerisation constants for [Pt(phen)DiBuBTu]$^+PF_6^-$, [Pt(4,7-diphenylphen)-DiBuBTu]$^+PF_6^-$ and [Pt(4,7-diphenylphen)DiBuNTu]$^+PF_6^-$

Table 3.14: Calculated K^D values for [Pt(phen)DiBuBTu]$^+PF_6^-$ in the temperature range 25-55 °C

TEMP °C	PROTON					
	H_2			H_9		
	K^D dm^3 mol^{-1}	LOWER LIMIT	UPPER LIMIT	K^D dm^3 mol^{-1}	LOWER LIMIT	UPPER LIMIT
25	22.73	20.62	24.94	28.66	25.66	31.82
30	22.12	20.16	24.18	27.47	24.96	30.10
35	20.48	18.30	22.80	26.50	23.60	29.56
40	20.23	17.11	23.60	25.66	21.71	29.93
45	18.34	17.30	19.42	22.51	21.04	24.03
50	15.87	14.16	17.67	20.68	18.49	23.00
55	14.33	12.22	16.59	16.13	15.02	17.29

Table 3.15: Calculated K^D values for [Pt(4,7-diphenylphen)DiBuBTu]$^+PF_6^-$ in the temperature range 25-55 °C

TEMP °C	PROTON					
	H_2			H_9		
	K^D dm^3 mol^{-1}	LOWER LIMIT	UPPER LIMIT	K^D dm^3 mol^{-1}	LOWER LIMIT	UPPER LIMIT
25	144.0	131.3	157.1	160.6	145.4	176.3
30	135.5	125.2	146.1	151.5	142.8	160.4
35	110.4	101.9	119.1	123.5	114.7	132.6
40	84.88	71.99	98.64	94.05	81.77	107.0
45	68.28	40.89	101.1	78.34	50.50	111.0
50	70.66	41.88	105.3	72.72	43.03	108.4
55	78.99	57.74	102.9	91.34	68.02	115.2

Table 3.16: Calculated K^D values for H_8 of $[Pt(4,7\text{-diphenylphen})DiBuNTu]^+PF_6^-$ in the temperature range 25-55 °C

TEMP °C	K^D $dm^3\ mol^{-1}$	LOWER LIMIT	UPPER LIMIT
25	78.99	71.43	86.81
30	70.08	55.88	85.38
35	66.07	48.29	85.67
40	58.01	43.32	74.04
45	47.52	31.79	65.09
50	66.00	51.62	81.55
55	56.52	33.23	83.52

3.2.4.2 Dimerisation constants for $[Pt(bipy)DiBuBTu]^+PF_6^-$, $[Pt(4,4'\text{-dimethylbipy})\text{-}DiBuNTu]^+PF_6^-$ and $[Pt(4,4'\text{-ditbutbipy})DiBuBTu]^+PF_6^-$

Table 3.17: Calculated K^D values for H_6, of $[Pt(bipy)DiBuBTu]^+PF_6^-$ in the temperature range 25-55 °C

TEMP °C	K^D $dm^3\ mol^{-1}$	LOWER LIMIT	UPPER LIMIT
25	9.701	4.649	15.40
30	5.585	2.027	9.544
35	4.227	1.287	7.463
40	3.370	0.649	6.364
45	5.057	3.269	6.944
50	6.555	4.280	8.978
55	3.383	1.073	5.883

Table 3.18: Calculated K^D values for H_6 of $[Pt(4,4'\text{-dimethylbipy})DiBuNTu]^+PF_6^-$ in the temperature range 25-55 °C

TEMP °C	K^D $dm^3\ mol^{-1}$	LOWER LIMIT	UPPER LIMIT
25	5.915	8.402	11.02
30	3.396	7.462	11.91
35	2.933	7.656	12.89
40	1.578	5.761	10.38
45	0.000	3.804	12.07
50	*a*		
55	*a*		

a. due to significant broadening of the ^1H NMR peaks of $[Pt(4,4'\text{-dimethylbipy})DiBuNTu]^+PF_6^-$ accurate determinations of the association constants were not possible

Table 3.19: Calculated K^D values for H_6 of $[Pt(4,4'\text{-ditbutbipy})DiBuBTu]^+PF_6^-$ in the temperature range 25-55 °C

TEMP °C	K^D $dm^3\ mol^{-1}$	LOWER LIMIT	UPPER LIMIT
25	19.63	17.05	22.34
30	16.21	14.29	18.22
35	14.19	11.29	17.32
40	13.37	9.103	18.21
45	12.44	9.328	15.85
50	8.092	3.399	13.80
55	0.000	0.000	4.106

3.2.5 Thermodynamic Parameters

The thermodynamic parameters of molecular self-association were determined from observed temperature dependencies of the ^{1}H NMR chemical shifts of the platinum(II) complexes. The dimerisation constants were determined for six [Pt(diimine)(*N*,*N*-di(*n*-butyl)-*N'*-acyl-thioureato)]$^+PF_6^-$ complexes at different temperatures. From a plot of lnK *vs.* 1/T, entropy (ΔS), enthalpy (ΔH) and Gibb's free energy (ΔG) were estimated using van't Hoff's equation:

$$\mathbf{lnK = \Delta S/R - \Delta H/RT} \qquad \text{(Equation 10)}$$

As observed from the van't Hoff plot for [Pt(phen)DiBuBTu]$^+PF_6^-$ (Figure 3.17) a considerable degree of scattering about the line is observed. The error bars associated with each K^D value (within 95% confidence limits) give an indication of the degree of error associated with K^D.

Figure 3.17: Graphical representation of lnK *vs.* T^{-1} for [Pt(phen)DiBuBTu]$^+PF_6^-$ with the upper and lower limits for each K^D value (within 95% confidence limits)

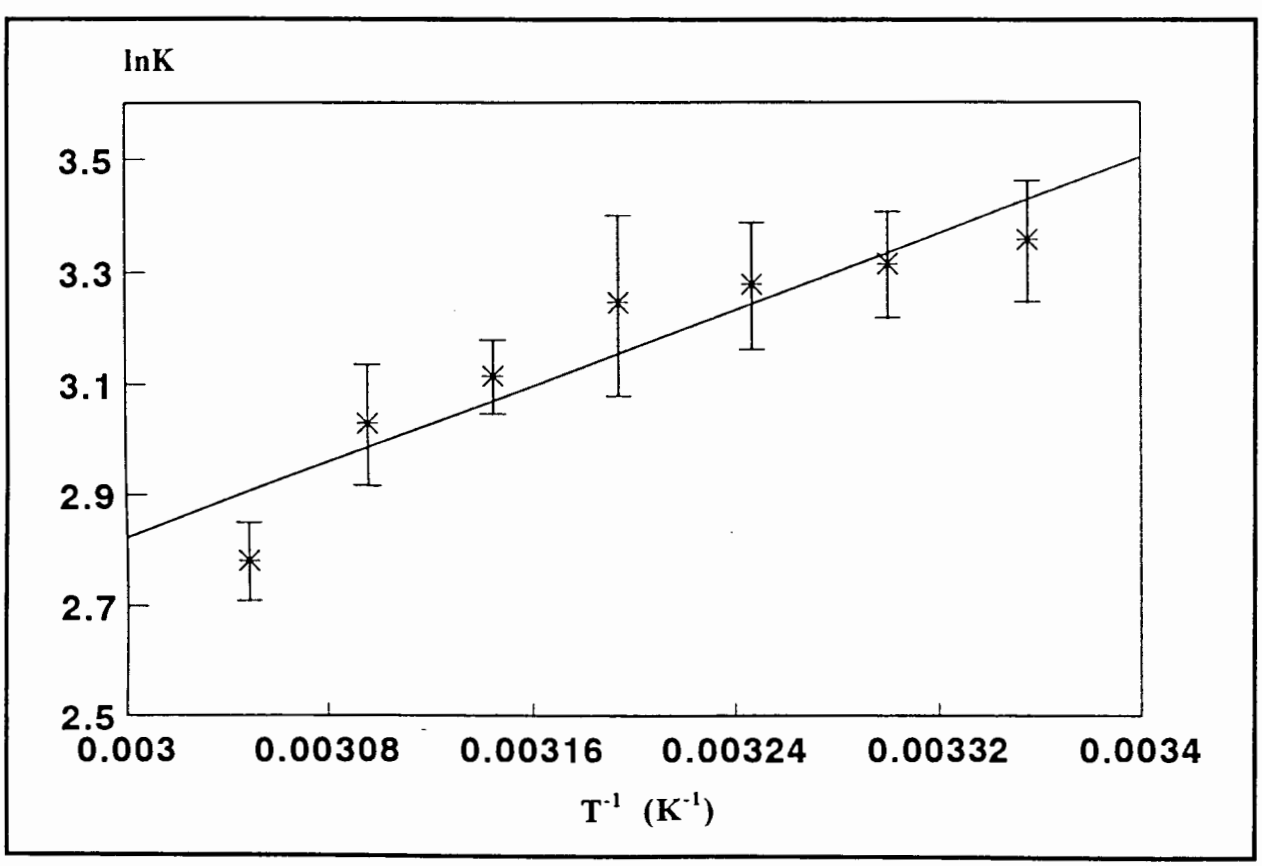

Gibbs's free energy (ΔG) values calculated using

$$\Delta G = RT\ln K \qquad \text{(Equation 11)}$$

compare favourably with those values determined from van't Hoff plots. The thermodynamic parameters determined for the platinum(II) complexes are summarised in Table 3.20 together with the average dimerisation constant for each complex.

Table 3.20: Thermodynamic constants determined for [Pt(diimine)(*N,N*-di(*n*-butyl)-*N'*-acyl-thioureato)]$^+PF_6^-$ complexes

COMPLEX	K^D / dm^3 mol^{-1}	ΔG^a / kJ mol^{-1}	ΔG^b / kJ mol^{-1}	ΔH^b / kJ mol^{-1}	ΔS^b / J K^{-1} mol^{-1}
[Pt(phen)DiBuBTu]$^+PF_6^-$	23.3 ± 3.3	-7.8	-7.9	-12.5	-15.4
[Pt(phen)DiBuNTu]$^+PF_6^-$	1 - 2	*c*			
[Pt(4,7-diphenylphen)DiBuBTu]$^+PF_6^-$	114 ± 18	-11.7	-12.5	-30.8	-61.3
[Pt(4,7-diphenylphen)DiBuNTu]$^+PF_6^-$	63 ± 8	-10.3	-10.9	-18.9	-27.1
[Pt(bipy)DiBuBTu]$^+PF_6^-$	2.7 ± 0.6	-2.5	-4.8	-15.8	-37.0
[Pt(bipy)DiBuNTu]$^+PF_6^-$	*d*				
[Pt(4,4'-dimethylbipy)DiBuBTu]$^+PF_6^-$	*e*				
[Pt(4,4'-dimethylbipy)DiBuNTu]$^+PF_6^-$	6.7 ± 1.4	-4.7	-5.5	-28.8	-78.3
[Pt(4,4'-ditbutbipy)DiBuBTu]$^+PF_6^-$	28.0 ± 3.1	-7.8	-7.4	-24.1	-56.0
[Pt(4,4'-ditbutbipy)DiBuNTu]$^+PF_6^-$	1.7 ± 0.4	*c*			

a: calculated from -RTlnK
b: determined from van't Hoff plots
c: K^D too low for temperature dependence study
d: K^D below 3 dm^3 mol^{-1}
e: poor solubility resulted in varied K^D values
estimated errors: $\Delta H = \pm 10\%$, $\Delta S = \pm 20\%$, $\Delta G = \pm 20\%$ determined from linear regression analysis

3.2.6 Solvent Study

As previously noted, the hydrophobic nature of aromatic molecules plays an important role in their self-association interactions in solution[32]. To illustrate this, we undertook a ^{1}H NMR concentration dependence experiment on [Pt(4,4'-ditbutbipy)DiBuNTu]$^+PF_6^-$ in acetonitrile-d_3. Aliquots of deuterium oxide were then added to the NMR tube containing a solution of the complex in 1.81 cm^3 acetonitrile-d_3, and the ^{1}H NMR spectrum recorded after each addition. A total of 0.25 cm^3 deuterium oxide was added before precipitation of the complex occurred.

Figure 3.18 illustrates graphically the upfield, concentration induced chemical shift of the complex protons in acetonitrile-d_3, and the significant upfield shifts on the addition of deuterium oxide (with subsequent dilution of the complex solution). This is also made evident in Table 3.21.

Table 3.21: ^{1}H NMR Chemical shift data of [Pt(4,4'-ditbutbipy)DiBuNTu]$^+PF_6^-$ in pure acetonitrile-d_3 and acetonitrile-d_3/deuterium oxide mixtures

CONC	^{1}H NMR CHEMICAL SHIFTS (ppm)			
mol dm^{-3}	**$H_{3'}$**	**H_3**	**$H_{6'}$**	**H_6**
acetonitrile-d_3				
4.697x10^{-3} [a]	8.362	8.319	8.670	8.603
1.774x10^{-2} [b]	8.310	8.268	8.592	8.525
Δδ	**0.052**	**0.051**	**0.078**	**0.078**
acetonitrile-d_3/deuterium oxide				
1.497x10^{-2} [a]	8.224	8.182	8.442	8.378
1.771x10^{-2} [b]	8.297	8.256	8.557	8.494
Δδ	**-0.073**	**-0.074**	**-0.115**	**-0.116**

a: lowest concentration at which ^{1}H NMR chemical shift data is measured
b: highest concentration at which ^{1}H NMR chemical shift data is measured
c: $\Delta\delta$ = chemical shift difference δ(Ca) - δ(Cb)

A plot of chemical shift *vs.* %D_2O, follows the same trend as that of chemical shift *vs.* concentration (i.e. an upfield resonance shift as %D_2O in the complex solution is increased) (Figure 3.19).

Figure 3.18: Graphical representation of chemical shift (ppm) *vs.* concentration (mol dm^{-3}) illustrating the effect of the addition of deuterium oxide to a solution of $[Pt(4,4'\text{-ditbutbipy})DiBuNTu]^{+}PF_6^{-}$ in acetonitrile-d_3

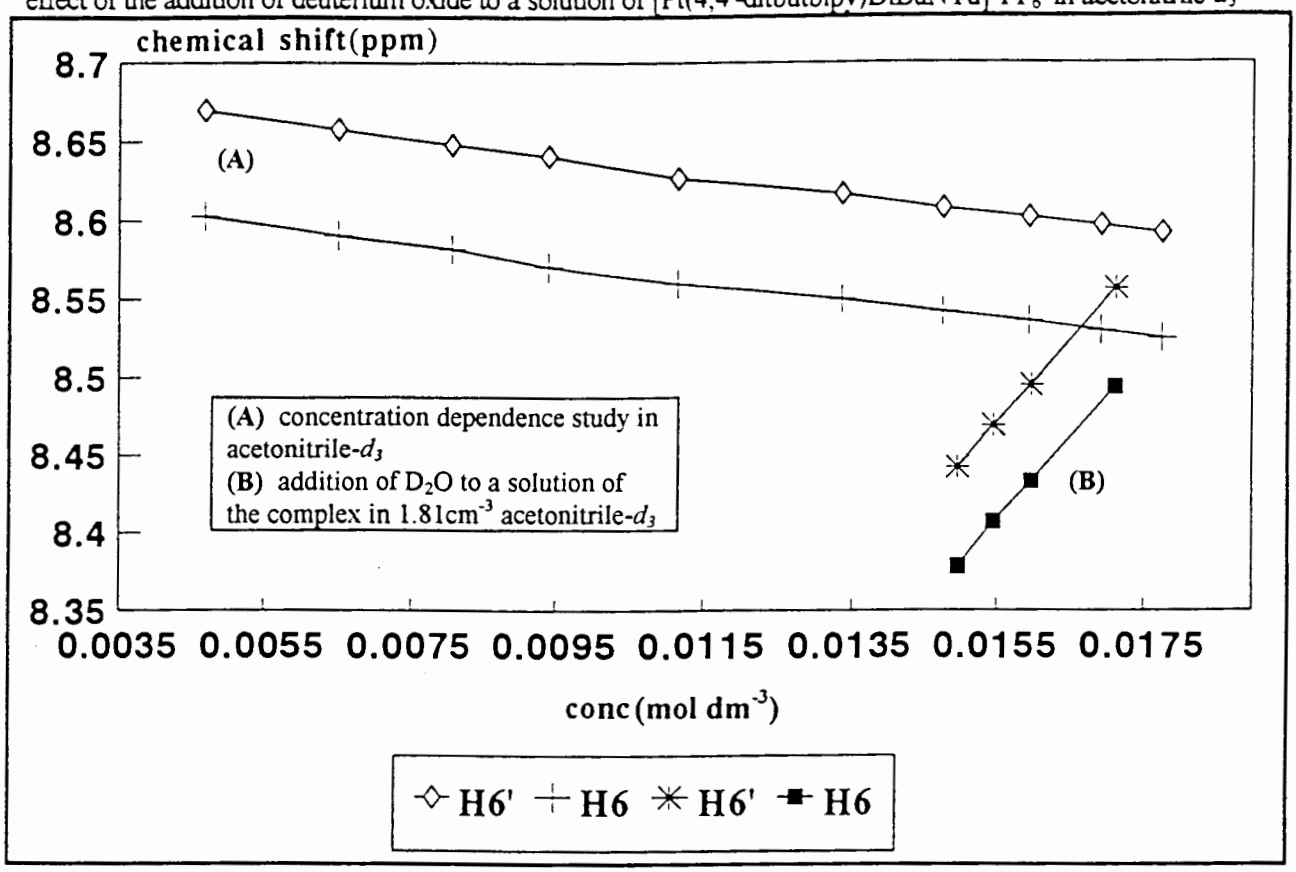

Figure 3.19: Graphical representation of chemical shift (ppm) *vs.* $\%D_20$ for $[Pt(4,4'\text{-ditbutbipy})\text{-}DiBuNTu]^{+}PF_6^{-}$

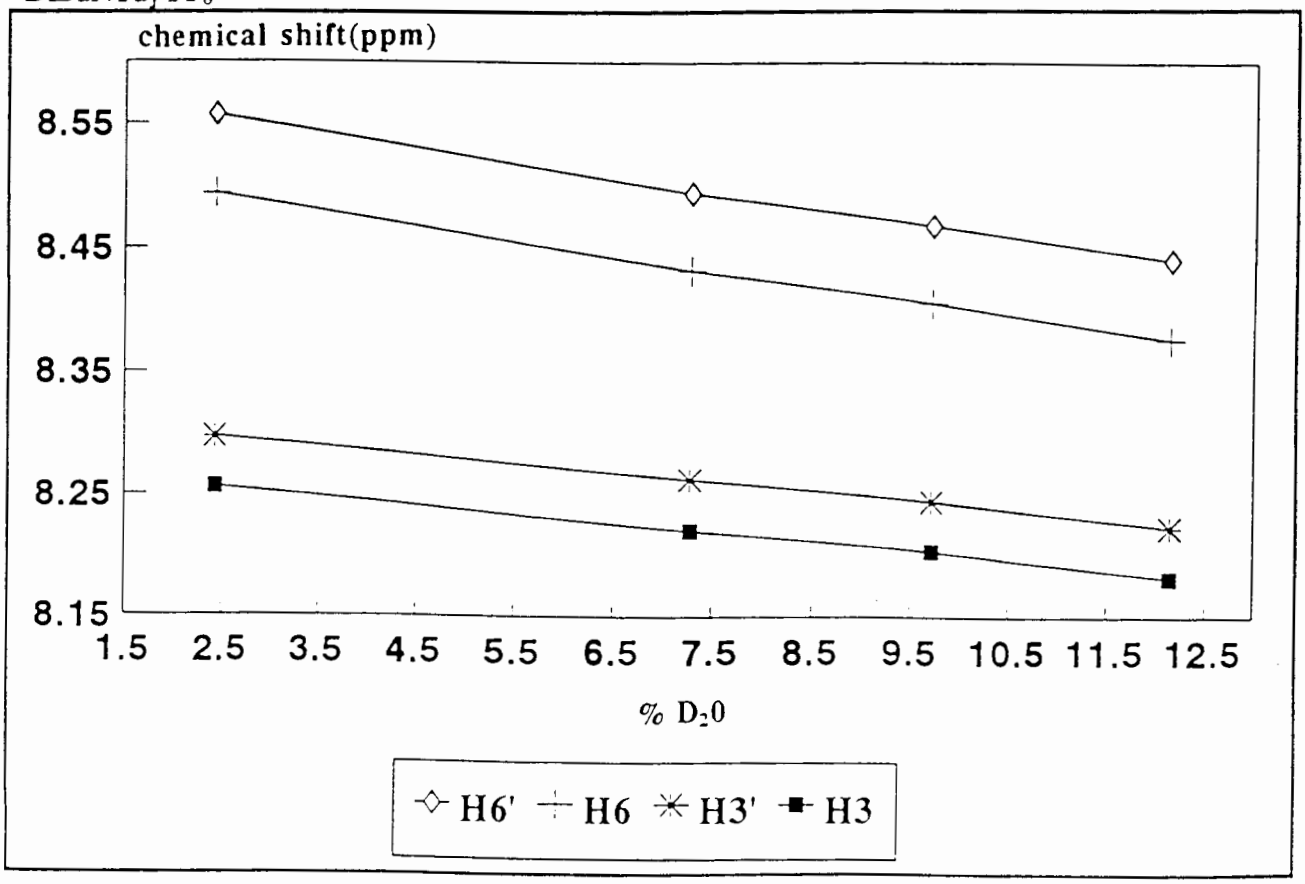

3.2.7 UV-Visible Spectroscopy

3.2.7.1 Introduction

Oligomerisation of d^8 complexes is well documented[12,23] and numerous association constants for aggregation interactions determined. The driving force for these associations is the formation of weak metal-metal bonds or hydrophobic stacking interactions between the ligands.

UV-visible spectroscopy has been used to determine association constants for various complexes[123,124]. In the determination of the association constants of (terpyridine)platinum(II) complexes, only the relative intensities of the electronic absorption bands were found to undergo change. The position of the bands remained constant[23]. Similarly, small changes were also observed for the dimerisation of bis(2,2'-bipyridyl)rhodium(I)[123]. This is in contrast to studies carried out on a series of isocyanide-rhodium complexes[124]. In these complexes, pronounced spectral shifts were found to occur due to the changes that occur in the energies of lowest unoccupied and highest occupied molecular orbitals when association takes place.

3.2.7.2 UV-visible Studies

In light of these findings, concentration dependence studies using UV-visible techniques were undertaken to determine association constants. The objective was to compare these results with those previously determined by ^{1}H NMR spectroscopy. Since ^{1}H NMR studies determined that [Pt(4,7-diphenylphen)DiBuBTu]$^+PF_6^-$ undergoes the strongest stacking interaction, the dimerisation of this complex and its naphthyl equivalent were studied.

The UV-visible spectrum of [Pt(4,7-diphenylphen)DiBuBTu]$^+PF_6^-$ in acetonitrile-d_3 (concentration, 8.865 x 10^{-6} mol dm^{-3}) possesses two intense bands at 230 nm (ε = 49 915 M^{-1} cm^{-1}) and 292 nm (ε = 56 417 M^{-1} cm^{-1}). The UV-visible spectrum of [Pt(4,7-diphenylphen)DiBuNTu]$^+PF_6^-$ in acetonitrile-d_3 (3.035 x 10^{-6} mol dm^{-3}), is very similar possessing two intense bands at 228 nm (ε = 82 388 M^{-1} cm^{-1}) and 296 nm (ε = 82 079 M^{-1} cm^{-1}). Unfortunately, these complexes exhibit intense UV-visible absorption bands, even at very low concentrations. Concentration dependence studies revealed that self-association at such low concentrations does not occur to an appreciable degree.

3.3 DISCUSSION

3.3.1 'Dimer' Model

The observed concentration dependence of the diimine proton chemical shifts of the platinum(II) mixed-ligand complexes, can only be explained in terms of molecular association. This can be attributed to the anisotropic shielding effect of the ring current from one diimine moiety of the aggregate upon its neighbour[108]. Molecular association is also supported by the observation of a decrease in proton chemical shift resonances with increasing temperature (at fixed complex concentration). This confirms that an associative/dissociative equilibrium exists. The occurrence of downfield chemical shifts with monomer formation is predicted since dissociation of the 'aggregate' is accompanied by a decrease in the anisotropic shielding effect.

The simplest self-association interaction is dimer formation which can be represented as follows:

$$2[\text{Pt(diimine)(L-}S,O)]^{+}PF_6^{-} \overset{K^D}{\rightleftharpoons} \{[\text{Pt(diimine)(L-}S,O)]_2\}^{2+}(PF_6^{-})_2 \qquad \text{(Equation 1)}$$

Initially only dimer formation was assumed to occur, and a method by Horman and Deux[119] employed to determine association constants. Since, the data appeared to fit the model extremely well, our assumption of only monomers and dimers existing in solution (under the experimental conditions outlined), proved to be correct.

The diimine proton chemical shifts were affected by concentration and temperature changes, while those of the benzyl or naphthyl group on the *N,N*-di(*n*-butyl)-*N'*-acylthiourea moiety of the complex did not appear to undergo significant changes. This suggests a regioselective interaction whereby only the diimine moiety of the complex is involved in the dimerisation process. By applying the rules determined by Hunter and Sanders[60] for favourable π-π interactions, a 'dimer' model can be postulated and is represented in Figure 3.20.

Figure 3.20 : Side-view of a [Pt(diimine)(*N,N*-di(*n*-butyl)-*N'*-acylthioureato)]$^+PF_6^-$ 'dimer', illustrating the regioselective interaction between the two diimine moieties of the monomers

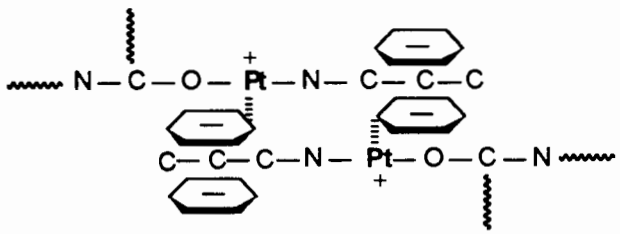

Additional evidence that the dimerisation model can be used to explain self-association occurring in solutions of our mixed-ligand platinum(II) complexes is provided below.

The temperature dependence of proton chemical shifts suggests that the platinum(II) complexes associate to form parallel dimers, and that the process is exothermic. Molecular association is also supported by the pronounced effect of solvent on the ^{1}H NMR chemical shifts.

Furthermore, (+)FAB mass spectra for selected platinum complexes, displayed peaks corresponding to monomeric and dimeric species only. Hence, these studies suggest that these molecules associate intermolecularly to form only dimers in solution as well as in the gas phase. The (+)FAB data for [Pt(bipy)DiBuBTu]$^+PF_6^-$ illustrates this: [Pt(N-N)(L-*S,O*)]$^+$ calc: 642.8 obs: 642.1; {[Pt(N-N)(L-*S,O*)]$_2$}$^{2+}$ (PF_6^-) calc: 1430.6 obs: 1428.7.

Excellent correlation was found between observed and calculated chemical shifts. This was found to be true for all the complexes studied and adds further evidence to the assumption that these platinum(II) complexes associate to form only dimers in solution.

A plot of observed chemical shift (δ_i) of the diimine protons *vs.* fraction of dimers present in solution (x_i), at a specific concentration and temperature, is linear. This only occurs if no higher aggregates are present, since the equation used to calculate the dimerisation constant would then no longer hold true.In addition, van't Hoff plots exhibit a linear relationship and this provides further evidence that the association constants calculated at different temperatures are correct.

3.3.2 Calculation of K^D

3.3.2.1 Comparison of dimerisation constants for [Pt(phen)DiBuBTu]$^+PF_6^-$, [Pt(phen)-DiBuNTu]$^+PF_6^-$, [Pt(4,7-diphenylphen)DiBuBTu]$^+PF_6^-$ and [Pt(4,7-diphenylphen)-DiBuNTu]$^+PF_6^-$

For all four complexes [Pt(phen)DiBuBTu]$^+PF_6^-$, [Pt(phen)DiBuNTu]$^+PF_6^-$, [Pt(4,7-diphenylphen)-DiBuBTu]$^+PF_6^-$ and [Pt(4,7-diphenylphen)DiBuNTu]$^+PF_6^-$, the H_2 and H_9 protons on the diimine moiety of the complex, experienced the largest upfield chemical shifts. In each case the shifts were of nearly equal magnitude. This dependence of ^1H chemical shifts is conceivable if a vertical stacking interaction occurs, in which the neighbouring diimine ligands overlap resulting in similar magnetic environments for H_2 and H_9. This will result in similar magnetic environments for H_4, H_7 and H_3, H_8.

Substituents on the diimine moiety, appear to have a significant effect on the degree of self-association. This is evident from varying association constants determined (Table 3.22).

Table 3.22: Average association constants determined in acetonitrile-d_3 at 25 °C

COMPLEX	K^D (dm^3 mol^{-1})
[Pt(phen)DiBuBTu]$^+PF_6^-$	23.28 ± 3.29
[Pt(phen)DiBuNTu]$^+PF_6^-$	1-2
[Pt(4,7-diphenylphen)DiBuBTu]$^+PF_6^-$	114.1 ± 18.7
[Pt(4,7-diphenylphen)DiBuNTu]$^+PF_6^-$	63.46 ± 8.06

Studies on tris(1,10-phenanthroline)ruthenium(III) complexes have shown that the 4,7-diphenyl-1,10-phenanthroline moiety of the complex is constrained to be nonplanar due to unfavourable steric interactions involving H_5 and H_6 and the ortho-protons of the phenyl substituents[125]. From the magnitude of their association constants, H_5 and H_6 in [Pt(4,7-diphenylphen)DiBuBTu]$^+PF_6^-$ and [Pt(4,7-diphenylphen)DiBuNTu]$^+PF_6^-$ appear to be less involved in the association interaction. This is possibly due to the presence of bulky phenyl groups at the 4 and 7 position of 1,10-phenanthroline interfering in the self-association interaction. The protons H_2 and H_3 both have lower K^D values than H_8 and H_9.

Since the phenyl rings of [Pt(4,7-diphenylphen)DiBuBTu]$^+PF_6^-$ are not in the plane of the complex, a low dimerisation constant would be expected. This is due to an unfavourable steric interaction occurring between the protons on the phenyl substituents and the phenyl ring of *N,N*-di(*n*-butyl)-*N'*-benzoylthiourea. Hence, the finding that the dimerisation constant of [Pt(4,7-diphenylphen)-DiBuBTu]$^+PF_6^-$ is five times that of [Pt(phen)DiBuBTu]$^+PF_6^-$ indicates that despite possible steric hindrances of the large phenyl groups, dimerisation is favoured in the former complex (Table 3.22). The prediction that an increase in π-surface will increase the association interaction is found to be true.

In intercalation studies of tris(4,7-diphenyl-1,10-phenanthroline)ruthenium(II), Barton *et al* have shown a strong tendency of the complex to intercalate into DNA despite non-planarity of the 4,7-diphenyl-1,10-phenanthroline moiety[126]. Wilson *et al* have demonstrated that molecules with unfused phenyl substituents can intercalate into DNA even though the binding affinity is lessened[31]. DNA is able to accommodate a certain amount of intrinsic twist of the intercalator ligands. In addition 4,7-diphenyl-1,10-phenanthroline may be more favoured than 1,10-phenanthroline for intercalation into the DNA-helix[32].

As previously mentioned, molecular shape is the most important factor which must be considered when designing a potential intercalator (Chapter 1.2). Therefore, the extended π-system of [Pt(4,7-diphenylphen)DiBuBTu]$^+PF_6^-$ is seen to counteract any decrease in self-association due to possible steric hindrances of its phenyl substituents, preventing close association of the monomeric units. In solution the free rotation of the phenyl groups about their bonds in a dynamic equilibrium might also lessen the steric factors.

The dimerisation constant for [Pt(phen)DiBuNTu]$^+PF_6^-$ could not be accurately determined due to its poor solubility in acetonitrile-d_3. It is estimated to be between 1-2 $dm^3\ mol^{-1}$. Therefore, dimerisation can be said to be negligible under these experimental conditions.

The nature of the *N,N*-di(*n*-butyl)-*N'*-acylthiourea ligand influences the magnitude of the dimerisation constants. Substitution of the benzyl for a naphthyl group has the effect of lowering the association constants determined. The naphthyl group therefore, does not appear to add stability to the dimer structure. However, its effect is not as great as that of altering the diimine

moiety of the complex. The average association constant for [Pt(4,7-diphenylphen)DiBuNTu]$^+PF_6^-$ is given in Table 3.22, showing that the dimerisation constant for this complex is almost less than half that of [Pt(4,7-diphenylphen)DiBuBTu]$^+PF_6^-$. Similarly, the association constant for [Pt(phen)-DiBuNTu]$^+PF_6^-$ is considerably lower than that for [Pt(phen)DiBuBTu]$^+PF_6^-$. This shows that variations on the *N,N*-di(*n*-butyl)-*N'*-acylthiourea moiety of the complex do affect the self-association interaction even though it is not thought to be directly involved in the association.

3.3.2.2 Comparison of dimerisation constants for [Pt(bipy)DiBuBTu]$^+PF_6^-$, [Pt(4,4'-dimethylbipy)DiBuNTu]$^+PF_6^-$, [Pt(4,4'-ditbutbipy)DiBuBTu]$^+PF_6^-$ and [Pt(4,4'-ditbutbipy)DiBuNTu]$^+PF_6^-$

$H_{6'}$ and H_6 of [Pt(bipy)DiBuBTu]$^+PF_6^-$, [Pt(4,4'-dimethylbipy)DiBuNTu]$^+PF_6^-$, [Pt(4,4'-ditbutbipy)-DiBuBTu]$^+PF_6^-$ and [Pt(4,4'-ditbutbipy)DiBuNTu]$^+PF_6^-$ undergo the greatest changes in chemical shifts which were again of similar magnitude (similarly $H_{5'}$ and H_5). These upfield shifts of the diimine proton resonances are due to anisotropic shielding effects. This is explained by a parallel, vertical stacking interaction between two monomers, resulting in similar magnetic environments for $H_{6'}$ and H_6.

We chose to study 4,4'-substituted 2,2'-bipyridyl platinum(II) complexes in an attempt to investigate the effect of electron density on the self-association interaction. The dimerisation constants determined are represented in Table 3.23.

Table 3.23: Average association constants determined in acetonitrile-d_3 at 25 °C

COMPLEX	K^D ($dm^3\ mol^{-1}$)
[Pt(bipy)DiBuBTu]$^+PF_6^-$	2.7 ± 0.6
[Pt(4,4'-dimethylbipy)DiBuNTu]$^+PF_6^-$	6.7 ± 1.4
[Pt(4,4'-ditbutbipy)DiBuBTu]$^+PF_6^-$	28.0 ± 3.1
Pt(4,4'-ditbutbipy)DiBuNTu]$^+PF_6^-$	1.7 ± 0.4

Steric factors could be expected to play a significant role in the magnitude of the association constants for the various complexes. Lower association constants for [Pt(4,4'-ditbutbipy)DiBuBTu]$^+PF_6^-$ and [Pt(4,4'-ditbutbipy)DiBuNTu]$^+PF_6^-$ were predicted on the

assumption that the bulky *tert*-butyl groups of 4,4'-di-*tert*-butyl-2,2'-bipyridyl, would inhibit the close association of two monomeric units. Substituting the *tert*-butyl group with a less bulky methyl was expected to have less of destabilising effect on the dimer structure.

The alkylpyridines are stronger bases than pyridine due to the inductive effect of the alkyl groups[127]. This suggests that σ-bonding arising from lone-pair donation between nitrogen (diimine) and platinum will be enhanced in the 4,4'-substituted bipyridyl complexes. This also allows for increased dπ-pπ back donation of electron density from the filled metal orbitals to the aromatic ring (Figure 3.21). The platinum atom is therefore left with a large δ+ charge and the π-ring with a δ- charge.

Figure 3.21: Bonding between platinum and the diimine ligand showing the π-back donation of electron density from platinum to the aromatic ring

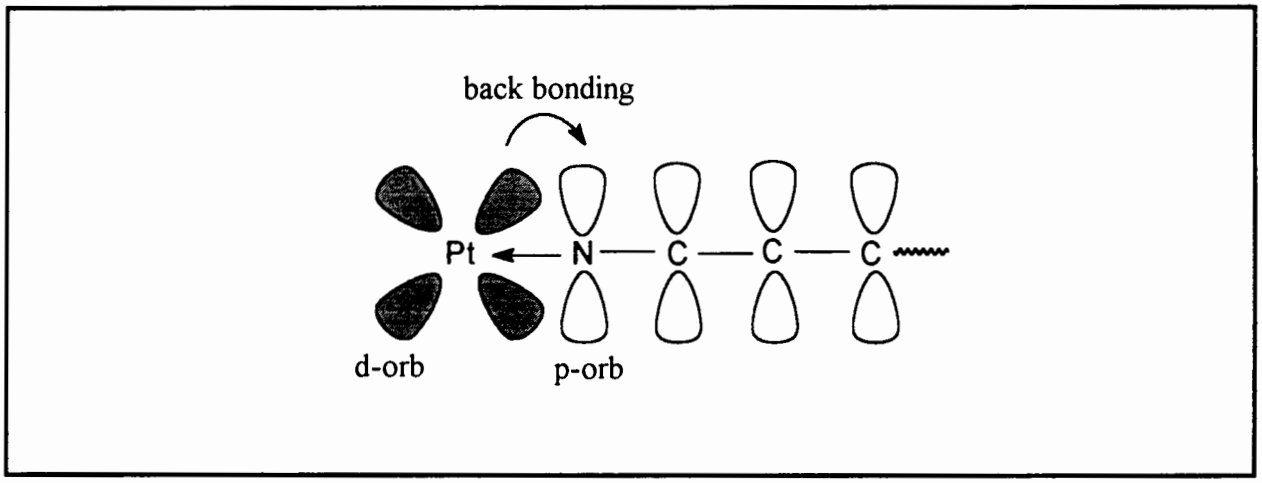

Contrary to expectations, the dimerisation constants for the 4,4'-dimethylbipy- and 4,4'-ditbutbipy complexes are greater than the bipy analogue. The negative effect the increased steric bulk of *tert*-butyl has on association, is counteracted by the increasing inductive releasing effect(+I) of these groups. These effects are predicted to account for increased self-association of the substituted 2,2'-bipyridyl platinum(II) complexes.

Since 2,2'-bipyridyl has previously been determined to be only marginally effective at inducing intercalative binding with DNA, we predicted a small dimerisation constant, which was observed (Table 3.23). Recent studies[45] on (2,2'-bipyridyl)platinum(II) complexes with co-ordinated pyridines, investigated the effect of the nature of substituents on the intercalative interaction. They found an increase in binding constants with increasing electron density of the 2,2'-bipyridyl moiety,

suggesting that stacking between the intercalated 2,2'-bipyridyl and nucleobases is driven by London dispersion forces rather than charge transfer interactions. This is in agreement with the results on the self-association of our (2,2'-bipyridyl)platinum(II) complexes. Substituents which lead to an increase in electron density of the 2,2'-bipyridyl moiety resulted in increased dimerisation constants. This is demonstrated by [Pt(4,4'-ditbutbipy)DiBuBTu]$^{+}PF_6^{-}$ which was found to have a larger association constant (28.00 dm^3 mol^{-1}) in comparison to [Pt(bipy)DiBuBTu]$^{+}PF_6^{-}$ (2.74 dm^3 mol^{-1}). The dimerisation constant of [Pt(4,4'-dimethylbipy)DiBuNTu]$^{+}PF_6^{-}$ (6.69 dm^3 mol^{-1}) is larger than [Pt(4,4'-ditbutbipy)DiBuNTu]$^{+}PF_6^{-}$ (1.72 dm^3 mol^{-1}) suggesting that steric hindrance of the bulky *tert*-butyl group prevents closer association of the molecules despite increased electron density of the 2,2'-bipyridyl moiety.

Thus, of the two effects seen to play a role in the stacking interaction, inductive effects appear to override steric factors (as seen from the magnitude of the association constants). However, steric effects of the ligand groups, are predicted to be more important in intercalative interactions.

Substitution of the benzyl group on the *N,N*-di(*n*-butyl)-*N'*-acylthiourea moiety with a naphthyl group has the effect of lowering the association constant as previously found for [Pt(phen)DiBuBTu]$^{+}PF_6^{-}$ and [Pt(4,7-diphenylphen)DiBuBTu]$^{+}PF_6^{-}$.

Due to the low association constant found for [Pt(bipy)DiBuBTu]$^{+}PF_6^{-}$, it was decided not to undertake studies on the naphthyl analogue.

In general, the variation in the dimerisation constants reflects the differing ability of the diimine ligands to overlap in the aggregate. Our studies show conclusively, that the nature of the diimine substituent on the [Pt(diimine)(*N,N*-di(*n*-butyl)-*N'*-acylthioureato)]$^{+}PF_6^{-}$ complexes, has a significant effect on the self-association interaction.

A plot of % dimer *vs.* concentration illustrates graphically those complexes which experience the strongest self-association interactions (Figure 3.22).

Figure 3.22: Graphical representation of % dimer *vs.* concentration (mol dm^{-3}) for the [Pt(diimine)(*N*,*N*-di(*n*-butyl)-*N'*-acylthioureato)]$^+PF_6^-$ complexes

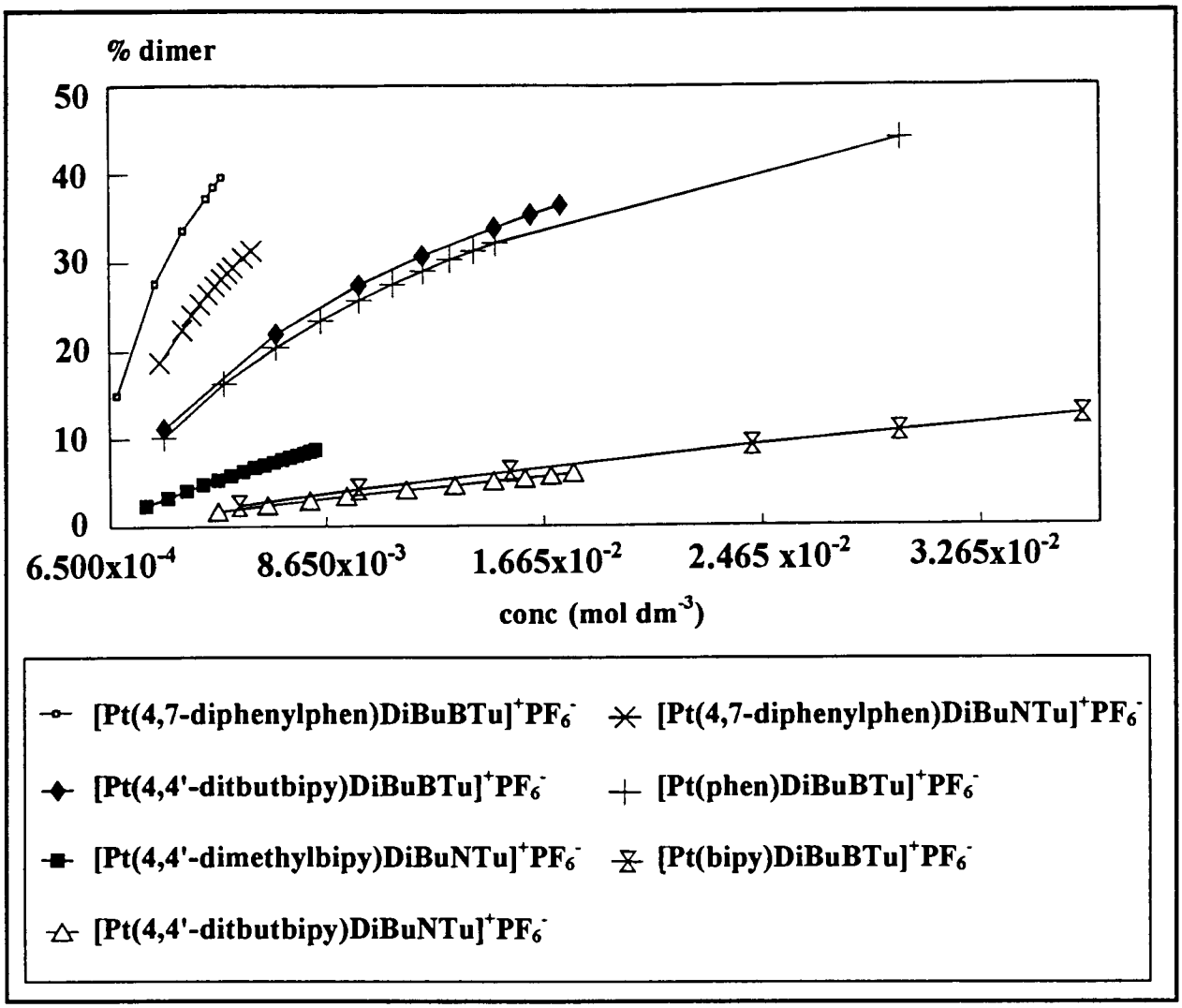

Previous studies[32,45] investigated factors governing intercalation of metal complexes into double-stranded DNA, and a trend for optimal complex geometry determined. The following trend was observed

2,2'-bipyridyl < 1,10-phenanthroline < 4,7-diphenyl-1,10-phenanthroline

This variation reflects the differing ability of the ligands to stack and the degree of overlap with the base pairs. This trend was mirrored in our dimerisation constants for the platinum(II) complexes.

[Pt(4,7-diphenylphen)DiBuNTu]$^+PF_6^-$ and [Pt(4,7-diphenylphen)DiBuBTu]$^+PF_6^-$ have significantly stronger dimerisation constants in comparison to the other complexes studied. This demonstrates the greater efficiency of extended aromatic systems at self-association. These results agree with the observation that effective metallointercalators tend to have large aromatic surfaces.

3.3.3 Thermodynamic Parameters

Exothermic reactions are typical for aggregation processes such as stacking interactions of molecules with unpaired electrons (for example purine bases and acridine dyes)[115]. Self-association of aromatic drugs is due to dispersive van der Waals interactions. These interactions are characterised by negative enthalpy and entropy contributions[128].

In the studies on our mixed-ligand platinum(II) complexes, the enthalpies of self-association in acetonitrile-d_3 are all negative. The high value of ΔH for [Pt(4,7-diphenylphen)DiBuBTu]$^+PF_6^-$ (-30.77 kJ mol^{-1}) is possibly due to substantial overlap of the diimine ligands in this complex. Enthalpy values determined, are a magnitude stronger than for van der Waals interactions (which are generally 0.1-10 kJ mol^{-1}) and two orders of magnitude weaker than for σ-bonds (100-1000 kJ mol^{-1}). Hence, a 'dimer' can be characterised as a weak π-bonded molecular complex.

The entropy change, ΔS, of self association, varies to a greater extent than the enthalpy change. Large negative values for ΔS, indicate some ordering of the solvent molecules in the vicinity of the aggregates. This indicates that entropy is an important component of these association reactions.

The observed trend in ΔG followed the order determined by the association constants. [Pt(4,7-diphenylphen)DiBuBTu]$^+PF_6^-$ (ΔG = -12.50 kJ mol^{-1}) has the largest energy associated with dimerisation and [Pt(bipy)DiBuBTu]$^+PF_6^-$ the smallest (ΔG = -4.76 kJ mol^{-1}). This shows increased ΔG values with larger π-surfaces. Studies of host-guest systems in which face-to-face arrangements occur, have suggested a possible increase in ΔG_{HG} with increasing surface of the π-systems[59].

3.3.4 Proposed 'dimer' structure

The use of NMR spectroscopy to determine association constants was reported in 1955[129]. Since then, NMR data has been used to evaluate stacking interactions of host-guest compounds[130-132], porphyrins[56] and nucleosides and bases[110-114,133].

^{1}H NMR studies were used to investigate nucleoside and base interactions[110-114,133] in an attempt to gain knowledge of the factors contributing to nucleic acid stabilisation. Chan *et al* undertook ^{1}H NMR studies on the self-association of purine and 6-methylpurine and concluded that they stack vertically with partial ring overlap[110]. This was found not to occur in the association of non-

aromatic uridine, cytidine and thymidine solutions. However, protons of these pyrimidine nucleosides were found to undergo upfield shifts with increasing purine concentration, which is indicative of a stacking interaction[111]. This suggests that a purine-nucleoside interaction takes place at the pyrimidine base through vertical ring stacking.

The concentration dependence of chemical shifts for various protons (specifically the magnitude of the chemical shift change), provide additional information about the average geometry of the stacks in solution. Two models were suggested for the stacking of nucleosides: (a) straight (face-to-back) - ribosyl substituents at N-9 on the same side of the stack (b) alternate (face-to-face or back-to-back) - ribosyl substituents are opposite to each other in the stack.

^{1}H NMR studies have also been carried out to determine the base-stacking interaction between two adenine rings in adenylyl-(3'-5')-adenosine. The stacking interaction was found to be relatively strong with the two adenine rings stacked in an *anti* conformation[133]. These studies were extended to examine the base-stacking interaction between adenine and cytosine bases in adenylyl-(3'-5')-cytidine and cytidylyl-(3'-5')-adenosine. Their stacking tendencies were found to be comparable, and consistent with stacked conformations in which both bases of the dinucleoside monophosphates are orientated in an *anti* conformation[114].

The model proposed by Hunter and Sanders[60] interprets π-π bonding as occurring due to favourable π-σ attractions rather than π-π electronic interactions. This is based on simplified Coulombic energy calculations. They stress that repulsive π-π interactions between arenes in a centrosymmetrical stack are transformed into attractive interactions by displacement of the ring planes, or through a charge redistribution brought about by heteroatoms in the ring. Hunter and Sanders have based their findings on studies of porphyrin self-association, however this model is now being used to explain π-π interactions in other systems[69].

A crystal structure determination of 4-picoline[4'-bis(2-hydroxyethyl)amino-2,2':6',2"-terpyridine]platinum(II) bis(tetrafluoroborate)[134] reveals that the terminal pyridine ring of the (2,2':6',2"-terpyridine)platinum(II) moieties overlap and are offset in accordance to the rules established by Hunter and Sanders[60]. The stacking is offset such that the electron-rich pyridine

nitrogen in one molecule is positioned over the electron-deficient central cavity of the pyridine ring above it.

Metallation of porphyrins has been found to result in their increased aggregation[68]. No affect on the geometry of the π-π interaction occurs. The placement of a metal within a porphyrin enhances aggregation by placing a large positive charge in the central cavity of the porphyrin π-system. This leads to a favourable interaction with the π-electrons of the pyrrole of the other porphyrin. The metal-π interaction is not classed as a bond but a weak electrostatic interaction between two charges. However, it is not a prerequisite for attractive π-π interactions.

These findings can be used to predict the dimer structure of our [Pt(diimine)(*N,N*-di(*n*-butyl)-*N'*-acylthioureato)]$^{+}PF_6^{-}$ complexes. The magnitude of the chemical shift differences for the various protons are used to determine which protons are most involved in the stacking interaction. Those protons undergoing the largest changes are presumed to be directly involved in the self-association interaction.

In [Pt(phen)DiBuBTu]$^{+}PF_6^{-}$, [Pt(phen)DiBuNTu]$^{+}PF_6^{-}$, [Pt(4,7-diphenylphen)DiBuBTu]$^{+}PF_6^{-}$ and [Pt(4,7-diphenylphen)DiBuNTu]$^{+}PF_6^{-}$, protons H_2 and H_9 undergo similar upfield chemical shifts due to the anisotropic shielding effect of one aggregate member upon its neighbour. A dimer structure is proposed for [Pt(phen)DiBuBTu]$^{+}PF_6^{-}$ in accordance with the guidelines set out by Hunter and Sanders[60] (Figure 3.23).

Figure 3.23: Proposed dimer structure of [Pt(phen)DiBuBTu]$^{+}PF_6$ **(A)** benzyl groups of *N,N*-di(*n*-butyl)-*N'*-benzoylthiourea are shown on the opposite side of the stack **(B)** benzyl groups of *N,N*-di(*n*-butyl)-*N'*-benzoylthiourea are shown on the same side of the stack

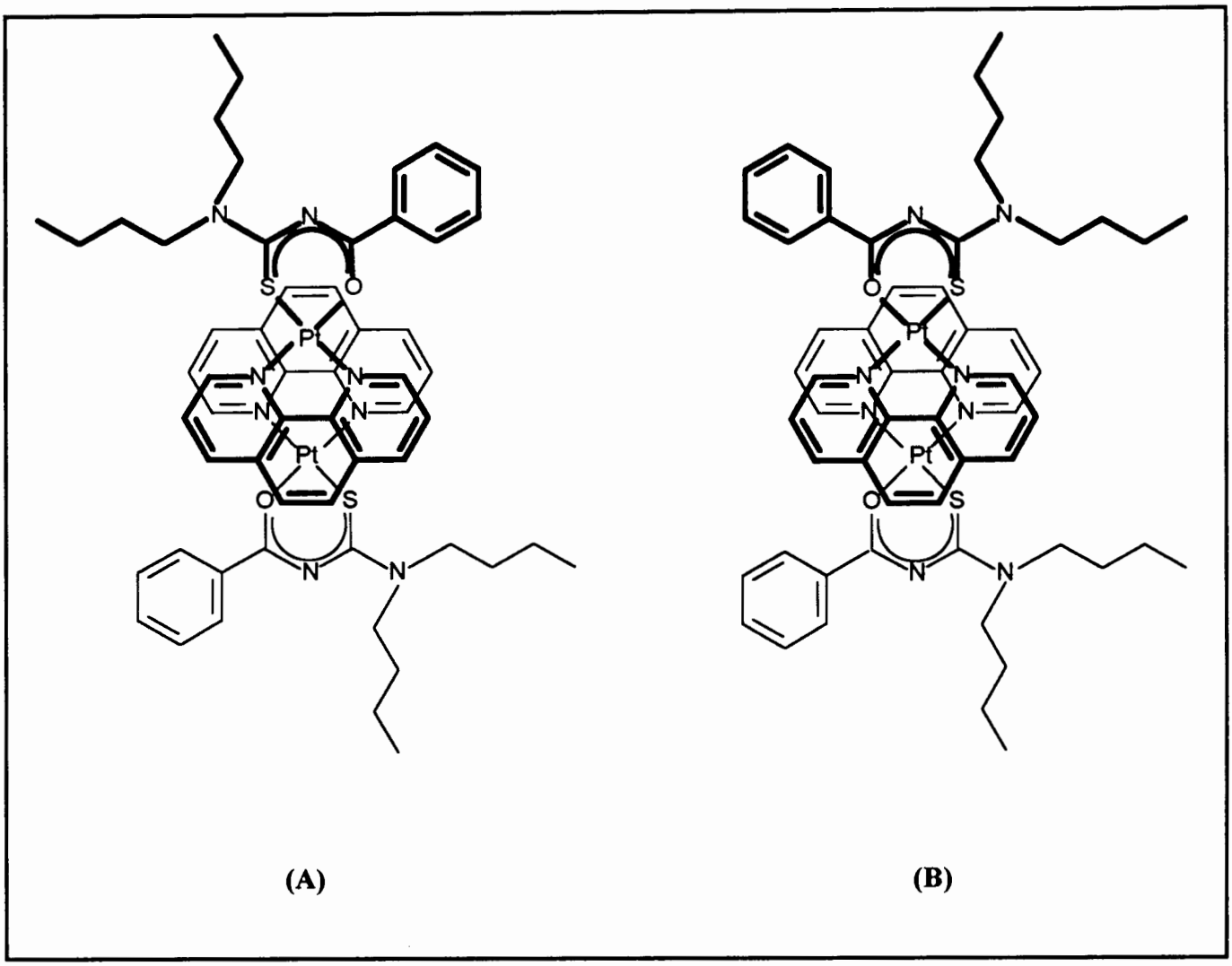

The (1,10-phenanthroline)platinum(II) moieties of the two molecules overlap and are offset such that the electron-rich pyridine nitrogen in one molecule is positioned over the electron-deficient central cavity of the pyridine ring in the second molecule[134]. The structure places H_2 and H_9 in similar magnetic environments, hence accounting for the similar observed chemical shift differences. The structure also illustrates the favourable attractive interaction between the positive platinum atom and the electron-rich centre ring of 1,10-phenanthroline. This is predicted to add increased stabilisation to the dimer-structure. Two possible structures are suggested; one in which the benzyl group of *N,N*-di(*n*-butyl)-*N'*-benzoylthiourea is found on the opposite side of the stack (**A**) and a second structure in which this group is on the same side of the stack (**B**) (Figure 3.23).

Figure 3.24: Proposed dimer structure of [Pt(4,7-diphenylphen)DiBuBTu]$^{+}PF_6$ illustrating the steric interference of the phenyl substituents at the 4,7 position of 1,10-phenanthroline, and the benzyl group of *N,N*-di(*n*-butyl)-*N'*-benzoylthiourea

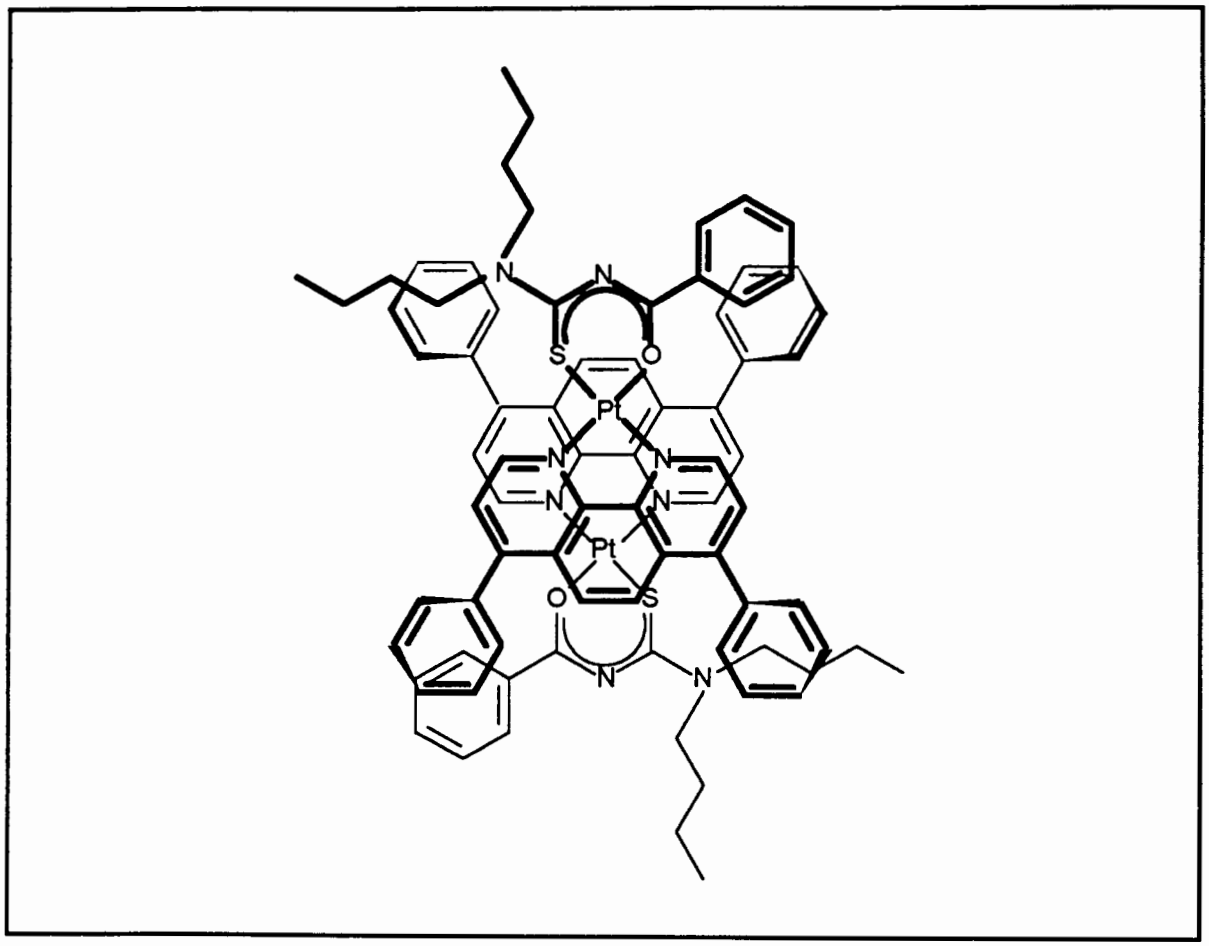

The two (1,10-phenanthroline)platinum(II) moieties in [Pt(4,7-diphenylphen)DiBuBTu]$^{+}PF_6^{-}$ are proposed as being overlapping and offset similar to [Pt(phen)DiBuBTu]$^{+}PF_6^{-}$. The phenyl groups of 4,7-diphenyl-1,10-phenanthroline are constrained to be out of the phenanthroline plane[125] due to unfavourable steric interactions between the ortho hydrogens of the phenyl substituents and the C_5 and C_6 hydrogens behind the centre ring (Figure 3.24).

A dimer structure is proposed for the (2,2'-bipyridyl)platinum(II) complexes and their derivatives in which possible steric effects of the bulky *tert*-butyl groups (Figure 3.25) are minimised and similar induced chemical shifts are observed for $H_{6'}$ and H_6.

Figure 3.25: Proposed dimer structures of $[Pt(bipy)DiBuBTu]^{+}PF_6^{-}$

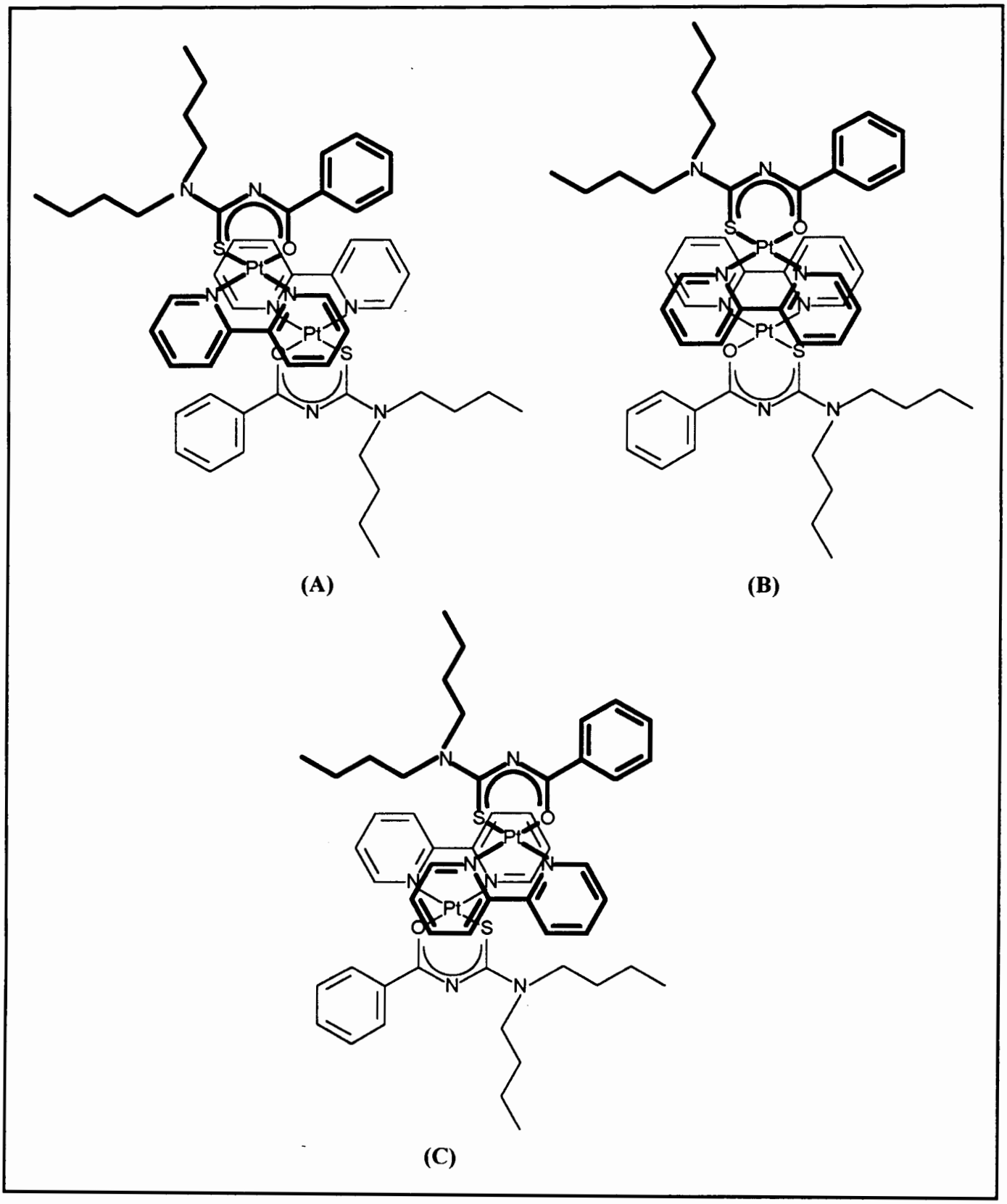

A dynamic equilibrium is suggested, in which the complexes fluctuated between three possible structures (**A**, **B** and **C**). This is predicted to occur quickly on the NMR time scale so only an average magnetic environment will contribute to the observed resonance shift. As previously noted, only a single set of resonances is observed for the monomer and dimer species at all concentrations.

A structure is proposed in which the bipyridyl rings of the two monomers overlap in an offset manner with the pyridine nitrogen's being centred over the electron-deficient cavity of the second molecule. In structure (**A**) (Figure 3.25), one ring of 2,2'-bipyridyl is positioned over the positive platinum atom of the second molecule, in (**B**) both rings of the 2,2'-bipyridyl moiety overlap and in structure (**C**) the second ring of 2,2'-bipyridyl overlaps the platinum atom of the second molecule.

3.3.5 Solvent Study

The effect of the addition of deuterium oxide to a solution of [Pt(4,4'-ditbutbipy)DiBuNTu]$^{+}PF_6^{-}$ in acetonitrile-d_3 was investigated. Two opposing factors must be considered. Dilution of the complex should result in a downfield shift of the diimine proton resonances as disaggregation occurs, while hydrophobic effects are expected to cause increased aggregation.

The addition of deuterium oxide caused significant upfield shifts of the diimine proton resonances. This suggests that the hydrophobic effect is the dominant influence, causing aggregation despite dilution of the complex solution.

A plot of chemical shift *vs.* %D_2O, follows the same trend as that of chemical shift *vs.* concentration (i.e. an upfield resonance shift as %D_2O is increased). This in accordance with the finding that aggregation[23] of terpyridineplatinum(II) cations is extensive in concentrated aqueous solutions, while non-aqueous solvents tend to minimise self-association. Hence, the observed increased aggregation is as a result of the hydrophobic nature of [Pt(4,4'-ditbutbipy)DiBuNTu]$^{+}PF_6^{-}$ and confirms the importance of this effect on stacking interactions in solution.

Potentially water-soluble platinum complexes of this type would thus be expected to show greater aggregation[23] due to increased solubility. Preliminary studies confirm this, but were not continued as part of this study.

CHAPTER 4

CONCLUSION

4 CONCLUSION

A series of mixed ligand [Pt(diimine)(*N,N*-di(*n*-butyl)-*N'*-acylthioureato)]$^{+}PF_6^{-}$ complexes has been successfully synthesised and characterised. ^{1}H NMR Studies on these platinum(II) complexes indicate that they interact with each other to form dimers in solution (specifically acetonitrile-d_3). It is postulated that the dimerisation interaction is regioselective since large chemical shift differences are observed for the diimine moiety of the complex.

For each complex, dimerisation constants (K^D), were calculated from significant chemical shift changes as a function of concentration. These results suggest that the self-association interaction is strongest for [Pt(4,7-diphenylphen)DiBuBTu]$^{+}PF_6^{-}$ (K^D = 114.1 ± 18.7 dm^3 mol^{-1}) and weakest for [Pt(phen)DiBuNTu]$^{+}PF_6^{-}$ (K^D = 1-2 dm^3 mol^{-1}).

A computer program allowed for the best estimation of the association constant (K^D) together with its upper and lower limits (within 95% confidence limits). In contrast to previous methods in which manual extrapolation of the chemical shift *vs.* concentration data was undertaken to determine the chemical shift of the monomer, the chemical shift values of the monomer and dimer are refined by the computer program.

The thermodynamic parameters (ΔG, ΔH and ΔS) for the dimerisation of these complexes in acetonitrile-d_3 solution, were obtained from temperature dependence studies using van't Hoff plots. These values are negative which indicates that the dimerisation interaction is energetically favourable.

Hunter and Sanders' model of π-π interactions can be used to explain the dimerisation interaction occurring, and to propose a dimer structure of the platinum(II) complexes in solution.

The following results substantiate this finding:

- Molecular association is supported by the pronounced effect of temperature and solvent on the ^{1}H NMR chemical shifts of the diimine protons

- +FAB mass spectra indicate the existence of only monomeric and dimeric species
- There is an excellent correlation between observed and calculated chemical shifts
- A plot of chemical shift of the diimine protons *vs.* fraction of dimers present in solution (at a specific concentration and temperature), is linear
- Van't Hoff plots exhibit a linear relationship

The nature of the diimine ligands has been found to have a significant effect on the extent of dimerisation in solution. By systematically varying the diimine moiety of the complexes, the role of ligand geometry on the self-association interaction was investigated. The nature of the substituents on the *N,N*-di(*n*-butyl)-*N'*-acylthiourea ligand also appeared to effect association, although to a much lesser degree.

The variation in the dimerisation constants reflects the differing ability of the diimine ligands to overlap in the aggregate. The overall dimerisation constants were found to follow the order:

[Pt(diimine)(*N,N*-di(*n*-butyl)-*N'*-benzoylthiourea)]$^+$$PF_6^-$

2,2'-bipyridyl < 1,10-phenanthroline < 4,4'-di-*tert*-butyl-2,2'-bipyridyl << 4,7-diphenyl-1,10-phenanthroline

[Pt(diimine)(*N,N*-di(*n*-butyl)-*N'*-naphthoylthiourea)]$^+$$PF_6^-$

1,10-phenanthroline < 4,4'-di-*tert*-butyl-2,2'-bipyridyl < 4,4'-dimethyl-2,2'-bipyridyl << 4,7-diphenyl-1,10-phenanthroline

The platinum(II) complexes with diimines having extended aromatic ligands, experienced greater association. The diimine, 4,7-diphenyl-1,10-phenanthroline, has a large surface area, therefore permitting substantial overlap of the complex monomers. This appears to enhance self-association, despite steric effects due to its non-planarity. This emphasises the importance of an extended π-surface for enhancing self-association.

In conclusion, our results for determining the optimum shape in self-association interactions, were found to agree with those determined for potential DNA-intercalators. Hence, it may be speculated that these complexes or similar platinum(II) complexes will interact with double-stranded DNA in an intercalative manner. Future work aimed at exploiting these findings to develop potentially new metallointercalator anticancer drugs could prove to be most rewarding.

CHAPTER 5

EXPERIMENTAL

5 EXPERIMENTAL

5.1 MATERIALS

The diimines used in the preparation of Pt(diimine)Cl_2 were commercially available from Aldrich Chemicals, except 4,4'-di-*tert*-butyl-2,2'-bipyridyl which was synthesised (5.3.1). 4-*Tert*-butyl-pyridine (Aldrich Chemicals) was distilled before use. Other reagents used in the synthesis of the platinum(II) complexes are commercially available and were used without additional purification.

5.2 INSTRUMENTATION

5.2.1 Mass Spectrometry

Mass spectra were taken with a VG micromass 16F mass-spectrometer by Mr P. Benincasa of the Department of Chemistry, University of Cape Town.

5.2.2 Nuclear Magnetic Resonance Spectroscopy

The ^1H and ^{13}C NMR spectra of 4,4'-di-*tert*-butyl-2,2'-bipyridyl were recorded in $CDCl_3$ using 5 mm tubes and a Varian VXR-200 FT-NMR spectrometer operating at 200.06 and 50.31 MHz respectively. The ^1H NMR spectra of the *N,N*-di(*n*-butyl)-*N'*-acylthiourea compounds were recorded in $CDCl_3$ using 5 mm tubes and a Varian VXR-200 FT-NMR spectrometer operating at 200.06 MHz. The ^{13}C NMR spectra were recorded using 5 mm tubes and a Varian UNITY-400 FT-NMR spectrometer operating at 100.58 MHz. All spectra were obtained at 25 °C unless otherwise stated. The ^1H NMR and 2D-COSY spectra of the [Pt(diimine)(*N,N*-di(*n*-butyl)-*N'*-acylthioureato)]$^+PF_6^-$ complexes were recorded in acetonitrile-d_3 in 5 mm tubes using a Varian UNITY-400 FT-NMR spectrometer operating at 399.95 MHz at 25 °C for the concentration dependence studies, as well as the range 25-55 °C (at 5 °C intervals) for the temperature dependence studies. All ^1H and ^{13}C chemical shifts were referred to the central line of the solvent resonance of known shifts relative to tetramethylsilane, and are estimated to be accurate to ±

0.05 ppm. Sufficient time between each spectrum recorded was allowed for the system to reach thermal equilibrium.

5.2.3 Melting Point

Melting points were measured on a Reichert-Jung thermovar attached to a DP-4 digital thermometer and are uncorrected.

5.2.4 Elemental Analysis

Elemental analysis for % C, H, N and S were carried out by Mr P. Benincasa of the Department of Chemistry, University of Cape Town on a Fissons Elemental Analyser EA 1108.

5.2.5 Positive Fast Atom Bombardment (+FAB)

(+FAB) mass spectra were obtained by courtesy of Dr. L. Fourie, University of Potchefstroom.

5.2.6 UV-Visible Spectroscopy

Absorbances were measured on a HP-8452A UV-Visible Diode-array spectrophotometer.

5.3 PREPARATION OF COMPOUNDS

5.3.1 Preparation of 4,4'-di-tert-butyl-2,2'-bipyridyl[94]

4-*Tert*-butyl-pyridine (25 ml) was purified by distillation under vacuum (0.2 mm Hg, 29-30 °C). 1g of palladium (10% on charcoal) was degassed in a schlenk flask overnight using an oil pump at 180 °C. The pyridine (23 ml) was added dropwise to the palladium catalyst under an inert (nitrogen) atmosphere. The mixture was left to heat under reflux for six days with stirring. After cooling, dry THF (75 ml) was added to the mixture before filtering (through celite) to remove the catalyst. Concentration of the solution to approximately 75 ml was followed by the addition of

catalyst. Concentration of the solution to approximately 75 ml was followed by the addition of neutral alumina (30 g), and then complete evaporation of the solvent. The solid alumina mixture was added to a sublimation apparatus connected to a trap and oil pump. Unreacted *tert*-butyl-pyridine was eliminated (approximately 8 ml) under vacuum (0.2 mm Hg, 60-130 °C) and 4,4'-di-*tert*-butyl-2,2'-bipyridyl was obtained by sublimation under vacuum (0.2 mm Hg, 130-160 °C). Further purification by recrystallisation from ethanol and water mixtures was carried out.

4,4'-di-*tert*-butyl-2,2'-bipyridyl (2.7969 g, 20.55 %), m.p. 156-159 °C (lit.,[94] 156 °C) (Found: C, 80.7; H, 8.9; N, 9.8%; M^+ 268. Calc. for $C_{18}H_{24}N_2$: C, 80.5; H, 9.0; N, 10.4%; M 268.194); δ_H(200.06 MHz; solvent $CDCl_3$; reference $SiMe_4$) 8.54 (2H, dd, J=5.23 and 0.68 Hz, H_6,$H_{6'}$), 8.35 (2H, dd, J=1.98 and 0.63 Hz, H_3,$H_{3'}$), 7.24 (2H, dd, J=5.24 and 1.99 Hz, H_5,$H_{5'}$), 1.33 (18H, s, Me's); δ_C(50.31 MHz; solvent $CDCl_3$; reference $SiMe_4$) 149.02 (C_6,$C_{6'}$), 120.70 (C_3,$C_{3'}$), 118.28 (C_5,$C_{5'}$), 30.63 $(CH_3)_6$, 160.96 (C_2,$C_{2'}$), 156.54 (C_4,$C_{4'}$), 34.99 (C_7,$C_{7'}$); *m/z* 268, 253, 237, 212, 119.

5.3.2. Preparation of N,N-di(n-butyl)-N'-acylthiourea ligands.

The *N,N*-di(*n*-butyl)-*N'*-acylthiourea compounds were synthesised according to the method reported by Douglass and Dains[72]. The acetone solvent was dried by heating to reflux in the presence of type 4 Å Linde molecular sieves and K_2CO_3, and distilled before use. Dry potassium thiocyanate (0.05 mol), was dissolved in dry acetone (30 ml) in a two necked round bottom flask. An equimolar amount of benzoyl or naphthoyl chloride dissolved in approximately 10 ml dry acetone, was added dropwise under a nitrogen atmosphere. The solution was heated to reflux under nitrogen for 30 minutes. Dibutylamine (0.05 mol), dissolved in 10 ml acetone was added dropwise, and the reaction mixture allowed to heat under reflux for a further 30 minutes. The solution was allowed to cool before being poured into ice water (approximately 200 ml) and left in the refrigerator overnight. The precipitated product was collected by filtration and dried. The ligands were recrystallised from ethanol (three times) to give a white crystalline material.

***N,N*-di(*n*-butyl)-*N'*-benzoylthiourea** (74.27 %), m.p. 90-92 °C (lit.[135], 93 °C), (Found: C, 65.4; H 8.3; N 9.5; S, 10.5%; M^+ 292. Calc. for $C_{16}H_{24}N_2OS$: C, 65.7; H, 8.3; N, 9.6 ; S 11.0%; M 292.48); δ_H (200.06 MHz, solvent $CDCl_3$; reference $SiMe_4$) 8.29 (1H, s, NH), 7.84 (2H, d, J=7.25

Hz, $H_{2'}$,$H_{6'}$), 7.58 (1H, t, J=7.35 Hz, $H_{4'}$), 7.47 (2H, t, J=7.38 Hz, $H_{3'}$,$H_{5'}$), 3.98 (2H, t, J=7.24 Hz, $H_{a'}$), 3.56 (2H, t, J=6.62 Hz, H_a), 1.80 (2H, m, $H_{b'}$), 1.67 (2H, m, H_b), 1.45 (2H, m, $H_{c'}$), 1.30 (2H, m, H_c), 0.99 (3H, t, J=7.24 Hz, $H_{d'}$), 0.91 (3H, t, J=7.17 Hz, H_d); δ_C (100.58 MHz, solvent $CDCl_3$; reference $SiMe_4$), 179.72 (C=S), 163.57 (C=O), 132.88($C_{4'}$), 132.77 ($C_{1'}$), 128.89 ($C_{2'}$,$C_{6'}$), 127.75 ($C_{3'}$,$C_{5'}$), 53.28 ($C_{a'}$), 53.11 (C_a), 30.14 ($C_{b'}$), 28.51 (C_b), 20.07 ($C_{c'}$,$C_{c'}$), 13.87 ($C_{d'}$), 13.72 (C_d); *m/z* 128, 105, 77, 44.

***N,N*-di(*n*-butyl)-*N'*-naphthoylthiourea** (88.02 %), m.p. 98-100 °C (lit.[92], 95-99 °C), (Found: C, 69.9; H, 7.7; N, 8.2; S, 8.8% M^+ 342. Calc. for $C_{20}H_{26}N_2OS$: C, 70.1; H, 7.7; N, 8.2; S, 9.4%; M 342.54) δ_H(200.06 MHz; solvent $CDCl_3$; reference $SiMe_4$) 8.47 (1H, d, J=8.21 Hz, $H_{8'}$), 8.21 (1H, s, NH), 8.00 (1H, d, J=8.23 Hz, $H_{2'}$), 7.91 (1H, d, J=7.69 Hz and J=1.33 Hz (long range coupling to $H_{2'}$), $H_{4'}$), 7.77 (1H, d, J=7.23 Hz and J=1.12 Hz (long range coupling to $H_{7'}$), $H_{5'}$), 7.46-7.66 (3H, m, $H_{3'}$,$H_{6'}$,$H_{7'}$), 4.01 (2H, t, J=7.25 Hz, $H_{a'}$), 3.69 (2H, t, J=7.25 Hz, H_a), 1.66-1.94 (2H, m, $H_{b'}$,H_b), 1.30-1.56 (2H, m, $H_{c'}$,H_c), 0.90-1.08 (6H, m, $H_{d'}$,H_d), δc(100.58 MHz, solvent $CDCl_3$; reference $SiMe_4$) 179.30 (C=S), 165.13 (C=O), 133.87 ($C_{1'}$), 132.43 ($C_{4'}$), 131.69 ($C_{9'}$), 130.25 ($C_{10'}$), 128.55 ($C_{2'}$), 127.80 ($C_{8'}$), 126.78 ($C_{5'}$), 126.27 ($C_{7'}$), 125.16 ($C_{3'}$), 124.52 ($C_{6'}$), 53.39 ($C_{a'}$,C_a), 30.25 ($C_{b'}$), 28.54 ($C_{b'}$), 20.20 ($C_{c'}$), 20.13 (C_c), 13.88 ($C_{d'}$), 13.78 (C_d); *m/z* 155, 127, 69, 55.

5.3.3 Preparation of Pt(diimine)Cl_2 Complexes[95]

K_2PtCl_4 (1.5 mmol) was dissolved in a boiling 2 M HCl/H_2O mixture (approximately 20 ml). This was added to a boiling solution of diimine (1.5 mmol) in a 2 M HCl/H_2O mixture (approximately 20 ml). The reaction was carried out in a beaker covered by a watchglass. The reaction mixture was left stirring for several days until a yellow precipitate formed and the red colour of the solution disappeared completely (indicating that all the platinum salt had reacted). The product was isolated by centrifuging followed by washing with water and diethylether. The washed product was dried in the oven overnight (60 °C). Evaporation of the filtrate resulted in a second crop of product being obtained.

1,10-phenanthrolinedichloroplatinum(II) (81.9 %) m.p. > 335 °C (Found: C, 32.8; H, 1.9; N 6.4%. Calc for $C_{12}H_8N_2PtCl_2$: C, 32.3; H, 1.8; N, 6.3%

4,7-diphenyl-1,10-phenanthrolinedichloroplatinum(II) (89.9 %) m.p. > 335 °C (Found: C, 48.6; H, 2.8; N 4.7%. Calc for $C_{24}H_{16}N_2PtCl_2$: C, 48.2; H, 2.7; N, 4.7%

2,2'-bipyridyldichloroplatinum(II) (92.6 %) m.p. > 335 °C (Found: C, 28.6; H, 1.9; N 6.5%. Calc for $C_{10}H_8N_2PtCl_2$: C, 28.4; H, 1.9; N, 6.6%

4,4'-dimethyl-2,2'-bipyridyldichloroplatinum(II) (74.9 %) m.p. > 335 °C (Found: C, 32.8; H, 2.7; N 6.2%. Calc for $C_{12}H_{12}N_2PtCl_2$: C, 32.0; H, 2.7; N, 6.2%

4,4'-di-*tert*-butyl-2,2'-bipyridyldichloroplatinum(II) (73.5 %) m.p. > 335 °C (Found: C, 40.9; H, 4.6; N 4.8%. Calc for $C_{18}H_{24}N_2PtCl_2$: C, 40.5; H, 4.5; N, 5.2%

5.3.4. Preparation of [Pt(diimine)(N,N-di(n-butyl)-N'-acylthioureato)]$^+PF_6^-$ complexes.

A suspension of Pt(diimine)Cl_2 (0.5 mmol) in acetonitrile (CH_3CN)(40 ml) was heated to reflux for approximately 10 minutes in a round bottom flask. A slight excess of *N,N*-di(*n*-butyl)-*N'*-acylthiourea (0.505 mmol) in CH_3CN (10 ml) was added, and the solution left to heat under reflux for 30 minutes. Sodium acetate (0.75 mmol) was added and the solution left to heat under reflux for a further 30-60 minutes or until the solution went clear and NaCl precipitated out. Excess NH_4PF_6 (5 x 0.5 mmol) was added to the reaction mixture which was left to heat under reflux for a further 30 minutes. The yellow solution was filtered through celite to remove NaCl and NH_4Cl salts and concentrated to 10-15 ml. An excess of diethyl ether was added and the solution placed in the freezer (-20 °C) overnight. Depending on the complex, the time taken for the product to precipitate varied. However in all cases the bulk of the product precipitated without further addition of ether. The precipitated complexes were isolated by centrifuging, followed by washing with ether and then dried in the oven (60 °C) overnight. Further drying under vacuum over silica gel was carried out. Concentration and cooling of the filtrate yielded a second crop of the complex. The complexes were recrystallised from acetonitrile/diethylether mixtures to give a bright yellow powder.

1,10-phenanthroline-*N,N*-di(*n*-butyl)-*N'*-benzoylthioureato(*S,O*)platinum(II) hexafluoro-phosphate (1) (80.3%) m.p. 270-272 °C (Found: C, 41.1; H, 3.8; N, 6.9. $C_{28}H_{31}N_4OSPtPF_6$

requires C, 41.4; H, 3.9; N, 6.9%) δ_H(399.95 MHz; solvent CD_3CN; reference $SiMe_4$) 0.95 (3H, t, H_d), 1.01 (3H, t, $H_{d'}$), 1.33 (2H, m, H_c), 1.38 (2H, m, $H_{c'}$), 1.48 (2H, m, H_b), 1.59 (2H, m, $H_{b'}$), 3.34 (2H, m, H_a), 3.36 (2H, m, $H_{a'}$), 7.29 (2H, t, $H_{3'}$,$H_{5'}$), 7.32 (1H, dd, H_8), 7.43 (1H, d, H_6), 7.48 (1H, d, H_5), 7.45 (2H, d, $H_{2'}$,$H_{6'}$), 7.54 (1H, t, $H_{4'}$), 7.68 (1H, dd, H_3), 7.91 (1H, dd, H_9), 8.18 (1H, dd, H_7), 8.22 (1H, dd, H_2), 8.24 (1H, dd, H_4)

1,10-phenanthroline-*N,N*-di(*n*-butyl)-*N'*-naphthoylthioureato(*S,O*)platinum(II) hexafluorophosphate (2) (76.3 %) m.p. 182-185 °C (Found: C, 43.3; H, 3.7; N, 6.4; S, 3.5. $C_{32}H_{33}N_4OSPtPF_6$ requires C, 44.6; H, 3.9; N, 6.5; S, 3.7%) δ_H(399.95 MHz; solvent CD_3CN; reference $SiMe_4$) 0.85 (3H, t, H_d), 1.07 (3H, t, $H_{d'}$), 1.29 (2H, m, H_c), 1.55 (2H, m, $H_{c'}$), 1.71 (2H, m, H_b), 1.80-2.00 (2H, m, $H_{b'}$), 3.80 (2H, t, H_a), 3.92 (2H, t, $H_{a'}$), 7.47 (1H, t, $H_{7'}$), 7.54 (1H, t, $H_{6'}$), 7.56 (1H, t, $H_{3'}$), 7.78-7.86 (2H, m, H_3,H_8), 7.98 (1H, d, $H_{5'}$), 8.00 (1H, d, $H_{4'}$), 8.03 (1H, d, H_6), 8.08 (1H, d, H_5), 8.09 (1H, d, $H_{2'}$), 8.41(1H, d, $H_{8'}$), 8.71 (1H, d, H_7), 8.73 (1H, d, H_4), 8.76 (1H, d, H_9), 8.83 (1H, d, H_2)

4,7-diphenyl-1,10-phenanthroline-*N,N*-di(*n*-butyl)-*N'*-benzoylthioureato(*S,O*)platinum(II) hexafluorophosphate (3) (50.3 %) m.p. 280-283 °C (Found: C, 48.5; H, 3.8; N, 6.0. $C_{40}H_{39}N_4OSPtPF_6$ requires C, 49.8; H, 4.1; N, 5.8%) δ_H(399.95 MHz; solvent CD_3CN; reference $SiMe_4$) 0.93 (3H, t, H_d), 1.03 (3H, t, $H_{d'}$), 1.38 (2H, m, H_c), 1.49 (2H, m, $H_{c'}$), 1.69 (2H, m, H_b), 1.75-2.00 (2H, m, $H_{b'}$), 3.79 (4H, m, $H_{a'}$,H_a), 7.50 (2H, t, $H_{3'}$,$H_{5'}$), 7.58-7.72 (2H, m, $H_{4'}$), 7.85 (1H, d, H_8), 8.04 (1H, d, H_6), 8.10 (1H, d, H_5), 8.15 (1H, m, H_3), 8.15 (2H, m, $H_{2'}$,$H_{6'}$), 8.89 (1H, d, H_9), 9.29 (1H, d, H_2)

4,7-diphenyl-1,10-phenanthroline-*N,N*-di(*n*-butyl)-*N'*-naphthoylthioureato(*S,O*)platinum(II) hexafluorophosphate (4) (34.0 %) m.p. 236-238 °C (Found: C, 51.2; H, 3.9; N, 5.7. $C_{44}H_{41}N_4OSPtPF_6$ requires C, 52.1; H, 4.1; N, 5.5%) δ_H(399.95 MHz; solvent CD_3CN; reference $SiMe_4$) 0.85 (3H, t, H_d), 1.05 (3H, t, $H_{d'}$), 1.28 (2H, m, H_c), 1.53 (2H, m, $H_{c'}$), 1.68 (2H, m, H_b), 1.80-2.00 (2H, m, $H_{b'}$), 3.78 (2H, t, H_a), 3.87 (2H, t, $H_{a'}$), 7.50-7.68 (3H, bm, $H_{3'}$,$H_{6'}$,$H_{7'}$), 7.80 (1H, d, H_8), 7.86 (1H, d, H_3), 7.96-8.08 (4H, m, H_5, H_6, $H_{4'}$,$H_{5'}$), 8.09 (1H, d, $H_{2'}$), 8.44 (1H, d, $H_{8'}$), 8.87 (1H, d, H_9), 8.90 (1H, d, H_2)

2,2'-bipyridyl-*N,N*-di(*n*-butyl)-*N'*-benzoylthioureato(*S,O*)platinum(II) hexafluorophosphate (5) (78.6 %) m.p. 250-253 °C (Found: C, 39.1; H, 3.9; N, 6.8; S, 3.7. $C_{26}H_{31}N_4OSPtPF_6$ requires C, 39.6; H, 4.0; N, 7.1; S, 4.1%) δ_H(399.95 MHz; solvent CD_3CN; reference $SiMe_4$) 0.96 (3H, t, H_d), 1.05 (3H, t, $H_{d'}$), 1.41 (2H, m, H_c), 1.49 (2H, m, $H_{c'}$), 1.70 (2H, m, H_b), 1.83 (2H, m, $H_{b'}$), 3.78 (4H, m, $H_{a'}$,H_a), 7.57 (1H, t, H_5), 7.50 (2H, t, $H_{3'}$,$H_{5'}$), 7.91 (1H, t, $H_{5'}$), 7.65 (1H, t, $H_{4'}$), 8.11 (2H, d, $H_{2'}$,$H_{6'}$), 8.17 (1H, d, H_3), 8.23 (1H, d, $H_{3'}$), 8.22 (1H, t, H_4), 8.31 (1H, t, $H_{4'}$), 8.57 (1H, d, H_6), 9.01 (1H, d, $H_{6'}$)

2,2'-bipyridyl-*N,N*-di(*n*-butyl)-*N'*-naphthoylthioureato(*S,O*)platinum(II) hexafluorophosphate (6) (73.8 %) m.p. 132-135 °C (Found: C, 42.3; H, 3.9; N, 6.7; S, 3.8. $C_{30}H_{33}N_4OSPtPF_6$ requires C, 43.0; H, 4.0; N, 6.7; S, 3.8%) δ_H(399.95 MHz; solvent CD_3CN; reference $SiMe_4$) 0.85 (3H, t, H_d), 1.06 (3H, t, $H_{d'}$), 1.29 (2H, m, H_c), 1.53 (2H, m, $H_{c'}$), 1.69 (2H, m, H_b), 1.88 (2H, m, $H_{b'}$), 3.78 (2H, m, H_a), 3.88 (2H, m, $H_{a'}$), 7.51-7.61 (3H, m, $H_{3'}$,$H_{6'}$,$H_{7'}$), 7.64 (1H, m, H_5), 7.68 (1H, m, $H_{5'}$), 8.01 (1H, d, $H_{5'}$), 8.02 (1H, d, $H_{2'}$), 8.11 (1H, d, $H_{4'}$), 8.30-8.33 (4H, m, $H_{3'}$,H_3,$H_{4'}$,H_4), 8.43 (1H, d, $H_{8'}$), 8.73 (1H, d, H_6), 8.78 (1H, d, $H_{6'}$)

4,4'-dimethyl-2,2'-bipyridyl-*N,N*-di(*n*-butyl)-*N'*-benzoylthioureato(*S,O*)platinum(II) hexafluorophosphate (7) (83.4 %) m.p. 272-275 °C (Found: C, 40.3; H, 4.3; N, 6.5; S, 3.7. $C_{28}H_{35}N_4OSPtPF_6$ requires C, 41.2; H, 4.3; N, 6.9; S, 3.9%) δ_H(399.95 MHz; solvent CD_3CN; reference $SiMe_4$) 0.95 (3H, t, H_d), 1.04 (3H, t, $H_{d'}$), 1.40 (2H, m, H_c), 1.49 (2H, m, $H_{c'}$), 1.69 (2H, m, H_b), 1.80-2.00 (2H, m, $H_{b'}$), 2.48 (3H, s, CH_3), 2.53 (3H, s, CH'_3), 3.78 (4H, m, $H_{a'}$,H_a), 7.38 (1H, d, H_5), 7.51 (2H, t, $H_{3'}$,$H_{5'}$), 7.65 (1H, t, $H_{4'}$), 7.70 (1H, d, $H_{5'}$), 8.00 (1H, s, H_3), 8.07 (1H, s, $H_{3'}$), 8.10 (2H, d, $H_{2'}$,$H_{6'}$), 8.37 (1H, d, H_6), 8.79 (1H, d, $H_{6'}$)

4,4'-dimethyl-2,2'-bipyridyl-*N,N*-di(*n*-butyl)-*N'*-naphthoylthioureato(*S,O*)platinum(II) hexafluorophosphate (8) (76.7 %) m.p. 206-209 °C (Found: C, 44.9; H, 4.2; N, 6.4, S, 3.5. $C_{32}H_{37}N_4OSPtPF_6$ requires C, 44.4; H, 4.3; N, 6.5; S, 3.7%) δ_H(399.95 MHz; solvent CD_3CN; reference $SiMe_4$) 0.84 (3H, t, H_d), 1.04 (3H, t, $H_{d'}$), 1.27 (2H, m, H_c), 1.51 (2H, m, $H_{c'}$), 1.67 (2H, m, H_b), 1.80-2.00 (2H, m, $H_{b'}$), 2:49 (3H, s, CH_3), 2.54 (3H, s, CH'_3), 3.76 (2H, t, H_a), 3.86 (2H, t, $H_{a'}$), 7.43 (1H, d, H_5), 7.48 (1H, d, $H_{5'}$), 7.50-7.60 (3H, m, $H_{3'}$,$H_{6'}$,$H_{7'}$), 7.99 (2H, d, $H_{2'}$), 8.00 (2H, d, $H_{5'}$), 8.09 (2H, d, $H_{4'}$), 8.13 (1H, s, H_3), 8.16 (1H, s, $H_{3'}$), 8.40 (1H, d, $H_{8'}$), 8.51 (1H, d, H_6), 8.56 (1H, d, $H_{6'}$)

4,4'-di-*tert*-butyl-2,2'-bipyridyl-*N,N*-di(*n*-butyl)-*N'*-benzoylthioureato(*S,O*)platinum(II) hexafluorophosphate (9) (71.6 %) m.p. 263-265 °C (Found: C, 45.4; H, 5.3; N, 6.1; S, 3.4. $C_{34}H_{47}N_4OSPtPF_6$ requires C, 45.4; H, 5.3; N, 6.2; S, 3.6%) δ_H(399.95 MHz; solvent CD_3CN; reference $SiMe_4$) 0.92 (3H, t, H_d), 1.04 (3H, t, $H_{d'}$), 1.35 (2H, m, H_c), 1.48 (2H, m, $H_{c'}$), 1.42 (9H, s, $(CH_3)_3$), 1.46 (9H, s, $(CH'_3)_3$), 1.64 (2H, m, H_b), 1.82 (2H, m, $H_{b'}$), 3.68-3.78 (4H, m, $H_{a'}$,H_a), 7.43 (2H, t, $H_{3'}$,$H_{5'}$), 7.51 (1H, dd, H_5), 7.60 (1H, t, $H_{4'}$), 7.86 (1H, dd, $H_{5'}$), 8.03 (2H, d, $H_{2'}$,$H_{6'}$), 8.18 (1H, d, H_3), 8.27 (1H, d, $H_{3'}$), 8.34 (1H, d, H_6), 8.83 (1H, d, $H_{6'}$)

4,4'-di-*tert*-butyl-2,2'-bipyridyl-*N,N*-di(*n*-butyl)-*N'*-naphthoylthioureato(*S,O*)platinum(II) hexafluorophosphate (10) (84.1 %) m.p. 212-215 °C (Found: C, 47.2; H, 5.2; N, 5.9; S, 3.2. $C_{38}H_{49}N_4OSPtPF_6$ requires C, 48.0; H, 5.2; N, 5.9; S, 3.4%) δ_H(399.95 MHz; solvent CD_3CN; reference $SiMe_4$) 0.84 (3H, t, H_d), 1.06 (3H, t, $H_{d'}$), 1.27 (2H, m, H_c), 1.50 (2H, m, $H_{c'}$), 1.42 (9H, s, $(CH_3)_3$), 1.44 (9H, s, $(CH'_3)_3$), 1.67 (2H, m, H_b), 1.87 (2H, m, $H_{b'}$), 3.74 (2H, t, H_a), 3.86 (2H, t, $H_{a'}$), 7.48-7.62 (3H, m, $H_{3'}$,$H_{6'}$,$H_{7'}$), 7.48-7.62 (2H, m, H_5,H_5), 7.97 (1H, d, $H_{2'}$), 8.00 (1H, d, $H_{5'}$), 8.08 (1H, d, $H_{4'}$), 8.27 (1H, d, H_3), 8.31 (1H, d, $H_{3'}$), 8.42 (1H, d, $H_{8'}$), 8.53 (1H, d, H_6), 8.60 (1H, d, $H_{6'}$)

5.4 AGGREGATION MEASUREMENTS

^{1}H NMR concentration dependence studies of [Pt(phen)DiBuBTu]$^+PF_6^-$, [Pt(phen)-DiBuNTu]$^+PF_6^-$, [Pt(4,7-diphenylphen)DiBuBTu]$^+PF_6^-$, [Pt(4,7-diphenylphen)DiBuNTu]$^+PF_6^-$, [Pt(bipy)DiBuBTu]$^+PF_6^-$, [Pt(4,4'-dimethylbipy)DiBuBTu]$^+PF_6^-$, [Pt(4,4'-dimethylbipy)-DiBuNTu]$^+PF_6^-$, [Pt(4,4'-ditbutbipy)DiBuBTu]$^+PF_6^-$ and [Pt(4,4'-ditbutbipy)DiBuNTu]$^+PF_6^-$ were carried out in acetonitrile-d_3 solution. The temperature dependence studies of the chemical shifts at fixed concentration of [Pt(phen)DiBuBTu]$^+PF_6^-$, [Pt(phen)DiBuNTu]$^+PF_6^-$, [Pt(4,7-diphenylphen)DiBuBTu]$^+PF_6^-$, [Pt(4,7-diphenylphen)DiBuNTu]$^+PF_6^-$, [Pt(bipy)DiBuBTu]$^+PF_6^-$, [Pt(4,4'-dimethylbipy)DiBuNTu]$^+PF_6^-$ and [Pt(4,4'-ditbutbipy)DiBuBTu]$^+PF_6^-$ were also undertaken in an attempt to determine thermodynamic parameters for the aggregation interactions.

For the chemical shift concentration dependence studies, a relatively concentrated solution (approximately 10^{-2} M) of each complex was prepared by weighing out an accurate mass of the

complex and dissolving it in a measured volume of acetonitrile-d_3 (typically 1 ml). 50 µl aliquots of the concentrated solution were then transferred using a micropippette into a NMR tube which contained exactly 0.5 ml acetonitrile-d_3 initially. After each addition, the ^{1}H NMR spectrum was recorded at 25°C, and the complex concentration calculated by assuming additive volumes.

For the temperature dependence studies, the spectra were recorded at 5 °C intervals (in the temperature range 25-55 °C) with a PAD (pre acquisition delay) of 180 s. This was to ensure that thermal equilibrium had been achieved. In general the temperature array experiments were carried out for five to eight different concentrations for each complex.

CHAPTER 6

REFERENCES

6 REFERENCES

(1) J. Swiatek, *J. Coord. Chem.*, 1994, **33**, 191.

(2) S.J. Lippard, *Acc. Chem. Res.*, 1978, **11**, 211.

(3) H.I. Heitner, S.J. Lippard, H.R. Sunshine, *J. Am. Chem. Soc.*, 1972, **94**, 8936.

(4) J.M. Wolfson, D.R. Kearns, *J. Am. Chem. Soc.*, 1974, **96**, 3653.

(5) M.J. Clarke, *Inorg. Chem.*, 1977, **16**, 738.

(6) K.G. Morallee, E. Nieboer, F.J.C. Rossotti, R.J.P. Williams, A.V. Xavier, R.A. Dwek, *Chem. Comm.*, 1970, 1132.

(7) K. Gasiorowski, J. Swiatek, H. Kozlowski, *Inorg. Chim. Acta.*, 1985, **106**, LI

(8) T.B Thederahn, M.D. Kuwabara, T.A. Larsen, D.S. Sigman, *J. Am. Chem. Soc.*, 1989, **111**, 4941.

(9) A.M.J. Fichtinger-Schepman, R.A. Baan, A. Luiten-Schnite, M. Van Dijk, P.M.M. Lohman, *Chem. Biol. Int.*, 1985, **55**, 275.

(10) W.D. Wilson, in *Nucleic Acids in Chemistry and Biology*, eds. G.M. Blackburn and M.J. Gait, Oxford University Press, Oxford, 1990, ch. 8.

(11) A.P. Zipp, S.G. Zipp, *J. Chem. Educ.*, 1977, **54**, 739.

(12) F.A. Cotton, G. Wilkinson, *Advanced Inorganic Chemistry*, Wiley-Interscience, U.S.A., 5th edn., 1988, ch. 119.

(13) B. Rosenberg, L. Van Camp, T. Krigas, *Nature*, 1965, **205**, 698.

(14) M. Peyrone, *Liebigs Ann. Chem.*, 1844, **51**, 1.

(15) C.A. McAuliffe, H.L. Sharma, N.D. Tinker, in *Chemistry of the Platinum Group Metals*, ed. F.R. Hartley, Elsevier Science Publishers B.V., Amsterdam, 1991, ch. 16.

(16) A.W. Prestayko, S.T. Crooke, S.K. Carter, N.A. Alder, eds., *Cisplatin: Current Status and New Developments*, Academic Press, New York, 1980.

(17) S.E. Sherman, S.J. Lippard, *Chem. Rev.*, 1987, **87**, 1153.

(18) U. Hollstein, *Chem. Rev.*, 1974, **74**, 625.

(19) R.B. Silverman, *The Organic Chemistry of Drug Designed Drug Action*, Academic Press Inc., New York, 1992, ch. 6.

(20) L.S. Lerman, *J. Mol. Biol.*, 1961, **3**, 18.

(21) U. Pindur, M. Haber, K. Sattler, *J. Chem. Educ.*, 1993, **70**, 263.

(22) O. Kennard, W.N. Hunter, *Angew. Chem. Int. Ed. Engl.*, 1991, **30**, 1254.

(23) K.W. Jennette, J.T. Gill, J.A. Sadownick, S.J. Lippard, *J. Am. Chem. Soc.*, 1976, **98**, 6159.

(24) G.P. Kreishman, S.I. Chan, W. Bauer, *J. Mol. Biol.*, 1971, **61**, 45.

(25) N.S. Angerman, T.A. Victor, C.L. Bell, S.S. Danyluk, *Biochemistry*, 1972, **11**, 2402.

(26) J.K. Barton, A.T. Danishefsky, J.M. Goldberg, *J. Am. Chem. Soc.*, 1984, **106**, 2172.

(27) P.J. Bond, R. Langridge, K.W. Jennette, S.J. Lippard, *Proc. Nat. Acad. Sci. U.S.A.*, 1975, **72**, 4825.

(28) S.J. Lippard, P.J. Bond, K.C. Wu, W.R. Bauer, *Science*, 1976, **194**, 726.

(29) F. Liu, K.A. Meadows, D.R. McMillin, *J. Am. Chem. Soc.*, 1993, **115**, 6699.

(30) R.J. Morgan, S. Chatterjee, A.D. Baker, T.C. Strekas, *Inorg. Chem.*, 1991, **30**, 2687.

(31) W.D. Wilson, L. Strekowski, F.A. Tanious, R.A. Watson, J.L. Mokrosz, A. Strekowska, G.D. Webster, S. Neidle, *J. Am. Chem. Soc.*, 1988, **110**, 8292.

(32) A.M. Pyle, J.P. Rehmann, R. Meshoyrer, C.V. Kumar, N.J. Turro, J.K. Barton, *J. Am. Chem. Soc.*, 1989, **111**, 3051.

(33) A.H. Wang, J. Nathans, G. van der Marel, J.H. van Boom, A. Rich, *Nature*, 1978, **276**, 471.

(34) Y.-S. Wong, S.J. Lippard, *J. Chem. Soc., Chem. Commun.*, 1977, 824.

(35) K.W. Jennette, S.J. Lippard, G.A. Vassiliades, W.R. Bauer, *Proc. Nat. Acad. Sci. U.S.A.*, 1974, **71**, 3839.

(36) G.M. Intille, C.E. Pflunger, W.A. Baker., Jr., *J. Cryst. Mol. Struct.*, 1973, **3**, 47.

(37) H.I. Heitner, S.J. Lippard, *Inorg. Chem.*, 1974, **13**, 815.

(38) D.M. Crothers, *Biopolymers*, 1968, **6**, 575.

(39) P.J. Bond, R. Langridge, K.W. Jennette, S.J. Lippard, *Proc. Nat. Acad. Sci. U.S.A.*, 1975, **72**, 4825.

(40) L. Kumar, N.R. Kandasamy, T.S. Srivastava, *Inorg. Chim. Acta.*, 1982, **67**, 139.

(41) K.H. Puthraya, T.S. Srivastava, A.J. Amonkar, M.K. Adwankar, M.P. Chitnis, *J. Inorg. Biochem.*, 1985, **25**, 207.

(42) K.H. Puthraya, T.S. Srivastava, A.J. Amonkar, M.K. Adwankar, M.P. Chitnis, *J. Inorg. Biochem.*, 1986, **26**, 45.

(43) R. Mital, K. Sen Ray, T.S. Srivastava, R.K. Bhattacharya, *J. Inorg. Biochem.*, 1986, **27**, 133.

(44) R. Mital, T.S. Srivastava, H.K. Parekh, M.P. Chitnis, *J. Inorg. Biochem.*, 1991, **41**, 93.

(45) M. Cusumano, M.L. Di Pietro, A. Giannetto, *J. Chem. Soc., Chem. Commun.*, 1996, 2527.

(46) S.A. Tysoe, R.J. Morgan, A.D. Baker, T.C. Strekas, *J. Phys. Chem.*, 1993, **97**, 1707.

(47) J.K. Barton, *Science*, 1986, **233**, 727.

(48) J.K. Barton, L.A. Basile, A. Danishefsky, A. Alexandrescu, *Proc. Natl. Acad. Sci. U.S.A.*, 1984, **81**, 1961.

(49) D.S. Sigman, *Acc. Chem. Res.*, 1986, **19**, 180.

(50) L.D. Williams, J. Thivierge, I.H. Goldberg, *Nucl. Acids. Res.*, 1988, **16**, 11607.

(51) W.D. Wilson, F.A. Tanious, R.A. Watson, H.J. Barton, A Strekowska, D.B. Harden, L. Strekowski, *Biochemistry*, 1989, **28**, 1984.

(52) R. Tamilarasan, D.R. McMillin, *Inorg. Chem.*, 1990, **29**, 2798.

(53) J.K. Barton, J.J. Damenberg, A.L. Raphael, *J. Am. Chem. Soc.*, 1982, **104**, 4967.

(54) C.K. Mathews, K.E. van Holde, *Biochemistry*, The Benjamin/Cummings Publishing Co., Inc., 1990.

(55) J.K. Barton, A.L. Raphael, *J. Am. Chem. Soc.*, 1994, **106**, 2466.

(56) K. Kuno, M. Takei, S. Hashimoto, *J. Phys. Chem.*, 1990, **94**, 2181.

(57) R.J. Abraham, B. Evans, K.M. Smith, *Tetrahedron*, 1978, **34**, 1213.

(58) G.R. Desiraju, A. Gavezzotti, *J. Chem. Soc., Chem. Commun.*, 1989, 621.

(59) H.-J. Schneider, *Angew. Chem. Int. Ed. Engl.*, 1991, **30**, 1417.

(60) C.A. Hunter, J.K.M. Sanders, *J. Am. Chem. Soc*, 1990, **112**, 5525.

(61) S.K. Burley, G. Petsko, *Science (Washington, D.C.)*, 1985, **229**, 23.

(62) S.K. Burley, G. Petsko, *J. Am. Chem. Soc.*, 1986, **108**, 7995.

(63) W.L. Jorgensen, D.L. Severance, *J. Am. Chem. Soc.*, 1990, **112**, 4768.

(64) A.V. Muehldorf, D. Van Engen, J.C. Warner, A.D. Hamilton, *J. Am. Chem. Soc.*, 1988, **110**, 6561.

(65) A.D. Hamilton, *J. Chem. Educ.*, 1990, **67**, 821.

(66) B. Askew, P. Ballester, C. Buhr, K.S. Jeong, S. Jones, K. Parris, K. Williams, J. Rebek., Jr., *J. Am. Chem. Soc.*, 1989, **111**, 1082.

(67) F. Cozzi, M. Cinquini, R. Annuziata, J.S. Siegel, *J. Am. Chem. Soc.*, 1993, **115**, 5330.

(68) R.J. Abraham, F. Eivazi, H. Pearson, K.M. Smith, *J. Chem. Soc., Chem. Commun.*, 1976, 699.

(69) D.V. Stynes, *Inorg. Chem.*, 1994, **33**, 5022.

(70) N. Kurnakow, *J. Prakt. Chem.*, 1894, **50**, 481.

(71) S.C. Shome, M. Mazumder, P.K. Haldar, D.K. Das, *J. Indian Chem. Soc*, 1977, LIV, 947.

(72) I.B. Douglass , F.B. Dains, *J. Am. Chem. Soc.*, 1934, **56**, 719.

(73) A. Takamizawa, K. Hira, K. Matsui, *Bull. Chem. Soc. Japan.*, 1963, **36**, 1214.

(74) D.T. Elmore, J.R. Ogle, *J. Chem. Soc.*, 1958, 1141.

(75) M.O. Lozinskii, P.S. Pel'kis, *Russ. Chem. Rev. (Engl. Transl.)*, 1968, **37**, 363.

(76) D.C. Schroeder, *Chem. Rev.*, 1955, **55** ,181.

(77) W.I. Congdon, J.T. Edward, *J. Am. Chem. Soc.*, 1972, **94**, 6096.

(78) W.I. Congdon, J.T. Edward, *J. Am. Chem. Soc.*, 1972, **94**, 6099.

(79) W.I. Congdon, J.T. Edward, *Can. J. Chem.*, 1974, **52**, 697.

(80) L. Beyer, E. Hoyer, H. Hennig, R. Kirmse, *J. Prakt. Chem.*, 1975, **317**, 829.

(81) R. Richter, L. Beyer, J. Kaiser, *Z. Anorg. Allg. Chem.*, 1980, **461**, 67.

(82) G. Fitzl, L. Beyer, J. Sieler, R. Richter, J. Kaiser, E. Hoyer, *Z. Anorg. Allg. Chem.*, 1977, **433**, 237.

(83) K.-H König, M. Schuster, B. Steinbrech, G. Schneeweis, R. Schlodder, *Fresenius' Z. Anal. Chem.*, 1985, **321**, 457.

(84) P. Vest, M. Schuster, K.-H König, *Fresenius' Z. Anal. Chem.*, 1989, **335**, 759.

(85) P. Vest, M. Schuster, K.-H König, *Fresenius' J. Anal. Chem.*, 1991, **339**, 142.

(86) P. Vest, M. Schuster, K.-H König, *Fresenius' J. Anal. Chem.*, 1991, **341**, 566.

(87) M. Schuster, *Fresenius' J. Anal. Chem.*, 1992, **342**, 791.

(88) M. Schuster, E. Unterreitmaier, *Fresenius' J. Anal. Chem.*, 1993, **346**, 630.

(89) S. Bourne, K.R. Koch, *J. Chem. Soc., Dalton Trans.*, 1993, 2071.

(90) K.R. Koch, C. Sacht, T. Grimmbacher, S. Bourne, *S. Afr. J. Chem.*, 1995, **48**, 71.

(91) A. Irving, K.R. Koch, M. Matoetoe, *Inorg. Chim. Acta*, 1993, **206**, 193.

(92) K.R. Koch, J. du. Toit, M.R. Caira, C. Sacht, *J. Chem. Soc., Dalton Trans.*, 1994, 785.

(93) K.R. Koch, C. Sacht, S. Bourne, *Inorg. Chim. Acta.*, 1995, **232**, 109.

(94) T.B. Hadda, H. Le Bozec, *Inorg. Chim. Acta*, 1993, **204**, 103.

(95) G.T. Morgan, F.H. Burstall, *J. Chem. Soc.*, 1934, 965.

(96) F.A. Palocsay, J.V. Rund, *Inorg. Chem*, 1969, **8**, 524.

(97) R.S. Osborn, D. Rodgers, *J. Chem. Soc., Dalton Trans.*, 1974, 1002.

(98) E. Bielli, P.M. Gidney, R.D. Gillard, B.T. Heaton, *J. Chem. Soc., Dalton Trans.*, 1974, 2133.

(99) T.W. Thomas, A.E. Underhill, *Chem. Soc. Rev.*, 1972, **1**, 99.

(100) A.J. Canty, B.W. Skelton, P.R. Traill, A.H. White, *Aust. J. Chem*, 1992, **45**, 417.

(101) S.R. Salman, G.Y. Sarkis, E.D. Faisal, *Can. J. Spectrosc.*, 1986, **31**, 167.

(102) T. Grimmbacher, Ph.D Thesis, University of Cape Town, August 1995.

(103) J. Miller, K.R. Koch, unpublished work.

(104) R.G. Pearson, *Science*, 1966, **151**, 172.

(105) D.F. Shriver, P.W. Atkins, C.H. Langford, *Inorganic Chemistry*, Oxford University Press, Oxford, 1990, ch. 7.

(106) P.E. Rosevear, W.H.F. Sasse, *J. Heterocycl. Chem.*, 1971, **8**, 483.

(107) K.R. Koch, M.C. Matoetoe, *Mag. Res. in Chem.*, 1991, **29**, 1158.

(108) H. Günter, *An Introduction to NMR Spectroscopy*, John Wiley & Sons, Ltd, Chichester, 1980.

(109) A.L. Thakkar, L.G. Tensmeyer, R.B. Hermann,W.L. Wilham, *Chem. Commun.*, 1970, 524.

(110) S.I. Chan, M.P. Schweizer, P.O.P. Ts'o, G.K. Helmkamp, *J. Am. Chem. Soc.*, 1964, **86**, 4182.

(111) M.P. Schweizer, S.I. Chan, P.O.P. Ts'o, *J. Am. Chem. Soc.*, 1965, **87**, 5241.

(112) A.D. Broom, M.P. Schweizer, P.O.P. Ts'o, *J. Am. Chem. Soc.*, 1967, **89**, 3612.

(113) M.P. Schweizer, A.D. Broom, P.O.P. Ts'o, D.P. Hollis, *J. Am. Chem. Soc.*, 1968, **90**, 1042.

(114) B.W. Bangerter, S.I. Chan, *J. Am. Chem. Soc.*, 1969, **91**, 3910.

(115) D.B. Davies, L.N. Djimant, A.N. Veselkov, *J. Chem. Soc., Faraday Trans.*, 1996, **92**, 383.

(116) C.S. Wilcox, in *Frontiers in Supramolecular Organic Chemistry and Photochemistry*, eds. H.-J. Schneider and H. Dürr, V.C.H Weinheim, New York, 1991, p.123.

(117) J. Granot, *J. Am. Chem. Soc.*, 1978, **100**, 6745.

(118) P.R. Mitchell, *J. Chem. Soc., Dalton Trans.*, 1980, 1079.

(119) I. Horman, B. Dreux, *Helvetica Chim. Acta*, 1984, **67**, 744.

(120) H. Jiang, Dept. of Statistical Science, University of Cape Town, 1994.

(121) R.J. Abraham, P.A. Burbidge, A.H. Jackson, P.B. MacDonald, *J. Chem. Soc. B*, 1966, 620.

(122) R.J. Abraham, B. Evans, K.M. Smith, *Tetrahedron*, 1978, **34**, 1213.

(123) M. Chou, C. Creutz, D. Mahajan, N. Sutin, A.P. Zipp, *Inorg. Chem.*, 1982, **21**, 3989.

(124) K.R. Mann, N.S. Lewis, R.M. Williams, H.B. Gray, J.G. Gordon, II, *Inorg. Chem.*, 1978, **17**, 828.

(125) B.M. Goldstein, J.K. Barton, H.M. Berman, *Inorg. Chem.*, 1986, **25**, 842.

(126) J.K. Barton, A.L. Raphael, *J. Am. Chem. Soc.*, 1984, **90**, 1042.

(127) M.H. Palmer, *The Structure and Reactions of Heterocyclic Compounds*, Edward Arnold, Pub., Ltd, London, 1967, ch. 2.

(128) P.D. Ross, S. Subramanian, *Biochemistry*, 1981, **20**, 3096.

(129) C.M. Huggins, G.C. Pimentel, J.N. Shoolery, *J. Chem. Phys.*, 1955, **23**, 1244.

(130) M.D. Cowart, I. Sucholeiki, R.R. Bukownik, C.S. Wicox, *J. Am. Chem. Soc.*, 1988, **110**, 6204.

(131) J.D. Kilburn, A.R. MacKenzie, W.C. Still, *J. Am. Chem. Soc.*, 1988, **110** 1307.

(132) S.C. Zimmerman, C.M. Van Zyl, G.S. Hamilton, *J. Am. Chem. Soc.*, 1989, **111**, 1373.

(133) S.I. Chan, J.M. Nelson, *J. Am. Chem. Soc.*, 1969, **91**, 168.

(134) A. Chernega, A.S. Droz, K. Prout, T. Vilaivan, G.W. Weaver, G. Lowe, *J. Chem. Research(S)*, 1996, 402.

(135) K.-H. König, M. Schuster, G. Schneeweis, B. Steinbrech, *Fresenius' Z. Anal. Chem.*, 1984, **319**, 66.

CHAPTER 7

APPENDICES

7.1 APPENDIX 1

Flow Chart of the Computer Program used to Calculate K^D, x_i, δ_o and $(\delta_o - \delta_\infty)$

Read data (All $(M_i)_o$, δ_i)

↓

$K^D = K_{first}$

↓

* Calculate set of x_i values for each $(M_i)_o$ from $x_i = (1 + y_i/2) - [(1 + y_i/2)^2 - 1]^{1/2}$

↓

Perform linear regression calculation for $\delta_i = f(x_i)$ according to $\delta_i = \delta_o - x_i(\delta_o - \delta_\infty)$

↓

For line obtained compute mean square deviation of experimental δ_i from this line (= relative standard deviation)

↓

If $K^D = K_{first}$, store K^D, δ_o(intercept), $(\delta_o - \delta_\infty)$(slope) and relative standard deviation

If $K^D \neq K_{first}$, store new values of K^D, intercept, slope and relative standard deviation only if new relative standard deviation < presently stored value of relative standard deviation

↓

Systematically vary K^D

↓

Repeat process from * until minimum relative standard deviation is found and K^D defined to desired precision.

↓

Calculate 95% upper and lower limits for K^D, δ_o and $(\delta_o - \delta_\infty)$

Report best values of K^D, δ_o and $(\delta_o - \delta_\infty)$ with their limits

7.2 APPENDIX 2

Table 7.2.1: ^{1}H NMR Chemical shift data (in ppm) for [Pt(phen)DiBuBTu]$^+PF_6^-$ in acetonitrile-d_3 at 25 °C

CONC (mol dm^{-3})	H_2	H_3	H_4	H_5	H_6	H_7	H_8	H_9	$H_{3''}$ $H_{5''}$	$H_{4''}$	$H_{2''}$ $H_{6''}$
2.699x10^{-3}	9.106	8.143	8.765	8.066	7.984	8.672	7.793	8.715	7.502	7.657	8.058
4.948x10^{-3}	8.941	8.050	8.672	7.945	7.883	8.580	7.702	8.555	7.471	7.644	7.941
6.852x10^{-3}	8.833	7.996	8.611	7.877	7.817	8.520	7.633	8.454	7.448	7.633	7.867
8.483x10^{-3}	8.758	7.958	8.568	7.831	7.770	8.478	7.615	8.385	7.430	7.624	7.814
9.897x10^{-3}	8.700	7.929	8.535	7.794	7.734	8.446	7.575	8.333	7.417	7.617	7.774
1.113x10^{-2}	8.653	7.905	8.508	7.764	7.705	8.421	7.550	8.290	7.406	7.611	7.742
1.223x10^{-2}	8.615	7.886	8.486	7.740	7.681	8.399	7.530	8.256	7.396	7.606	7.724
1.320x10^{-2}	8.584	7.870	8.468	7.720	7.662	8.382	7.514	8.228	7.388	7.602	7.691
1.406x10^{-2}	8.557	7.856	8.452	7.703	7.645	8.367	7.500	8.204	7.382	7.598	7.676
1.485x10^{-2}	8.534	7.844	8.439	7.688	7.630	8.354	7.488	8.184	7.376	7.594	7.660
2.970x10^{-2}	8.223	7.679	8.242	7.480	7.429	8.177	7.324	7.914	7.287	7.537	7.445

Table 7.2.2: ^{1}H NMR Chemical shift data (in ppm) for [Pt(phen)DiBuNTu]$^+PF_6^-$ in acetonitrile-d_3 at 25 °C

CONC (mol dm^{-3})	H_2	H_4	H_5	H_6	H_7	H_3H_8	H_9	$H_{2''}$	$H_{4''}$	$H_{3''}$ $H_{6''}$	$H_{5''}$	$H_{7''}$	$H_{8''}$
1.438x10^{-3}	9.043	8.867	8.209	8.166	8.847	7.94-8.00	9.030	8.068	8.117	7.56-7.62	8.024	7.538	8.496
1.891x10^{-3}	9.022	8.857	8.199	8.157	8.836	7.92-8.00	9.010	8.064	8.115	7.56-7.62	8.023	7.536	8.491
2.078x10^{-3}	9.013	8.852	8.194	8.152	8.831	7.92-7.98	9.000	8.059	8.115	7.56-7.62	8.023	7.532	8.488
2.244 10^{-3}	9.008	8.849	8.192	8.149	8.828	7.92-7.98	8.996	8.058	8.114	7.56-7.62	8.023	7.532	8.485
2.393x10^{-3}	9.002	8.845	8.187	8.145	8.824	7.92-7.98	8.989	8.055	8.114	7.56-7.62	8.022	7.530	8.483
2.649x10^{-3}	8.993	8.839	8.182	8.140	8.818	7.90-7.98	8.977	8.052	8.112	7.56-7.62	8.021	7.526	8.479
2.861x10^{-3}	8.981	8.832	8.176	8.134	8.812	7.90-7.96	8.964	8.048	8.112	7.56-7.62	8.019	7.525	8.475

Table 7.2.3: ^{1}H NMR Chemical shift data (in ppm) for [Pt(4,7-diphenylphen)DiBuBTu]$^+PF_6^-$ in acetonitrile-d_3 at 25 °C

CONC (mol dm^{-3})	H_2	H_3	H_5	H_6	H_8	H_9	$H_{3''}$ $H_{5''}$	$H_{4''}$	$H_{2''}$ $H_{6''}$
$9.336x10^{-4}$	9.292	8.153	8.100	8.036	7.847	8.891	7.496	7.58-7.72	8.153
$2.370x10^{-3}$	9.160	8.087	8.053	7.985	7.786	8.753	7.449	7.54-7.70	8.053
$3.423x10^{-3}$	9.099	8.057	8.030	7.961	7.757	8.691	7.427	7.52-7.70	8.006
$4.299x10^{-3}$	9.064	8.037	8.016	7.946	7.741	8.655	7.414	7.50-7.70	7.92-8.06
$4.564x10^{-3}$	9.050	8.031	8.012	7.941	7.735	8.643	7.409	7.50-7.70	7.90-8.06
$4.865x10^{-3}$	9.037	8.025	8.006	7.935	7.729	8.629	7.404	7.50-7.70	7.90-8.04

Table 7.2.4: ^{1}H NMR Chemical shift data (in ppm) for [Pt(4,7-diphenylphen)DiBuNTu]$^+PF_6^-$ in acetonitrile-d_3 at 25 °C

CONC (mol dm^{-3})	H_2	H_3	H_5 H_6	H_8	H_9	$H_{2''}$	$H_{3''}$ $H_{6''}$ $H_{7''}$	$H_{4''}$ $H_{5''}$	$H_{8''}$
$2.543x10^{-3}$	8.900	7.856	7.96-8.08	7.804	8.871	8.094	7.50-7.68	7.96-8.08	8.436
$3.390x10^{-3}$	8.858	7.833	7.94-8.06	7.777	8.830	8.087	7.46-7.66	7.94-8.06	8.414
$3.747x10^{-3}$	8.844	7.827	7.94-8.04	7.768	8.811	8.084	7.46-7.66	7.94-8.04	8.406
$4.068x10^{-3}$	8.831	7.821	7.94-8.04	7.760	8.798	8.081	7.46-7.66	7.94-8.04	8.400
$4.359x10^{-3}$	8.821	7.816	7.92-8.04	7.755	8.788	8.079	7.44-7.64	7.92-8.04	8.396
$4.623x10^{-3}$	8.812	7.812	7.92-8.04	7.749	8.778	8.078	7.44-7.64	7.92-8.04	8.391
$4.864x10^{-3}$	8.804	7.808	7.92-8.04	7.744	8.770	8.076	7.44-7.64	7.92-8.04	8.387
$5.085x10^{-3}$	8.795	7.802	7.90-8.02	7.738	8.761	8.074	7.44-7.64	7.90-8.02	8.382
$5.288x10^{-3}$	8.790	7.800	7.90-8.02	7.735	8.755	8.073	7.44-7.64	7.90-8.02	8.380
$5.650x10^{-3}$	8.777	7.794	7.90-8.02	7.728	8.743	8.071	7.44-7.66	7.90-8.02	8.373
$5.962x10^{-3}$	8.769	7.789	7.90-8.02	7.722	8.735	8.070	7.44-7.66	7.90-8.02	8.370

Table 7.2.5: ^{1}H NMR Chemical shift data (in ppm) for [Pt(4,4'-dimethylbipy)DiBuBTu]$^+PF_6^-$ in acetonitrile-d_3 at 25 °C

CONC (mol dm^{-3})	$H_{3'}$	H_3	$H_{5'}$	H_5	$H_{6'}$	H_6	$H_{3''}$ $H_{5''}$	$H_{4''}$	$H_{2''}$ $H_{6''}$
$2.128x10^{-3}$	8.073	8.003	7.695	7.375	8.790	8.367	7.509	7.651	8.100
$2.554x10^{-3}$	8.052	7.981	7.677	7.360	8.765	8.345	7.506	7.651	8.084
$2.902x10^{-3}$	8.035	7.964	7.64-7.70	7.345	8.746	8.327	7.504	7.651	8.070
$3.192x10^{-3}$	8.022	7.950	7.64-7.70	7.337	8.729	8.311	7.503	7.651	8.061
$3.438x10^{-3}$	8.013	7.939	7.64-7.70	7.328	8.716	8.301	7.501	7.652	8.053

Table 7.2.6: ^{1}H NMR Chemical shift data (in ppm) for [Pt(4,4'-dimethylbipy)DiBuNTu]$^+PF_6^-$ in acetonitrile-d_3 at 25 °C

CONC (mol dm^{-3})	$H_{3'}$	H_3	$H_{5'}$	H_5	$H_{6'}$	H_6	$H_{2''}$	$H_{4''}$	$H_{5''}$	$H_{3''}$ $H_{6''}$ $H_{7''}$	$H_{8''}$
2.014x10^{-3}	8.157	8.130	7.477	7.432	8.564	8.505	7.988	8.090	8.004	7.50-7.60	8.402
2.820x10^{-3}	8.139	8.114	7.462	7.413	8.545	8.485	7.978	8.089	8.004	7.48-7.60	8.395
3.525x10^{-3}	8.124	8.100	7.451	7.398	8.532	8.471	7.971	8.089	8.004	7.48-7.60	8.389
4.147x10^{-3}	8.110	8.089	7.440	7.385	8.520	8.458	7.964	8.088	8.004	7.46-7.60	8.385
4.700x10^{-3}	8.098	8.077	7.431	7.374	8.509	8.447	7.959	8.088	8.003	7.46-7.60	8.380
5.195x10^{-3}	8.095	8.075	7.423	7.367	8.500	8.436	7.954	8.087	8.003	7.46-7.60	8.376
5.640x10^{-3}	8.077	8.063	7.418	7.360	8.492	8.429	7.951	8.085	8.003	7.46-7.60	8.372
6.043x10^{-3}	8.073	8.055	7.411	7.347	8.482	8.417	7.944	8.084	8.000	7.46-7.60	8.369
6.409x10^{-3}	8.071	8.049	7.404	7.340	8.475	8.410	7.941	8.084	8.000	7.46-7.60	8.366
6.743x10^{-3}	8.061	8.044	7.399	7.335	8.470	8.404	7.939	8.084	8.000	7.46-7.60	8.364
7.050x10^{-3}	8.056	8.039	7.396	7.331	8.466	8.399	7.935	8.083	8.000	7.44-7.60	8.362
7.332x10^{-3}	8.051	8.034	7.392	7.325	8.460	8.392	7.932	8.082	7.999	7.44-7.60	8.360
7.592x10^{-3}	8.046	8.031	7.388	7.321	8.456	8.388	7.930	8.082	7.999	7.44-7.60	8.358
7.833x10^{-3}	8.042	8.027	7.384	7.317	8.452	8.383	7.928	8.081	7.999	7.44-7.60	8.356
8.057x10^{-3}	8.039	8.024	7.382	7.314	8.449	8.381	7.927	8.081	7.999	7.44-7.60	8.355
8.266x10^{-3}	8.035	8.020	7.378	7.310	8.444	8.376	7.924	8.081	7.999	7.44-7.60	8.353

Table 7.2.7: ^{1}H NMR Chemical shift data (in ppm) for [Pt(4,4'-ditbutbipy)DiBuBTu]$^+PF_6^-$ in acetonitrile-d_3 at 25 °C

CONC (mol dm^{-3})	$H_{3'}$	H_3	$H_{5'}$	H_5	$H_{6'}$	H_6	$H_{3''}$ $H_{5''}$	$H_{4''}$	$H_{2''}$ $H_{6''}$
2.695x10^{-3}	8.355	8.278	7.964	7.610	8.980	8.515	7.507	7.60-7.66	8.171
6.840x10^{-3}	8.321	8.238	7.920	7.565	8.919	8.440	7.481	7.624	8.115
9.880x10^{-3}	8.303	8.218	7.899	7.543	8.888	8.403	7.466	7.616	8.086
1.220x10^{-2}	8.292	8.206	7.885	7.530	8.869	8.380	7.456	7.611	8.068
1.482x10^{-2}	8.281	8.194	7.873	7.517	8.851	8.358	7.448	7.605	8.050
1.617x10^{-2}	8.276	8.189	7.867	7.511	8.842	8.348	7.441	7.602	8.041
1.729x10^{-2}	8.273	8.185	7.863	7.507	8.836	8.340	7.438	7.601	8.035

Table 7.2.8: ^{1}H NMR Chemical shift data (in ppm) for [Pt(4,4'-ditbutbipy)DiBuNTu]$^+$PF$_6^-$ in acetonitrile-d_3 at 25 °C

CONC (mol dm^{-3})	$H_{3'}$	H_3	$H_{5'}$ H_5	$H_{6'}$	H_6	$H_{2''}$	$H_{4''}$	$H_{5''}$	$H_{3''}$ $H_{6''}$ $H_{7''}$	$H_{8''}$
4.697x10^{-3}	8.362	8.319	7.64-7.70	8.670	8.603	8.020	8.107	8.020	7.54-7.64	8.446
6.503x10^{-3}	8.354	8.311	7.64-7.70	8.658	8.591	8.010	8.103	8.013	7.52-7.62	8.442
8.051x10^{-3}	8.348	8.305	7.64-7.70	8.648	8.582	8.006	8.101	8.015	7.52-7.62	8.439
9.393x10^{-3}	8.342	8.300	7.60-7.66	8.641	8.574	7.999	8.098	8.015	7.50-7.60	8.436
1.160x10^{-2}	8.332	8.290	7.50-7.66	8.627	8.560	7.992	8.094	8.009	7.50-7.66	8.431
1.335x10^{-2}	8.326	8.284	7.50-7.66	8.617	8.550	7.986	8.090	8.005	7.50-7.64	8.428
1.476x10^{-2}	8.320	8.278	7.50-7.66	8.608	8.542	7.981	8.088	8.001	7.50-7.64	8.425
1.593x10^{-2}	8.316	8.274	7.48-7.62	8.602	8.536	7.978	8.085	7.999	7.48-7.62	8.423
1.691x10^{-2}	8.312	8.271	7.48-7.62	8.597	8.530	7.974	8.083	8.000	7.48-7.62	8.421
1.774x10^{-2}	8.310	8.268	7.48-7.62	8.592	8.525	7.971	8.082	7.997	7.48-7.62	8.419

Table 7.2.9: ^{1}H NMR Chemical shift data (in ppm) for [Pt(bipy)DiBuBTu]$^+$PF$_6^-$ in acetonitrile-d_3 at 25 °C

CONC (mol dm^{-3})	$H_{3'}$	H_3	$H_{4'}$	H_4	$H_{5'}$	H_5	$H_{6'}$	H_6	$H_{3''}$ $H_{5''}$	$H_{4''}$	$H_{2''}$ $H_{6''}$
5.484x10^{-3}	8.236	8.167	8.311	8.217	7.914	7.568	9.005	8.566	7.504	7.648	8.105
9.851x10^{-3}	8.180	8.107	8.270	8.180	7.873	7.523	8.937	8.492	7.487	7.642	8.054
1.538x10^{-2}	8.113	8.045	8.226	8.136	7.829	7.469	8.865	8.415	7.469	7.634	8.000
2.426x10^{-2}	8.019	7.951	8.157	8.074	7.762	7.408	8.753	8.299	7.439	7.619	7.917
2.965x10^{-2}	7.970	7.903	8.122	8.044	7.727	7.372	8.695	8.239	7.424	7.610	7.875
3.639x10^{-2}	7.909	7.844	8.076	8.001	7.680	7.327	8.623	8.166	7.401	7.598	7.822

7.3 APPENDIX 3

Table 7.3.1: ^{1}H NMR Chemical shift data (in ppm) for [Pt(phen)DiBuBTu]$^+PF_6^-$ in acetonitrile-d_3 for various temperatures

TEMP (°C)	H_2	H_4	H_7	H_9
CONC (mol dm^{-3})	$2.709x10^{-3}$			
25	9.106	8.766	8.676	8.716
30	9.143	8.787	8.697	8.755
35	9.179	8.807	8.717	8.793
40	9.211	8.825	8.735	8.825
45	9.242	8.840	8.750	8.857
50	9.269	8.855	8.765	8.885
55	9.296	8.869	8.779	8.913
CONC (mol dm^{-3})	$6.877x10^{-3}$			
25	8.835	8.612	8.521	8.455
30	8.881	8.638	8.548	8.502
35	8.930	8.664	8.574	8.548
40	8.974	8.688	8.598	8.593
45	9.019	8.714	8.623	8.638
50	9.058	8.736	8.646	8.676
55	9.095	8.755	8.667	8.713
CONC (mol dm^{-3})	$1.120x10^{-2}$			
25	8.661	8.513	8.426	8.298
30	8.711	8.542	8.454	8.346
35	8.764	8.569	8.482	8.395
40	8.811	8.596	8.508	8.439
45	8.847	8.618	8.531	8.475
50	8.888	8.640	8.562	8.512
55	8.928	8.666	8.576	8.565
CONC (mol dm^{-3})	$1.410x10^{-2}$			
25	8.560	8.455	8.370	8.207
30	8.612	8.483	8.398	8.256
35	8.660	8.509	8.424	8.300
40	8.703	8.537	8.451	8.339
45	8.757	8.568	8.481	8.391
50	8.811	8.595	8.508	8.440
55	8.856	8.622	8.536	8.490

TEMP (°C)	H_2	H_4	H_7	H_9
CONC (mol dm^{-3})	$2.970x10^{-2}$			
25	8.228	8.257	8.182	7.919
30	8.287	8.290	8.215	7.971
35	8.342	8.325	8.246	8.022
40	8.399	8.355	8.279	8.072
45	8.445	8.385	8.308	8.112
50	8.491	8.413	8.336	8.157
55	8.535	8.439	8.361	8.197

Table 7.3.2: ^1H NMR Chemical shift data (in ppm) for $[Pt(phen)DiBuNTu]^+PF_6^-$ in acetonitrile-d_3 for various temperatures

TEMP (°C)	H_4	H_5	H_6	H_7
CONC (mol dm^{-3})	$2.861x10^{-3}$			
25	8.832	8.176	8.134	8.812
30	8.840	8.183	8.141	8.819
35	8.845	8.190	8.148	8.827
40	8.854	8.197	8.155	8.834
45	8.861	8.202	8.160	8.840
50	8.862	8.204	8.163	8.842
55	8.864	8.205	8.165	8.845

Table 7.3.3: ^1H NMR Chemical shift data (in ppm) for $[Pt(4,7\text{-diphenylphen})DiBuBTu]^+PF_6^-$ in acetonitrile-d_3 for various temperatures

TEMP (°C)	H_2	H_3	H_5	H_6	H_8	H_9
CONC (mol dm^{-3})	$9.245x10^{-4}$					
25	9.308	8.162	8.110	8.045	7.857	8.908
30	9.334	8.174	8.118	8.055	7.869	8.936
35	9.358	8.184	8.126	8.064	7.879	8.962
40	9.378	8.193	8.133	8.071	7.889	8.984
45	9.398	8.202	8.139	8.078	7.897	9.006
50	9.416	8.210	8.144	8.084	7.905	9.025
55	9.429	8.216	8.148	8.088	7.911	9.040

TEMP (°C)	H_2	H_3	H_5	H_6	H_8	H_9
CONC (mol dm^{-3})	$2.347x10^{-3}$					
25	9.171	8.092	8.058	7.990	7.791	8.765
30	9.203	8.107	8.070	8.004	7.806	8.800
35	9.235	8.10-8.16	8.082	8.016	7.820	8.833
40	9.263	8.137	8.091	8.027	7.832	8.863
45	9.290	8.149	8.100	8.037	7.844	8.891
50	9.314	8.160	8.108	8.046	7.856	8.918
55	9.336	8.171	8.116	8.053	7.866	8.941
CONC (mol dm^{-3})	$3.390x10^{-3}$					
25	9.112	8.064	8.037	7.967	7.764	8.705
30	9.144	8.079	8.049	7.981	7.779	8.738
35	9.177	8.094	8.061	7.993	7.793	8.773
40	9.209	8.109	8.072	8.007	7.807	8.807
45	9.238	8.122	8.083	8.017	7.820	8.837
50	9.263	8.134	8.092	8.028	7.832	8.866
55	9.282	8.12-8.18	8.099	8.036	7.842	8.880
CONC (mol dm^{-3})	$4.188x10^{-3}$					
25	9.080	8.047	8.024	7.954	7.749	8.673
30	9.113	8.062	8.037	7.968	7.763	8.706
35	9.146	8.078	8.049	7.981	7.779	8.741
40	9.178	8.093	8.061	7.994	7.793	8.775
45	9.209	8.107	8.072	8.006	7.806	8.807
50	9.230	8.08-8.14	8.080	8.015	7.817	8.830
55	9.247	8.128	8.088	8.023	7.827	8.851
CONC (mol dm^{-3})	$5.085x10^{-3}$					
25	9.043	8.028	8.009	7.938	7.731	8.635
30	9.077	8.044	8.023	7.953	7.747	8.670
35	9.110	8.059	8.035	7.966	7.761	8.704
40	9.138	8.073	8.046	7.978	7.774	8.735
45	9.158	8.00-8.10	8.057	7.989	7.787	8.756
50	9.184	8.00-8.10	8.02-8.10	8.000	7.798	8.783
55	9.218	8.04-8.14	8.06-8.10	8.013	7.814	8.818

TEMP (°C)	H_2	H_3	H_5	H_6	H_8	H_9
CONC (mol dm^{-3})	$6.102x10^{-3}$					
25	9.012	8.012	7.997	7.925	7.717	8.604
30	9.047	8.029	8.011	7.940	7.733	8.641
35	9.080	8.044	8.024	7.954	7.747	8.675
40	9.111	8.056	8.036	7.967	7.761	8.707
45	9.142	8.073	8.047	7.980	7.775	8.739
50	9.172	8.02-8.10	8.059	7.992	7.789	8.770
55	9.199	8.02-8.10	8.070	8.002	7.801	8.798

Table 7.3.4: ^1H NMR Chemical shift data (in ppm) for $[Pt(4,4'\text{-ditbutbipy})DiBuBTu]^+PF_6^-$ in acetonitrile-d_3 for various temperatures

TEMP (°C)	$H_{3'}$	H_3	$H_{5'}$	H_5	$H_{6'}$	H_6
CONC (mol dm^{-3})	$2.723x10^{-3}$					
25	8.354	8.276	7.964	7.610	8.981	8.519
30	8.357	8.280	7.972	7.60-7.64	8.994	8.532
35	8.360	8.284	7.977	7.60-7.64	9.000	8.541
40	8.363	8.287	7.982	7.62-7.66	9.008	8.552
45	8.365	8.289	7.987	7.62-7.66	9.014	8.558
50	8.367	8.292	7.989	7.62-7.66	9.021	8.567
55	8.368	8.293	7.993	7.62-7.66	9.026	8.575
CONC (mol dm^{-3})	$6.912x10^{-3}$					
25	8.319	8.237	7.921	7.567	8.923	8.448
30	8.326	8.245	7.933	7.580	8.939	8.467
35	8.332	8.252	7.941	7.590	8.950	8.483
40	8.337	8.258	7.951	7.601	8.965	8.497
45	8.341	8.263	7.959	7.608	8.974	8.510
50	8.345	8.268	7.966	7.60-7.63	8.983	8.524
55	8.350	8.273	7.974	7.60-7.63	8.995	8.536

TEMP (°C)	$H_{3'}$	H_3	$H_{5'}$	H_5	$H_{6'}$	H_6
CONC (mol dm^{-3})	9.983×10^{-3}					
25	8.300	8.215	7.897	7.543	8.889	8.408
30	8.307	8.223	7.909	7.556	8.906	8.428
35	8.313	8.230	7.920	7.568	8.920	8.445
40	8.319	8.237	7.929	7.577	8.932	8.459
45	8.325	8.245	7.940	7.589	8.947	8.477
50	8.330	8.251	7.948	7.58-7.61	8.959	8.493
55	8.335	8.258	7.957	7.60-7.64	8.972	8.508
CONC (mol dm^{-3})	1.233×10^{-2}					
25	8.289	8.203	7.885	7.531	8.871	8.387
30	8.297	8.212	7.898	7.545	8.888	8.408
35	8.304	8.221	7.908	7.557	8.903	8.425
40	8.310	8.228	7.920	7.569	8.919	8.444
45	8.316	8.236	7.930	7.580	8.934	8.462
50	8.323	8.244	7.940	7.58-7.61	8.947	8.479
55	8.327	8.248	7.92-7.98	7.56-7.62	8.961	8.496
CONC (mol dm^{-3})	1.498×10^{-2}					
25	8.277	8.189	7.870	7.516	8.851	8.361
30	8.285	8.198	7.883	7.529	8.867	8.381
35	8.292	8.207	7.894	7.542	8.883	8.401
40	8.299	8.216	7.906	7.555	8.899	8.420
45	8.304	8.223	7.919	7.570	8.918	8.443
50	8.310	8.229	7.90-7.94	7.56-7.60	8.932	8.460
55	8.315	8.237	7.90-7.94	7.56-7.62	8.945	8.475
CONC (mol dm^{-3})	1.634×10^{-2}					
25	8.273	8.185	7.865	7.512	8.844	8.353
30	8.280	8.194	7.878	7.525	8.860	8.375
35	8.288	8.203	7.888	7.539	8.878	8.393
40	8.295	8.212	7.902	7.551	8.893	8.413
45	8.301	8.219	7.916	7.54-7.60	8.912	8.436
50	8.305	8.224	7.88-7.94	7.54-7.60	8.925	8.451
55	8.309	8.229	7.88-7.96	7.54-7.62	8.933	8.460

TEMP (°C)	$H_{3'}$	H_3	$H_{5'}$	H_5	$H_{6'}$	H_6
CONC (mol dm^{-3})	$1.747x10^{-2}$					
25	8.267	8.178	7.858	7.505	8.834	8.342
30	8.275	8.188	7.871	7.518	8.851	8.362
35	8.283	8.197	7.884	7.531	8.867	8.383
40	8.288	8.203	7.897	7.545	8.887	8.405
45	8.298	8.214	7.88-7.92	7.52-7.58	8.903	8.425
50	8.299	8.217	7.88-7.94	7.54-7.60	8.912	8.439
55	8.303	8.221	7.88-7.94	7.54-7.60	8.920	8.451

Table 7.3.5: ^{1}H NMR Chemical shift data (in ppm) for [Pt(4,4'-dimethylbipy)DiBuNTu]$^+PF_6^-$ in acetonitrile-d_3 for various temperatures

TEMP (°C)	$H_{3'}$	H_3	$H_{5'}$	H_5	$H_{6'}$	H_6
CONC (mol dm^{-3})	$2.224x10^{-3}$					
25	8.157	8.132	7.475	7.432	8.565	8.506
30	8.163	8.135	7.480	7.440	8.575	8.515
35	8.169	8.138	*a*	*a*	8.582	8.523
40	8.172	8.142	*a*	*a*	8.589	8.530
45	8.175	8.146	*a*	*a*	8.595	8.535
50	8.178	8.149	*a*	*a*	8.602	8.542
55	8.183	8.151	*a*	*a*	8.608	8.543
CONC (mol dm^{-3})	$3.893x10^{-3}$					
25	8.124	8.099	7.450	7.399	8.533	8.472
30	8.133	8.108	7.458	7.412	8.546	8.484
35	8.141	8.116	*a*	*a*	8.556	8.495
40	8.149	8.122	*a*	*a*	8.565	8.505
45	8.156	8.128	*a*	*a*	8.576	8.514
50	8.163	8.132	*a*	*a*	8.584	8.522
55	8.168	8.140	*a*	*a*	8.594	8.532

TEMP (°C)	$H_{3'}$	H_3	$H_{5'}$	H_5	$H_{6'}$	H_6
CONC (mol dm^{-3})	5.190×10^{-3}					
25	8.096	8.075	7.429	7.373	8.507	8.444
30	8.109	8.094	7.439	7.386	8.521	8.458
35	8.119	8.096	7.447	7.398	8.532	8.470
40	8.129	8.097	7.456	7.410	8.545	8.483
45	8.137	8.112	*a*	*a*	8.556	8.493
50	8.147	8.120	*a*	*a*	8.572	8.507
55	8.154	8.125	*a*	*a*	8.577	8.518
CONC (mol dm^{-3})	6.228×10^{-3}					
25	8.074	8.062	7.416	7.358	8.491	8.427
30	8.095	8.074	7.427	7.372	8.507	8.443
35	8.106	8.094	7.437	7.386	8.520	8.457
40	8.119	8.096	7.447	7.399	8.535	8.472
45	8.129	8.097	7.455	7.412	8.548	8.485
50	8.140	8.114	7.467	7.426	8.563	8.499
55	8.147	8.120	*a*	*a*	8.572	8.508
CONC (mol dm^{-3})	6.673×10^{-3}					
25	8.073	8.054	7.409	7.349	8.482	8.417
30	8.091	8.072	7.420	7.364	8.497	8.433
35	8.095	8.074	7.429	7.376	8.511	8.448
40	8.111	8.093	*a*	*a*	8.526	8.462
45	8.123	8.096	*a*	*a*	8.545	8.480
50	*a*	*a*	*a*	*a*	8.553	8.490
55	*a*	*a*	*a*	*a*	8.560	8.501
CONC (mol dm^{-3})	7.077×10^{-3}					
25	8.072	8.050	7.406	7.342	8.477	8.412
30	8.083	8.063	7.417	7.360	8.494	8.430
35	8.094	8.073	7.426	7.374	8.508	8.444
40	8.106	8.082	*a*	*a*	8.522	8.458
45	8.120	8.095	*a*	*a*	8.538	8.475
50	8.129	8.096	*a*	*a*	8.551	8.487
55	*a*	*a*	*a*	*a*	8.554	8.497

TEMP (°C)	$H_{3'}$	H_3	$H_{5'}$	H_5	$H_{6'}$	H_6
CONC (mol dm^{-3})	7.785×10^{-3}					
25	8.055	8.038	7.395	7.333	8.465	8.398
30	8.071	8.052	7.408	7.347	8.482	8.416
35	8.091	8.071	7.419	7.364	8.497	8.431
40	8.094	8.073	*a*	*a*	8.513	8.448
45	8.111	8.094	*a*	*a*	8.529	8.465
50	*a*	*a*	*a*	*a*	8.538	8.477
55	*a*	*a*	*a*	*a*	8.539	8.485

a: peaks too broad to be accurately assigned

Table 7.3.6: ^{1}H NMR Chemical shift data (in ppm) for [Pt(4,7-diphenylphen)DiBuNTu]$^+PF_6^-$ in acetonitrile-d_3 for various temperatures

TEMP (°C)	H_2	H_9	H_3	H_8
CONC (mol dm^{-3})	1.584×10^{-3}			
25	8.975	8.953	7.891	7.854
30	8.998	8.981	7.903	7.871
35	9.019	9.004	7.914	7.879
40	9.037	9.022	7.922	7.890
45	9.044	9.029	7.932	7.899
50	9.068	9.053	7.942	7.912
55	9.081	9.066	7.946	7.930
CONC (mol dm^{-3})	2.773×10^{-3}			
25	8.905	8.877	7.858	7.808
30	8.931	8.908	7.870	7.825
35	8.950	8.932	7.879	7.838
40	8.966	8.952	7.888	7.850
45	8.990	8.976	7.897	7.866
50	9.011	8.997	7.907	7.876
55	9.034	9.020	7.918	7.892

TEMP (°C)	H_2	H_9	H_3	H_8
CONC (mol dm^{-3})	3.697×10^{-3}			
25	8.861	8.830	7.835	7.779
30	8.886	8.860	7.847	7.795
35	8.889	8.875	7.858	7.808
40	8.914	8.900	7.869	7.825
45	8.947	8.933	7.880	7.840
50	8.968	8.954	7.891	7.855
55	8.999	8.985	7.904	7.874
CONC (mol dm^{-3})	4.086×10^{-3}			
25	8.848	8.816	7.829	7.771
30	8.875	8.850	7.842	7.789
35	8.886	8.872	7.852	7.801
40	8.921	8.907	7.863	7.816
45	8.934	8.920	7.876	7.835
50	8.975	8.961	7.885	7.847
55	8.996	8.982	7.894	7.863
CONC (mol dm^{-3})	4.436×10^{-3}			
25	8.832	8.779	7.821	7.761
30	8.857	8.827	7.832	7.776
35	8.876	8.853	7.843	7.791
40	8.905	8.882	7.856	7.807
45	8.918	8.904	7.869	7.825
50	8.947	8.933	7.882	7.842
55	8.978	8.964	7.887	7.850
CONC (mol dm^{-3})	5.041×10^{-3}			
25	8.814	8.781	7.812	7.750
30	8.842	8.813	7.825	7.767
35	8.869	8.843	7.838	7.784
40	8.898	8.874	7.850	7.800
45	8.911	8.904	7.863	7.819
50	8.933	8.919	7.872	7.833
55	8.968	8.940	7.881	7.847

TEMP (°C)	H_2	H_9	H_3	H_8
CONC (mol dm^{-3})	$5.304x10^{-3}$			
25	8.801	8.768	7.806	7.743
30	8.828	8.799	7.819	7.758
35	8.858	8.828	7.831	7.773
40	8.862	8.848	7.842	7.789
45	8.898	8.884	7.859	7.810
50	8.920	8.906	7.866	7.824
55	8.934	8.920	7.877	7.839

H_2 and H_9:: values are estimates due to significant peak broadening

Table 7.3.7: ^{1}H NMR Chemical shift data (in ppm) for $[Pt(bipy)DiBuBTu]^+PF_6^-$ in acetonitrile-d_3 for various temperatures

TEMP (°C)	$H_{4'}$	H_4	$H_{5'}$	H_5	$H_{6'}$	H_6
CONC (mol dm^{-3})	$1.823x10^{-3}$					
25	8.373	*a*	7.977	*a*	9.118	8.694
30	8.379	*a*	7.983	*a*	9.128	8.707
35	8.388	*a*	7.988	*a*	9.138	8.718
40	*a*	*a*	7.991	*a*	9.146	8.728
45	*a*	*a*	7.995	*a*	9.154	8.737
50	*a*	*a*	7.997	*a*	9.163	8.745
55	*a*	*a*	7.996	*a*	9.167	8.752
CONC (mol dm^{-3})	$2.449x10^{-3}$					
25	8.370	*a*	7.971	*a*	9.108	8.682
30	8.376	*a*	7.977	*a*	9.119	8.695
35	8.383	*a*	7.982	*a*	9.130	8.706
40	8.385	*a*	7.986	*a*	9.139	8.716
45	*a*	*a*	7.989	*a*	9.143	8.726
50	*a*	*a*	7.992	*a*	9.151	8.734
55	*a*	*a*	7.997	*a*	9.157	8.741

TEMP (°C)	$H_{4'}$	H_4	$H_{5'}$	H_5	$H_{6'}$	H_6
CONC (mol dm^{-3})	3.343×10^{-3}					
25	8.347	*a*	7.948	*a*	9.069	8.639
30	8.357	*a*	7.958	*a*	9.087	8.660
35	8.365	*a*	7.965	*a*	9.102	8.677
40	8.373	*a*	7.972	*a*	9.115	8.691
45	8.377	*a*	7.978	*a*	9.125	8.706
50	8.383	*a*	7.984	*a*	9.137	8.717
55	8.388	*a*	7.988	*a*	9.147	8.728
CONC (mol dm^{-3})	4.436×10^{-3}					
25	8.335	*a*	7.940	7.597	9.053	8.623
30	8.345	*a*	7.949	*a*	9.071	8.643
35	8.354	*a*	7.955	*a*	9.084	8.659
40	8.361	*a*	7.961	*a*	9.100	8.676
45	8.368	*a*	7.968	*a*	9.107	8.687
50	8.372	*a*	7.973	*a*	9.120	8.699
55	8.377	*a*	7.978	*a*	9.128	8.708
CONC (mol dm^{-3})	7.463×10^{-3}					
25	8.292	8.202	7.897	7.550	8.982	8.543
30	8.305	*a*	7.909	7.564	9.005	8.568
35	8.317	*a*	7.916	7.577	9.024	8.588
40	8.325	*a*	7.929	7.585	9.040	8.608
45	8.335	*a*	7.936	7.596	9.054	8.625
50	8.343	*a*	7.944	7.603	9.069	8.640
55	8.355	*a*	7.952	*a*	9.087	8.633
CONC (mol dm^{-3})	9.622×10^{-3}					
25	8.266	*a*	7.872	7.522	8.940	8.496
30	8.280	*a*	7.884	7.538	8.965	8.523
35	8.293	*a*	7.894	7.550	8.987	8.546
40	8.305	*a*	7.905	7.562	9.004	8.568
45	8.318	*a*	7.917	7.577	9.025	8.590
50	8.329	*a*	7.926	7.587	9.043	8.609
55	8.339	*a*	7.936	*a*	9.063	8.629

TEMP (°C)	$H_{4'}$	H_4	$H_{5'}$	H_5	$H_{6'}$	H_6
CONC (mol dm^{-3})	$1.133x10^{-2}$					
25	8.249	*a*	7.850	7.493	8.908	8.461
30	8.261	*a*	7.864	7.516	8.933	8.487
35	8.273	*a*	7.877	7.529	8.954	8.510
40	8.288	*a*	7.889	7.543	8.977	8.538
45	8.301	*a*	7.901	7.560	8.997	8.561
50	8.313	*a*	7.912	7.571	9.020	8.582
55	8.326	*a*	7.922	7.585	9.039	8.590

a: peaks too broad to be accurately assigned